

**REPORT DOCUMENTATION PAGE**

Form Approved OMB No. 0704-0188

Public reporting burden for this collection of information is estimated to average 1 hour per response, including the time for reviewing instructions, searching existing data sources, gathering and maintaining the data needed, and completing and reviewing the collection of information. Send comments regarding this burden estimate or any other aspect of this collection of information, including suggestions for reducing the burden, to Department of Defense, Washington Headquarters Services, Directorate for Information Operations and Reports (0704-0188), 1215 Jefferson Davis Highway, Suite 1204, Arlington, VA 22202-4302. Respondents should be aware that notwithstanding any other provision of law, no person shall be subject to any penalty for failing to comply with a collection of information if it does not display a currently valid OMB control number.

**PLEASE DO NOT RETURN YOUR FORM TO THE ABOVE ADDRESS.**

<b>1. REPORT DATE (DD-MM-YYYY)</b> 25-08-2005	<b>2. REPORT TYPE</b> Final Report	<b>3. DATES COVERED (From – To)</b> 1 September 2004 - 01-Sep-05
--	---------------------------------------	---

<b>4. TITLE AND SUBTITLE</b>  Fabrication and Evaluation of Ceramic Microtubes by Extrusion of Pre ceramic Polymers	<b>5a. CONTRACT NUMBER</b> FA8655-04-1-3055
	<b>5b. GRANT NUMBER</b>
	<b>5c. PROGRAM ELEMENT NUMBER</b>

<b>6. AUTHOR(S)</b>  Professor Paolo Colombo	<b>5d. PROJECT NUMBER</b>
	<b>5d. TASK NUMBER</b>
	<b>5e. WORK UNIT NUMBER</b>

<b>7. PERFORMING ORGANIZATION NAME(S) AND ADDRESS(ES)</b> University of Bologna Viale Risorgimento, 2 Bologna I-40136 Italy	<b>8. PERFORMING ORGANIZATION REPORT NUMBER</b>  N/A
---	--

<b>9. SPONSORING/MONITORING AGENCY NAME(S) AND ADDRESS(ES)</b>  EOARD PSC 821 BOX 14 FPO 09421-0014	<b>10. SPONSOR/MONITOR'S ACRONYM(S)</b>
	<b>11. SPONSOR/MONITOR'S REPORT NUMBER(S)</b> Grant 04-3055

**12. DISTRIBUTION/AVAILABILITY STATEMENT**  
Approved for public release; distribution is unlimited.

**13. SUPPLEMENTARY NOTES**

**14. ABSTRACT**

This report results from a contract tasking University of Bologna as follows: This work will explore the fabrication of microtubes using commercially available, specialized equipment developed for micro-extrusion of conventional polymers. In this project, pre ceramic polymers, yielding Si-(O)-(N)-C upon pyrolysis at high temperature, will be used instead of conventional thermoplastic polymers. Microtubes of various diameters will be manufactured using both a single extrusion and a co-extrusion approach. In the latter method, a sacrificial material will be co-extruded with the pre ceramic polymer, and later eliminated to reveal the desired porosity. Multilumen microtubes will also be produced. The fabricated microtubes will be characterized in terms of mechanical properties and morphology, using several available analytical techniques.

**15. SUBJECT TERMS**  
EOARD, Ceramics, Microcavities, Materials Process Design, micro scale flows

<b>16. SECURITY CLASSIFICATION OF:</b>			<b>17. LIMITATION OF ABSTRACT</b> UL	<b>18. NUMBER OF PAGES</b>  78	<b>19a. NAME OF RESPONSIBLE PERSON</b> JOAN FULLER
<b>a. REPORT</b> UNCLAS	<b>b. ABSTRACT</b> UNCLAS	<b>c. THIS PAGE</b> UNCLAS			<b>19b. TELEPHONE NUMBER (Include area code)</b> +44 (0)20 7514 3154

**European Office for Aerospace Research and Development**

**Grant # 043055**

**Fabrication and Evaluation of Ceramic Microtubes by Extrusion of  
Pre ceramic Polymers**

*P.I.: Prof. Paolo Colombo  
Department of Applied Chemistry and Materials Science (DICASM)  
University of Bologna, viale Risorgimento 2  
40136 Bologna, Italy*

**Final Report  
Report 4**

31/8/2005

## 1.1. Modification of the extruder heads

The main general goal of this project is to characterize single and multilumen ceramic microtubes produced from preceramic polymers by co-extrusion. In order to achieve this, as specified in the budget details, extruders heads suitable for processing preceramic polymers, in particular silicone resins, need to be produced at Macgi/Gimac (Castronno, Varese, Italy) starting from conventional available heads.

The modification of the existing extruder heads concerned especially the design and testing of suitable pathways for uniformly distributing the molten resin within the head, assuring the production of well defined and good quality microtubes.

In this first stage of the contract, a head capable of producing single-lumen microtubes by co-extrusion was developed. With this head, a structure comprised of a sacrificial filler constituting a core surrounded by a layer of the silicone resin can be formed; upon pyrolysis (heating at high temperature -  $> 800^{\circ}\text{C}$  - in inert atmosphere in order to produce a silicon oxycarbide ceramic material) the filler in the core decomposes, while the preceramic polymer ceramizes yielding a SiOC ceramic microtube (see later).

The assembled equipment that was tested for the production of ceramic microtubes (Model TR 12/24 LD, Gimac, Castronno (VA), Italy) is constituted by:

- two loading trays, for the introduction of granulated or powdered materials
- two extruder cylinders (fitted with three thermocouples each), containing the extruding screws
- the extruder's head, where the two material fluxes are mixed and the microtubes are formed

In Figure 1-2 are reported images of the microextruder used in these experiments, showing also a detail of the extruder's head, while the microextruder in operation during the fabrication of microtubes from preceramic polymers is shown in Figure 3.

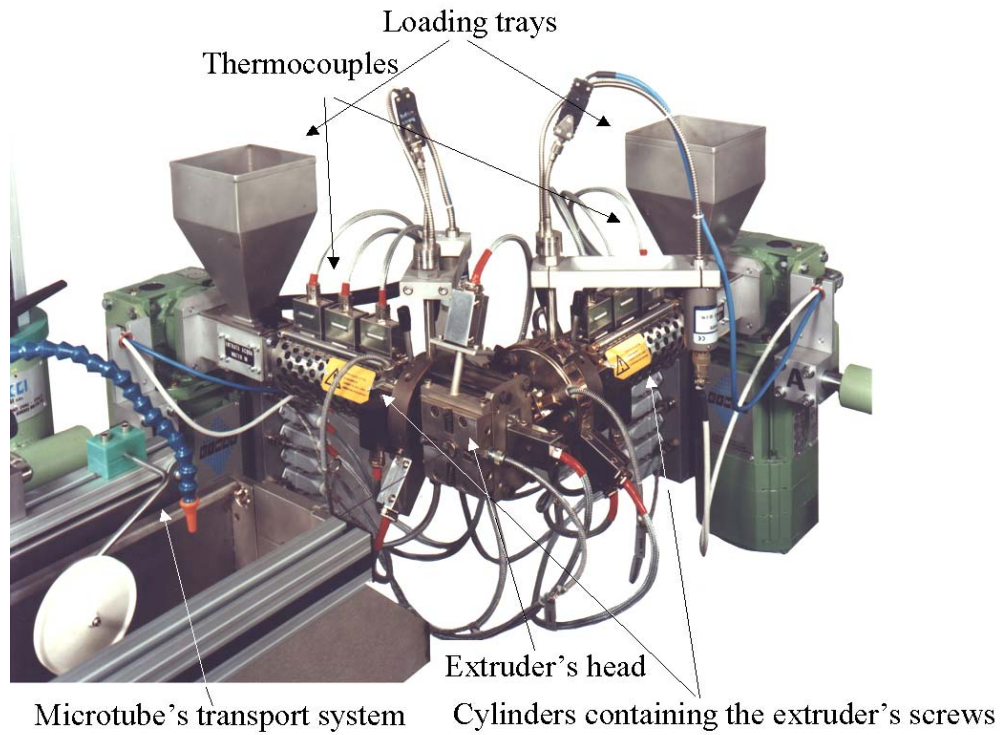


Figure 1. Detail of the co-extruder (image used in manufacturer's brochures – all rights belong to Gimac).

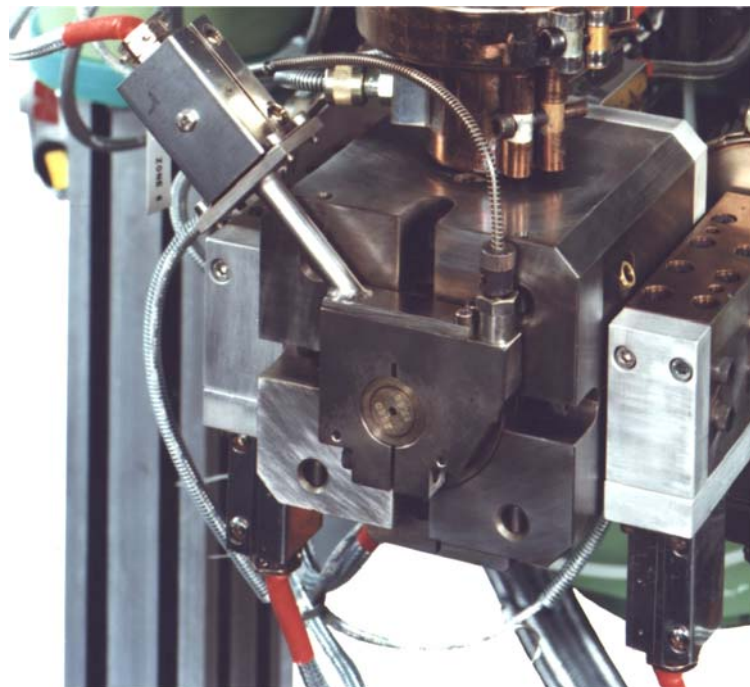


Figure 2. Detail of the co-extruder's head. The microtubes exit from the central orifice (image used in manufacturer's brochures – all rights belong to Gimac).

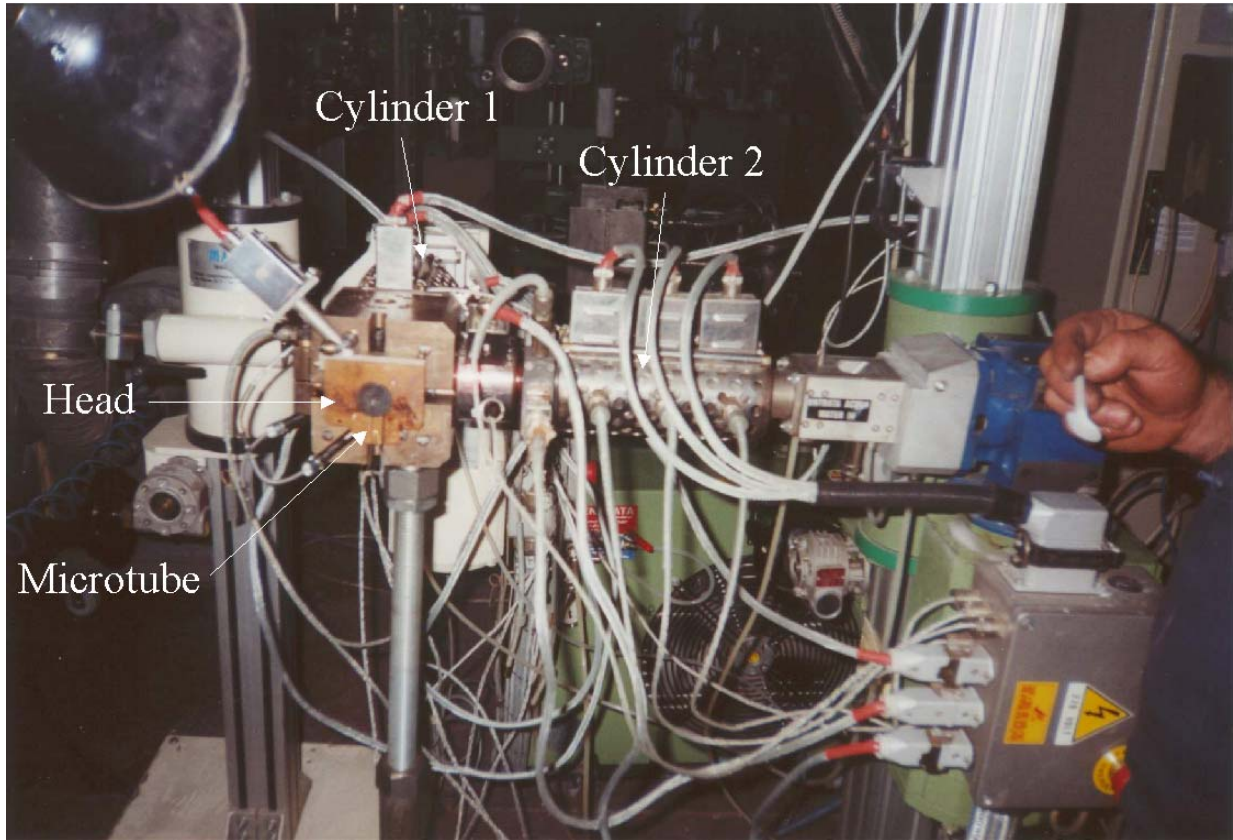


Figure 3. Fabrication of microtubes by co-extrusion (image used in manufacturer's brochures – all rights belong to Gimac).

## 1.2. Production of preceramic-polymer-based microtubes by co-extrusion

The concept of producing a ceramic microtube from the co-extrusion of a preceramic polymer and a filler (sacrificial) core is based on the fact that, upon heating, a preceramic polymer undergoes the polymer-to-ceramic transition (at temperatures in the range  $\sim 600$  to  $800^\circ\text{C}$ ) resulting in the formation of an amorphous ceramic material with substantial yield (in the range  $\sim 60$ - $90$  wt%). If the preceramic polymer is cross-linked, then upon heating no softening but only the ceramization process occurs, with weight density increase and significant shrinkage, and the ceramic product will retain the original shape it had while still in the polymeric stage. When heated in a similar way the sacrificial filler, depending on its molecular weight, composition and structure, will decompose leaving behind a limited residue.

Thus, if a suitable filler and a preceramic polymer are coupled in the way depicted in Figure 4, the formation of a hollow ceramic microtube after pyrolysis can be expected as the other material will act as a sacrificial filler.

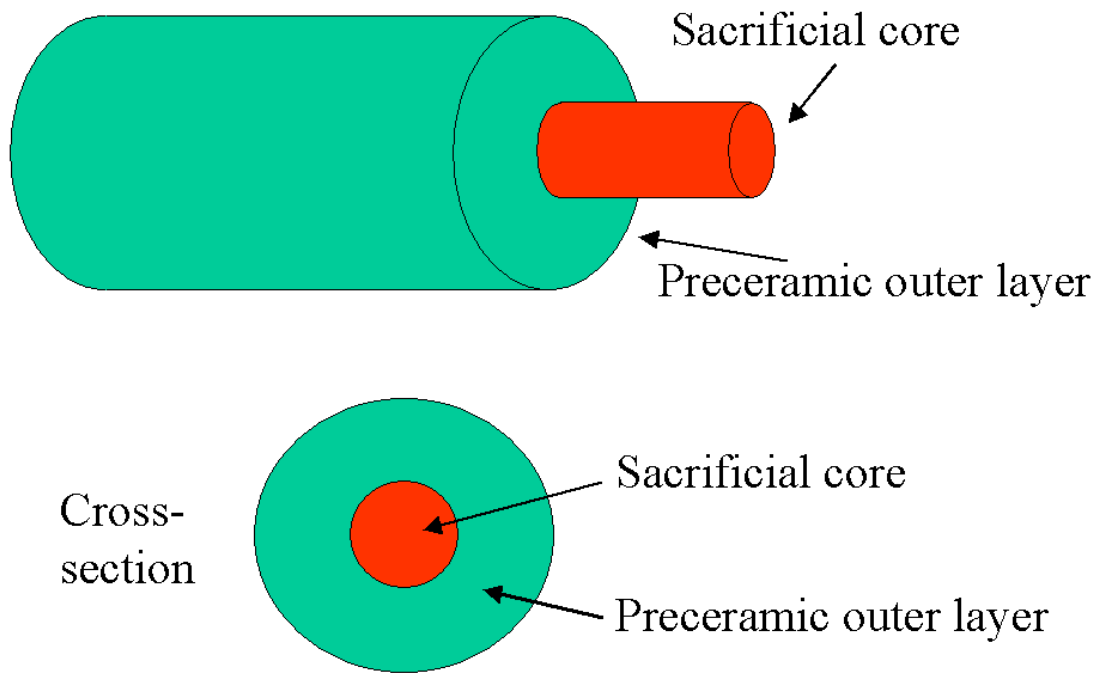


Figure 4. Schematic concept for the realization of a ceramic microtube from a preceramic polymer (outer shell) and a filler material (sacrificial core) by co-extrusion.

The characteristics that a material needs to possess in order to act as a sacrificial filler/template are:

- a) decomposition temperature interval higher than the cross-linking temperature of the preceramic polymer (to avoid the collapse of the preceramic polymer and the loss of the axial void)
- b) decomposition temperature interval higher than the processing temperature of the preceramic polymer (to avoid decomposition during forming when in contact with the preceramic polymer)
- c) should decompose leaving the least amount of char (to avoid decreasing the high temperature capability of the ceramic microtube) and possibly releasing a limited amount of gases (decomposition gases need to permeate through the preceramic polymer during heating and could create stresses and defects in the preceramic polymer outer shell). decomposition rate should be compatible with the pyrolysis rate and the rate of weight loss/transformation in the preceramic polymer
- d) processing temperature should be compatible with that of the preceramic polymer (to avoid mixing of the two material when they get into contact during forming or transformation of the preceramic polymer)
- e) rheology and mechanical properties compatible with the preceramic polymer (as both core and outer shell cool at a different rate and are extracted simultaneously at the same speed from the equipment).

- f) compatibility of the coefficient of thermal expansion (as the sacrificial filler material and the preceramic polymers are heated when joined/interlocked, and this could create undesirable stresses)
- g) chemical compatibility with the preceramic polymer (to avoid unwanted contaminations)

Of course, the specific values for the characteristics listed above which are required for the material to act as sacrificial filler depend on the general physical-chemical properties of the preceramic polymer (in particular its cross-linking temperature, its processing temperatures, its thermo-mechanical properties). In order to limit the range of variables, at this stage only a type of preceramic polymer (a silicone resin) and three different fillers were selected for the experiments.

Finally, several processing variables need to be considered when extruding; among them are:

- a) the direction of the extrusion
- b) the speed of the extrusion
- c) the atmosphere surrounding the microtube being formed (still, circulating)
- d) the rate of cooling

The silicone resin employed was a methyl-silicone (SOC-A35, Starfire Systems, Malta, NY). This preceramic polymer is sold in powder form (suitable for directly loading the extruder), is not hazardous, has a glass transition temperature of about 45°C, a softening temperature of about 90°C. It crosslinks via reaction of Si-OH groups (see later), its molecular weight is in the range of 400-6600 g/mole and its viscosity (at 90°C) is of the order of 200 Pa·s. Upon heating in inert atmosphere it forms an amorphous silicon oxycarbide (SiOC) ceramic material, with a ceramic yield of about 85 wt%. Such a high yield is due to the molecular structure of the silicone resin, typical of a silsesquioxane (see Figure 5). In the case of SOC-A35, R are methyl (-CH<sub>3</sub>) groups.

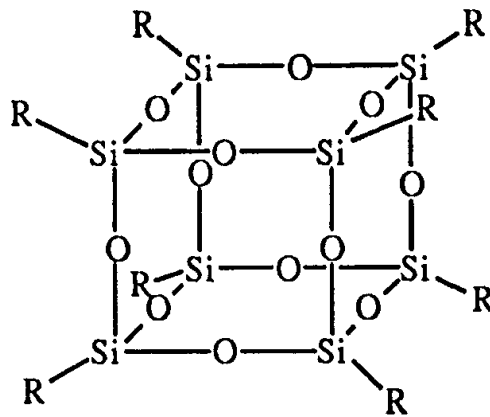


Figure 5. Building block of a silicone silsesquioxane resin.

The fillers chosen (labeled Filler #1, Filler #2 and Filler #3) have different characteristics but are known to burn out cleanly and can be processed easily using a microextruder. What differentiates them is the decomposition temperature range (that will be assessed using thermal gravimetric analysis), the decomposition rate and their mechanical properties (in particular Filler #3 is an elastomer).

In a first set of experiments, Filler #1 was used to fabricate the inner core, and the extrusion was carried out by processing the silicone resin at a temperature of about 90-110°C, while the Filler #1 reached temperatures in the range of 220-240°C. Despite several attempts, varying also the cooling rate, it was not possible to successfully fabricate structures such as the one shown in Figure 4. In fact all the samples produced did not maintain the morphology required because the hot Filler #1 would interact negatively with the silicone resin outer layer leading to its re-melting and partial decomposition. Attempts at reducing the processing temperature of the Filler #1 did not lead to any significant improvement, due to the loss of quality in the extrusion because the processing temperature was not optimal for the Filler #1. Thus Filler #1, at least in this initial stage of the investigation, was abandoned as a possible sacrificial filler material. No images of the samples are here reported as no microtubes were obtained.

It should be noted that it is technically possible to co-extrude materials with such a high difference in processing temperature. However, in order to do so, one should for instance use a technology proprietary to Gimac which employs specifically designed extruder heads, whose cost is outside the range of the budget available to this project.

In a second set of experiments, Filler #2 was used to fabricate the inner core, and the extrusion was carried out by processing the silicone resin at a temperature of about 90-110°C, while the Filler #2 reached temperatures in the range of 180-200°C. In this case, successful co-extrusion was achieved, as demonstrated by the SEM images shown in Figures 6-8, which refer to samples in which the silicone resin was cross-linked (see later), but before pyrolysis. Thus the sacrificial inner core is still present.

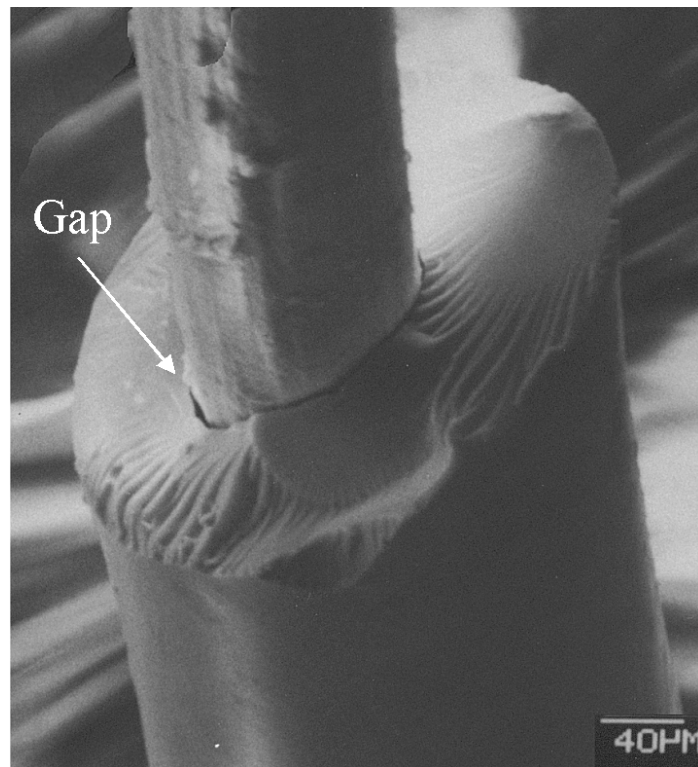


Figure 6. SEM image of a preceramic silicone resin outer shell on a Filler #2 inner core (the silicone resin was cut below the end of the microtube leaving exposed the inner core).

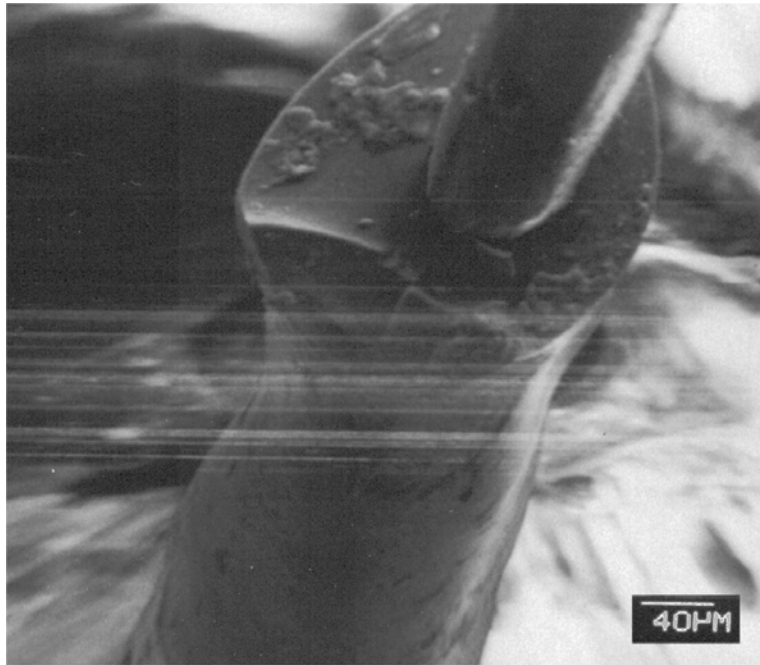


Figure 7. SEM image of a preceramic silicone resin outer shell on a Filler #2 inner core (lines are due to charging problems in the SEM).

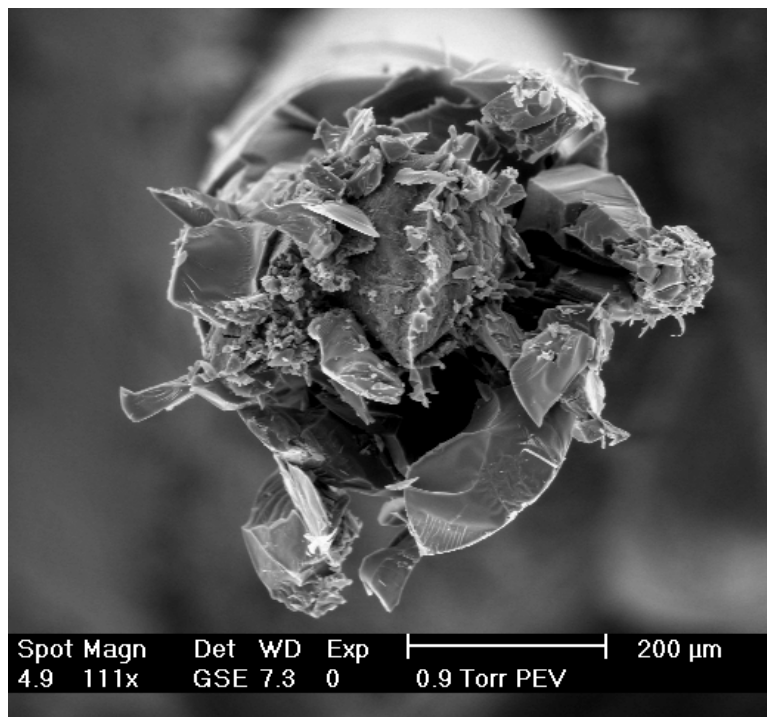


Figure 8. SEM image of a preceramic silicone resin outer shell on a Filler #2 inner core (due to the different mechanical properties between the two materials, cutting the co-extruded composite microtube led to brittle crushing of the outer silicone layer).

The following images (Figures 9-12), obtained with an optical stereo-microscope, were taken on samples before cross-linking and show again that successful co-extrusion of the silicone resin with Filler #2 was obtained, with continuous shell/core structures in which the thickness of the core is rather homogeneous as well as its placement within the preceramic polymer, and no significant cracks in the outer shell can be observed.

However, these images highlight also a potential problem of this approach. In fact, in some pictures one can observe the presence of few bubbles (indicated by the arrows) within the preceramic polymer outer shell. At this stage of the investigation, we believe that this feature is probably due to the fact that when the microtube is formed, Filler #2 is at a higher temperature than the preceramic polymer and when it gets into contact with the silicone resin it provokes its (partial) condensation via the condensation of Si-OH groups (see later), which in turn form bubbles (probably constituted of water vapor). In fact, if one puts the silicone resin into an oven at, say, 150°C for some time, it first melts and then hardens into a transparent solid containing several bubbles. Moreover, these defects were not observed in the samples produced using filler #3 (although more samples need to be investigated). Anyway, in the cross-sections reported in Figures 6-8 and 13-14 these defects are not observable indicating that their presence is not highly recurrent within the microtubes.

It has to be noted that, being the bubbles inside the preceramic polymer and not at its surface, any adverse effect on mechanical properties is probably limited (that is, they do not create a surface flaw that would drastically decrease the strength of the brittle ceramic material). Thus, we do not believe this problem is caused by a not optimal mixing of the fluxes within the extruder's head, even if we will consider this possibility in more detail in the next few months of experimentation. We have, however, a few options available for working around this problem one of which is, obviously, using a silicone resin that crosslinks via another mechanism (for instance via vinyl groups).

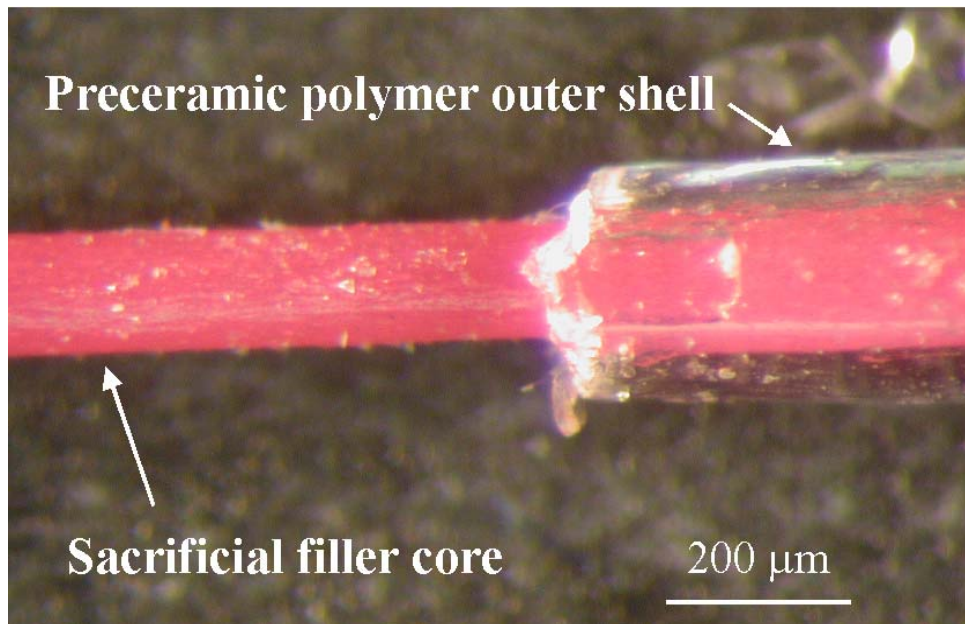


Figure 9. Optical stereomicroscope image of a preceramic silicone resin outer shell on a Filler #2 inner core.

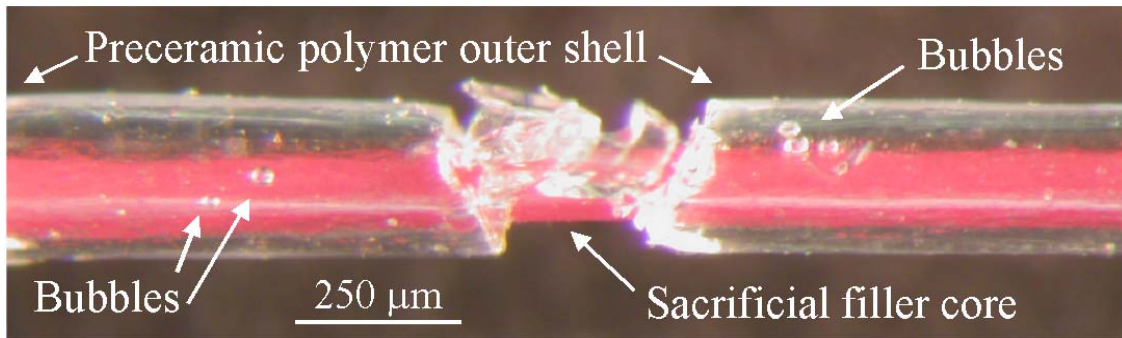


Figure 10. Optical stereomicroscope image of a preceramic silicone resin outer shell on a Filler #2 inner core.

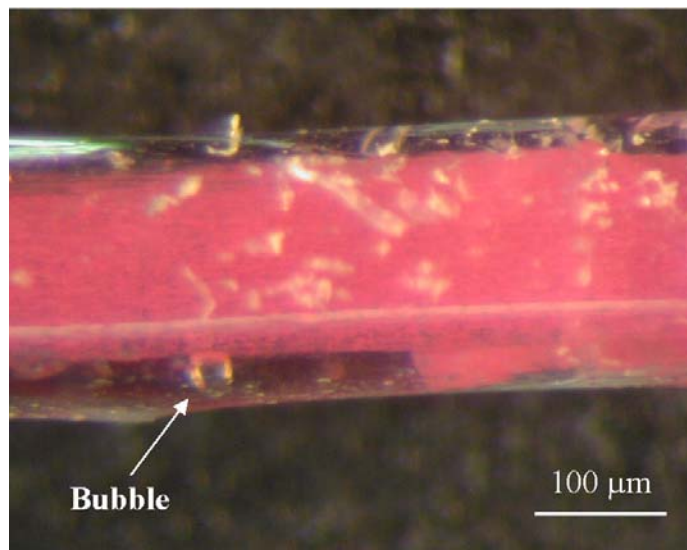


Figure 11. Optical stereomicroscope image of a preceramic silicone resin outer shell on a Filler #2 inner core.

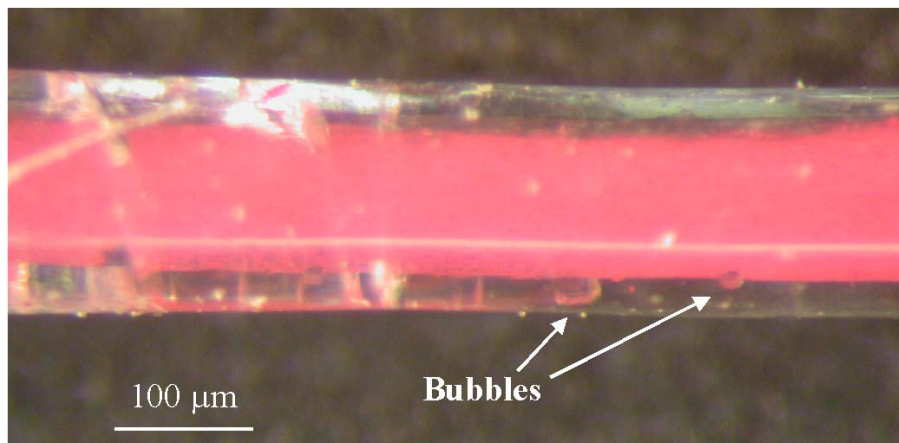


Figure 12. Optical stereomicroscope image of a preceramic silicone resin outer shell on a Filler #2 inner core.

It has to be remembered that at room temperature the silicone resin is below its glass transition temperature, thus displaying brittle fracture. Because of the compatible and suitable mechanical properties of the silicone resin and the Filler #2, it was also possible to manually extract the inner core before pyrolysis (but after cross-linking), at least for samples of a limited length, and thus observe both the outer and inner surfaces (see Figure 13 and 14).

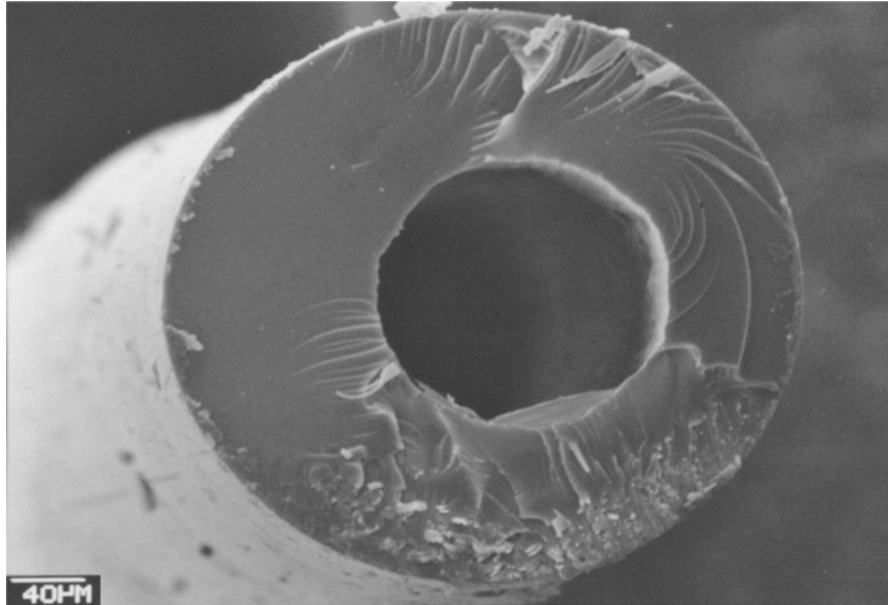


Figure 13. SEM image of a preceramic silicone microtube after manual extraction of the inner Filler #2 core (before pyrolysis).

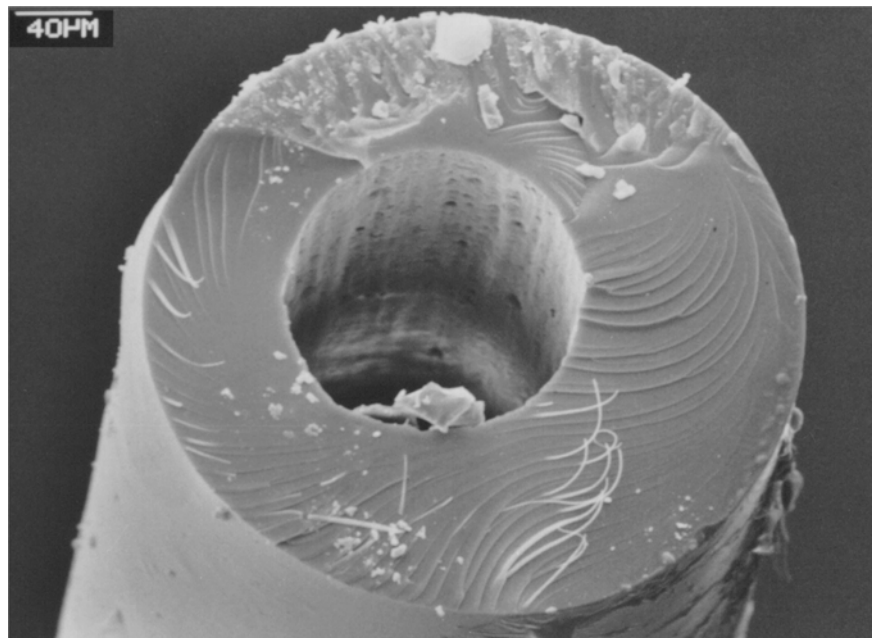


Figure 14. SEM image of a preceramic silicone microtube after manual extraction of the inner Filler #2 core (before pyrolysis).

As shown in Figures 15 and 16, there seems to be a difference in roughness between the outer surface and the inner surface (the inner surface is rougher), but the reason for this needs to be investigated in more details.

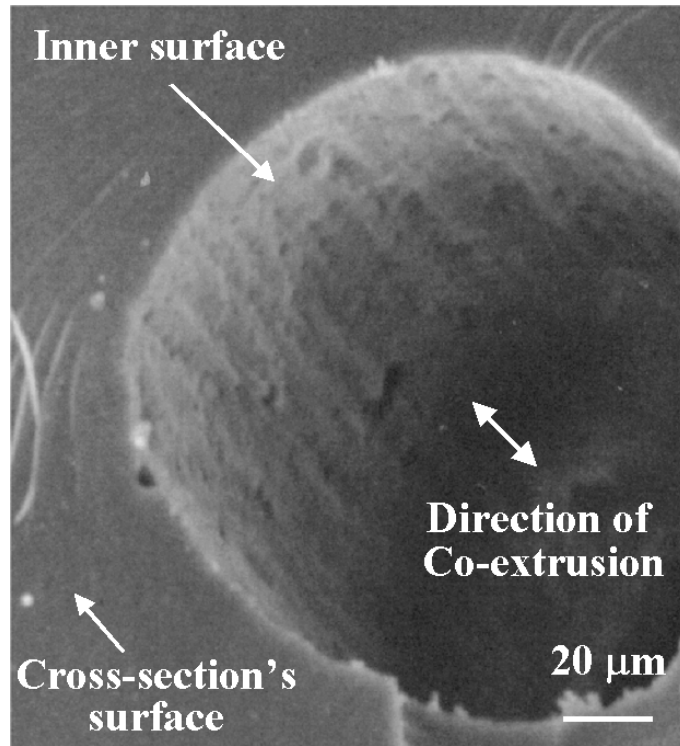


Figure 15. SEM image of the inner surface a preceramic silicone microtube after manual extraction of the inner Filler #2 core (before pyrolysis).

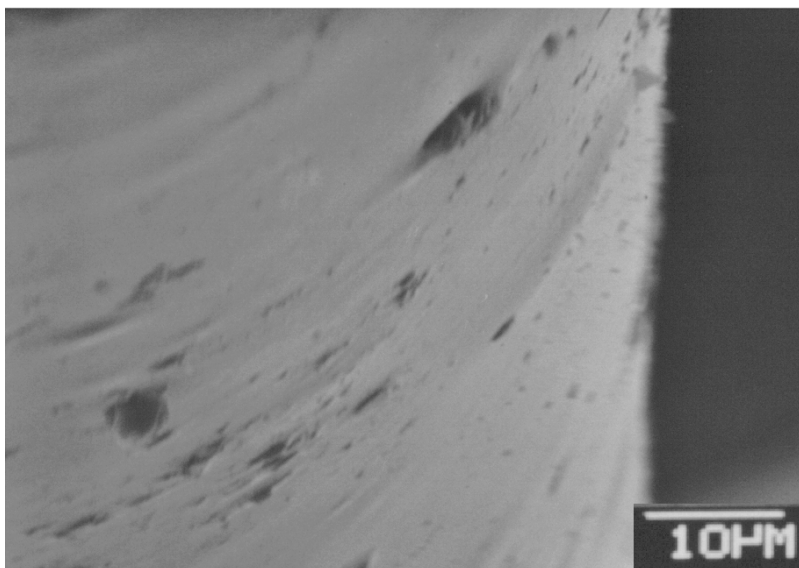


Figure 16. SEM image of the outer surface a preceramic silicone microtube after manual extraction of the inner Filler #2 core (before pyrolysis).

It has to be noted that the outer surface of the Filler #2 inner rod seems to have a rougher surface than the outer surface of the silicone outer shell (see especially Figure 6 and 9), suggesting that the difference could be attributed to the different nature of the materials comprising the co-extruded structure.

In this set of experiments, the size of the preceramic silicone microtube had an OD ranging from ~180 to 340  $\mu\text{m}$ , with an ID ranging from ~80 to 140  $\mu\text{m}$  (the data are referred to samples before pyrolysis; after pyrolysis a linear shrinkage of about 25% is expected). This was achieved by varying the speed at which the co-extruded microtube was drawn from the machine (typical speed ranged from 2 to 15 rpm). There seems to be some problems with the centering of the inner rod within the silicone shell (leading eventually to non a homogeneous thickness of the ceramic microtube's wall), but this can be attributable to the limited amount of material processed and there does not seem to be any intrinsic reason why some improvements can't be achieved continuing the experimentations.

The possibility to extract the inner core is certainly due to the fact that the adhesion between the silicone and the Filler #2 was very limited (see the presence of a small gap between the inner and outer core – see arrow in Figure 6 - probably due to different thermal contraction of the two materials upon cooling) and there was no unwanted mixing between the two materials during the processing of the co-extruded microtubes. Thus, Filler #2 is a very good candidate as sacrificial polymer for the production of microtubes by co-extrusion. This has however to be confirmed after the pyrolysis of the structures. Preliminary, limited experiments indicate that this is the case in that crack-free, ceramic microtubes can actually be produced by heating at 1200°C these co-extruded samples.

In a third set of experiments, Filler #3 was used to fabricate the inner core, and the extrusion was carried out by processing the silicone resin at a temperature of about 90-110°C, while Filler #3 reached temperatures in the range of 100 to 130°C. Also in this case, the thermal compatibility between the silicone resin and the Filler #3 was good, and it was possible to manufacture shell-core structures (see Figures 17-18, again relative to non-pyrolyzed specimens before cross-linking). Due to the elastomeric nature of the Filler #3 at room temperature it was not easy to cleanly cut the microtube for observing the inner core (as done with the Filler #2 samples) without destroying the silicone resin in a way that prevented a clear observation of the structure (Figure 18, for example, is an attempt at a longitudinal cross-section). More investigations will have to be performed and efforts made in order to suitably prepare these samples for SEM observations. Also, at this stage of the investigation, we cannot exclude that a possible higher adhesion between the silicone resin and the Filler #3 exists, which nevertheless should not be a problem for the subsequent pyrolysis treatment. Pyrolysis of these specimens is currently undergoing, and only after this step we'll be able to assess the full compatibility of the two materials (Filler #3 and the silicone resin), and in particular we should be able to understand if some unwanted mixing of the two materials occurred during processing, leading to the loss of the desired morphology (lack of a well defined axial hole within the ceramic microtube).

However, we should note that when processing microtubes by co-extrusion using Filler #3 and a silicone resin a problem was observed. As it can be seen in Figures 19 and 20, some cracks appear to be present in some specimens running perpendicularly to the drawing direction (the main axis).

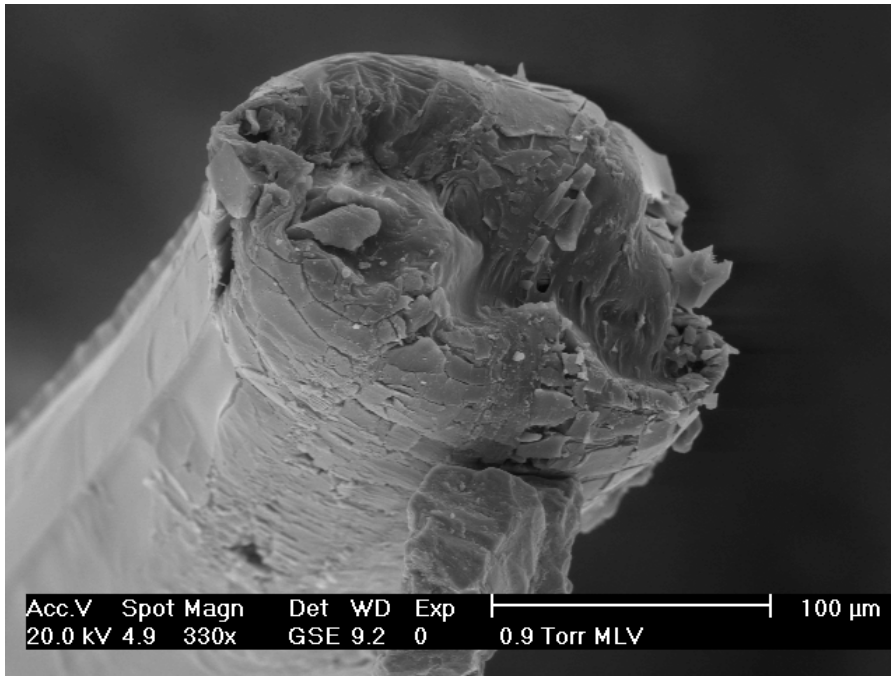


Figure 17. SEM image of a preceramic silicone microtube co-extruded with Filler #3 (before pyrolysis).

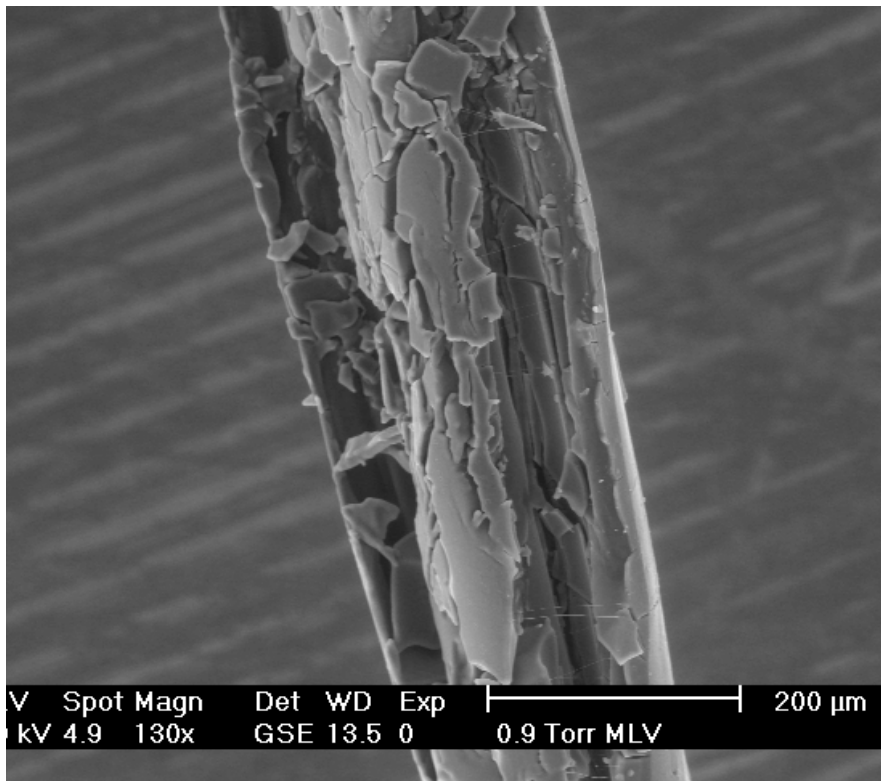


Figure 18. SEM image of the axial cross-section of a preceramic silicone microtube co-extruded with Filler #3 (before pyrolysis).

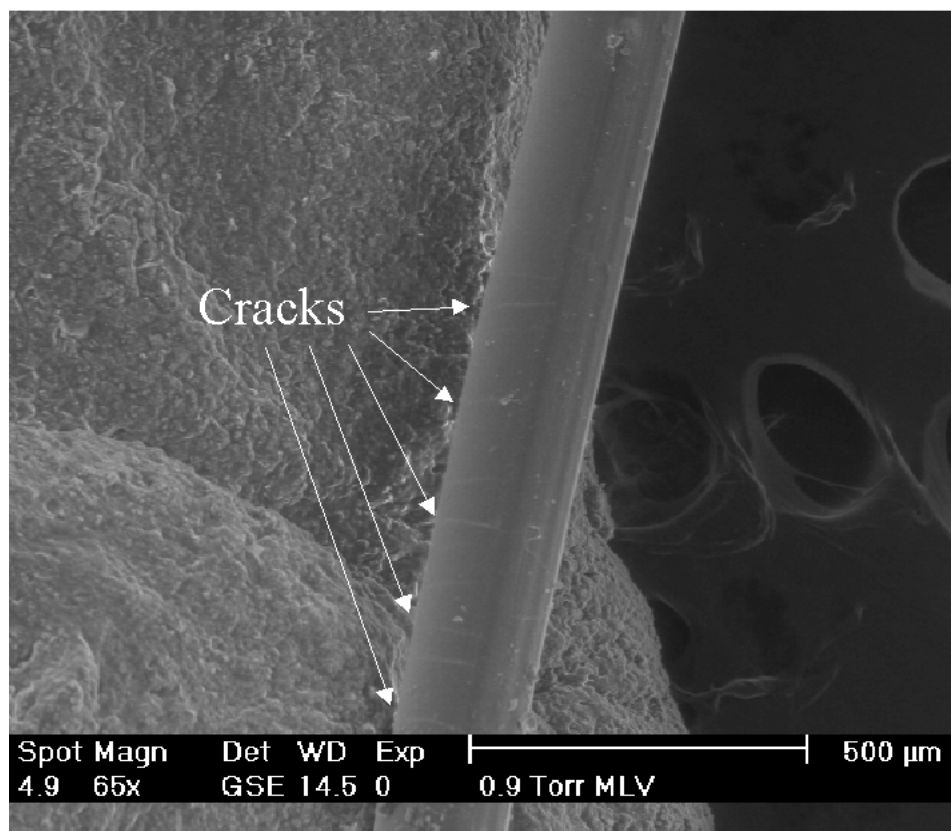


Figure 19. SEM image of a preceramic silicone microtube co-extruded with Filler #3 (before pyrolysis). The presence of tangential cracks is highlighted.

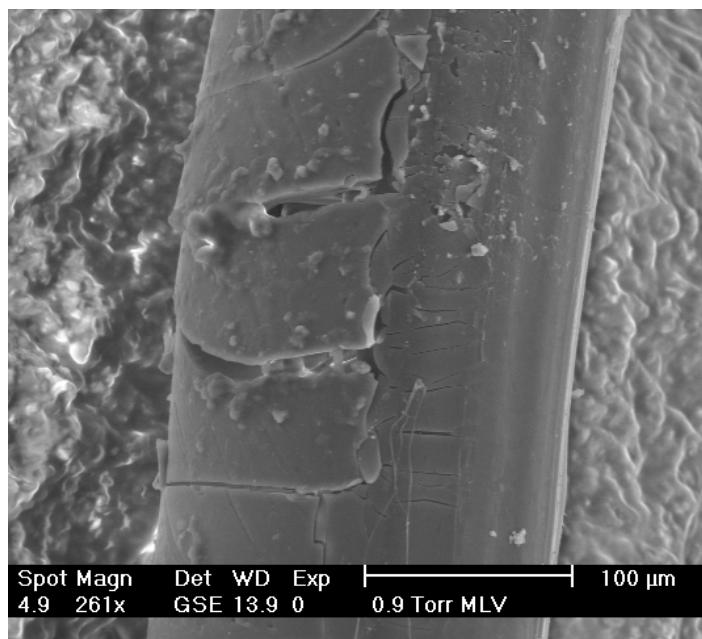


Figure 20. SEM image of a preceramic silicone microtube co-extruded with Filler #3 (before pyrolysis). Detail showing tangential cracks.

At this stage of the investigation, it is believed that the reason for this cracking is related to the large difference in mechanical properties between Filler #3 and the silicone resin (filler #3 was chosen for its thermal compatibility with the preceramic polymer). During drawing, the elastomeric Filler #3 is capable of more stretching than the silicone resin, possibly resulting in tangential cracking. However, this phenomenon was not observed in all specimens (see Figure 21), and this seems to suggest that it can be solved by varying the drawing parameters or the handling procedure.

The OD size for the co-extruded microtubes was in the 180-300  $\mu\text{m}$  range.

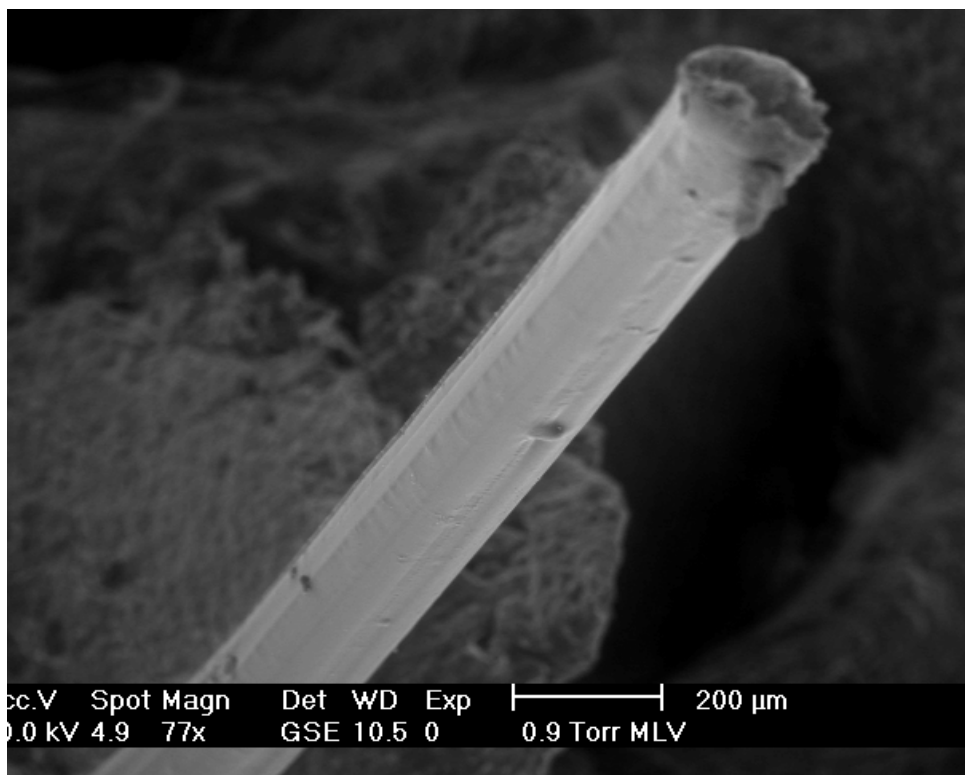


Figure 21. SEM image of a preceramic silicone microtube co-extruded with Filler #3 (before pyrolysis). No tangential cracks are visible.

### 1.3. Cross-linking of the preceramic polymer

In order to maintain its shape during pyrolysis, the preceramic polymer needs to be cross-linked. This is one of the main reasons (together with commercial availability, low cost, ability to be processed in air at elevated temperature -  $< 250^{\circ}\text{C}$  -) that led us to the use of thermosetting silicone resins.

The silicone resin chosen can crosslink via the condensation of Si-OH groups (which are contained in the amount of about 5%), and the achievement of the cross-linking can be monitored for instance by FTIR. In Figure 22 are reported the FTIR spectra for the as received preceramic polymer and after cross-linking (crushed microtubes, after elimination of the Filler #2 core), showing the elimination of the Si-OH band at about  $900\text{ cm}^{-1}$ , which is present in the fresh silicone resin. As a general comment, it has also to be observed that this class of silicone

resins can undergo spontaneous condensation of the Si-OH groups with the proceeding of time (shelf life, at room temperature is of the order of 6 months to a year), and thus the rheological characteristics of the preceramic polymer may vary depending on its age.

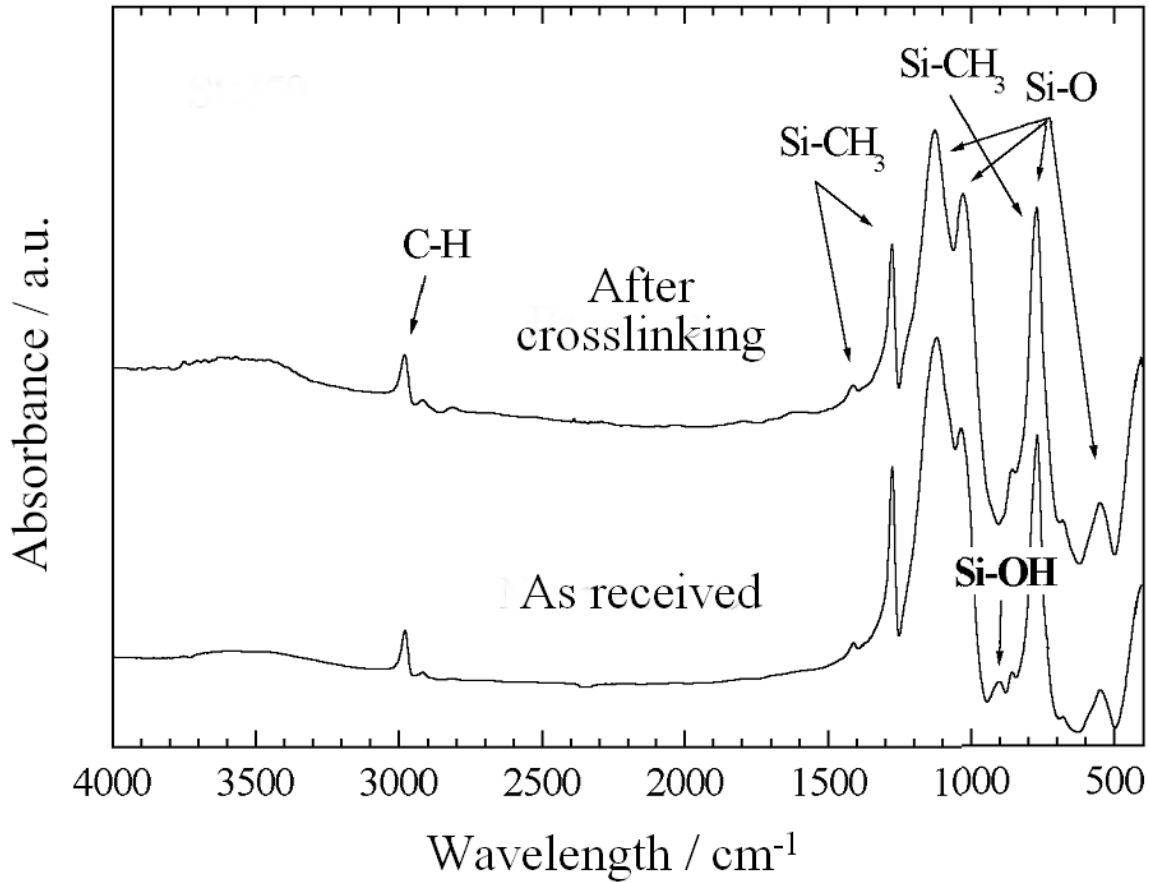


Figure 22. FTIR spectra of a silicone resin microtube before and after cross-linking. Note the disappearing of the Si-OH band.

For the silicone resin used in these experiments, after cross-linking a variation in color and transparency can be observed by the naked eye, as the microtubes goes from transparent to “whitish”/opaque (see Figure 23). No images taken with the stereo-optical microscope are here reported as under that instrument no significant difference can be observed between a cross-linked and a non-cross-linked microtube (probably due to the way the samples are lighted).

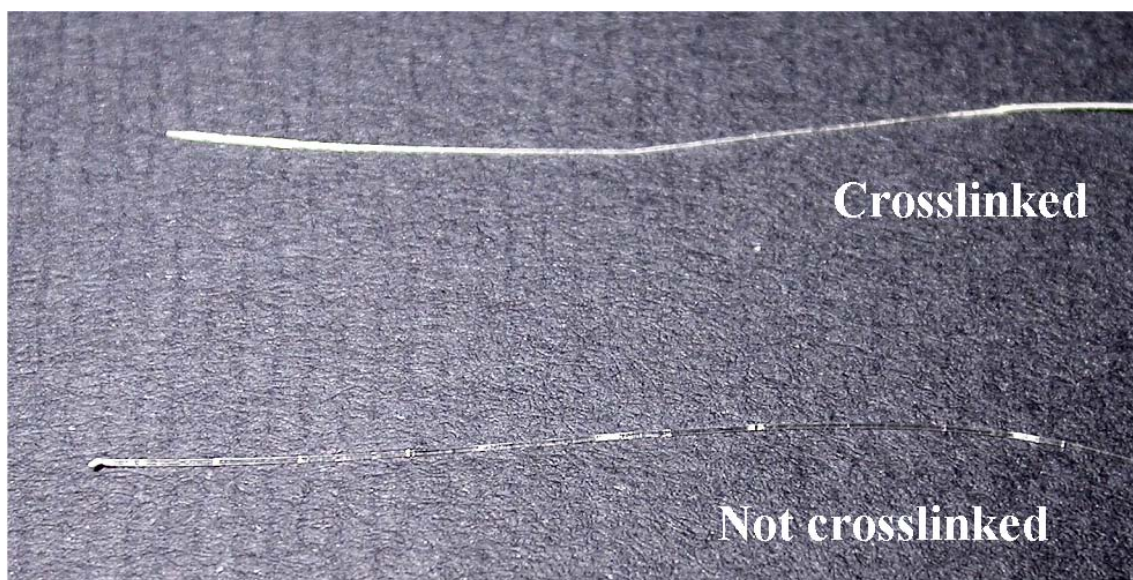


Figure 23. Image showing the difference between not-cross-linked and cross-linked microtubes (Filler #3).

Another way of assessing if cross-linking occurred is to pyrolyze the material in inert atmosphere; depending on the degree of cross-linking either melting of the microtube with loss of its shape can happen, or surface cracks or deformation (bulging) can appear, or the resulting ceramic microtube can have a homogeneous morphology.

### 2.1. Further experimentation (with filler #3 and filler #4)

Filler #3 was used again to try to produce single-lumen microtubes by co-extrusion (with silicone resin SOC-A35) varying several extrusion parameters (temperature, speed, direction of drawing). However, no better success than in the first set of experiments was achieved, and the microtubes obtained all contained transversal cracks in the polymeric stage, such as those depicted in Figures 19-20. However, we will use again filler #3 to try to produce multi-lumen microtubes by co-extrusion, as the smaller size of the extruded filler filament in that case might allow the production of un-cracked components.

Another filler (filler #4), possessing rheological and decomposition characteristics different from the ones relative to the other fillers, was also tested. However, as it happened with filler #1, also in this case it was not possible to fabricate microtubes with a good morphology by co-extrusion with silicone resin SOC-A35. At this stage of the investigation, we believe that the reason for the macroscopic distortion in shape that the the microtubes possessed after co-extrusion is possibly twofold. First of all, the rheological characteristics of the filler, being quite different from those of the silicone resin, might not be adequate for a co-extrusion process (for instance transferring shear stress to the preceramic polymer layer in an unfavorable way); secondly, as silicone resin and filler have a different coefficient of thermal expansion, if the axial filament is not well aligned, this could result in differential contraction upon cooling, leading to grossly deformed microtubes. Further experimentation is necessary to fully assess the possibility of using Filler #4 as a sacrificial filler material for co-extrusion with silicone resins. For the rest

of this research period we concentrated on the pyrolysis and characterization of the microtubes that were previously successfully co-extruded.

## **2.2. Co-extrusion experiments using a different preceramic polymer**

A different preceramic polymer, a methyl-phenyl silicone resin (H44, Wacker Chemie), was also used for manufacturing single-lumen microtubes by co-extrusion with filler #2. Some difference in the rheological behavior was observed with respect to the methyl silicone resin SOC-A35, and was attributed to a higher degree of cross-linking/molecular weight of the as-received H44 silicone resin. Nevertheless, it was possible to produce good quality microtubes (at least in the polymeric stage) using also this preceramic polymer. There does seem to be a lower amount of trapped bubbles in the material, probably due to a more limited release of condensation water during processing, due to the different molecular structure of the starting preceramic polymer. In the next period these microtubes will be cross-linked and pyrolyzed, and if the results are satisfying then this preceramic polymer will also be used for the production of multi-lumen microtubes.

## **2.3. Ceramization of the single-lumen, co-extruded microtubes**

### **2.3.1. TGA analysis**

In order to follow the pyrolysis process of co-extruded single-lumen microtubes, simultaneous Thermal Gravimetric and Differential Thermal Analysis (TGA/DTA) was performed on both the microtubes and the filler materials. The analysis were performed at a constant heating rate (2°C/min) under a nitrogen gas flux on tubes cut into short pieces or on cross-linked preceramic polymer powders. The data collected allowed to assess both the thermal range of decomposition of the sacrificial fillers and the amount of char (not volatilized residue, composed mainly of carbon) that might have remained deposited in the inside of the ceramic microtubes. The results are reported in Figure 24.

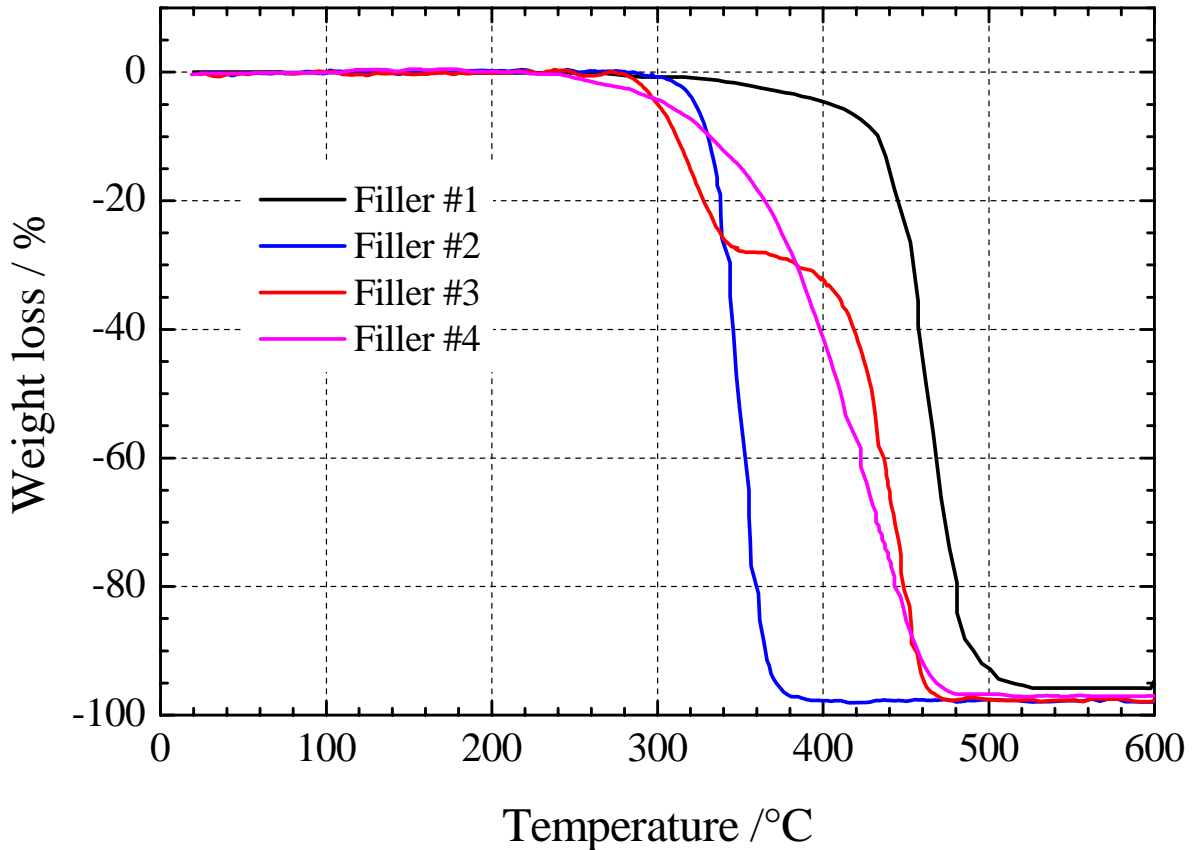


Figure 24. TGA curves for the various fillers

It is useful, at least from a theoretical point of view, to have a filler that decomposes in a range of temperatures compatible with the polymer to ceramic conversion of the preceramic polymer, as during this stage the filler will release gas that needs to escape from the component. In fact, there is a transient open porosity (up to ~20 vol%) that develops in the preceramic polymer material at this stage, that is eliminated by densification as higher temperatures (>800°C) are reached. Also, the preceramic polymer shrinks quite considerably (~60 vol%; ~25 linear %) during the ceramization process, and the presence of a filler material would interfere with this volumetric change leading probably to the development of cracks. As it can be seen, all the tested fillers had a favorable behavior, in that they decomposed at suitably low temperatures leaving behind with a minimal char (less than 4 wt%). Filler #1 started decomposing at ~300°C and completed its decomposition at ~380°C, with a char yield of ~2.3 wt%; Filler #2 started decomposing at ~330°C and completed its decomposition at ~520°C, with a char yield of ~4.5 wt%; Filler #3 started decomposing at ~280°C and completed its decomposition at ~470°C, with a char yield of ~2.5 wt%; Filler #4 started decomposing at ~250°C and completed its decomposition at ~480°C, with a char yield of ~3.3 wt%

The TGA data for the preceramic polymers used (SOC-A35 and H44) is as well of great importance, and was obtained under the same conditions on powders that were cross-linked following the procedure adopted for the microtubes. The results are reported in Figure 25.

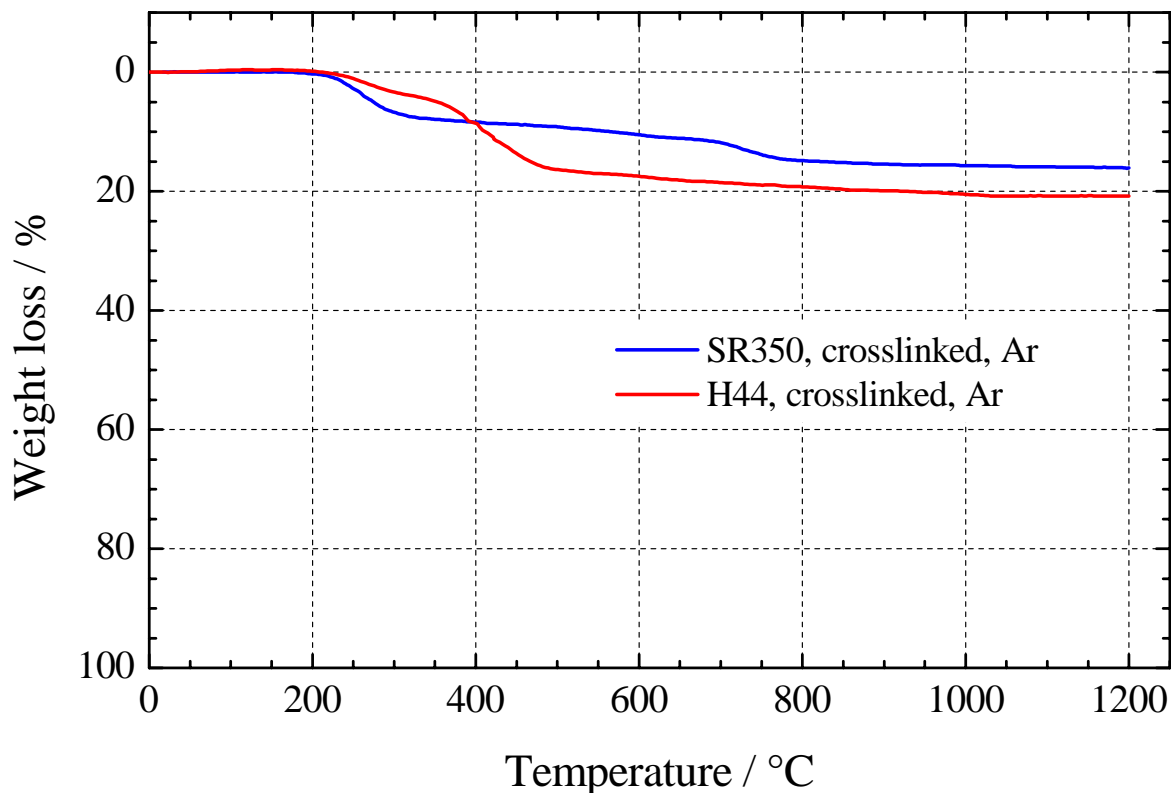


Figure 25. TGA curves for the various preceramic polymers

It can be seen that there are two regions in which there is weight loss for both preceramic polymers; one in the temperature range  $\sim 200\text{-}500^\circ\text{C}$ ; the other one in the temperature range  $\sim 600\text{-}800^\circ\text{C}$ . The first one is related to the elimination of low molecular weight species such as silanes, toluene, isopropyl alcohol and condensation water (for the H44 polymer, further condensation with loss of water goes on around  $400^\circ\text{C}$ ). The second weight loss (more evident for the SOC-A35 silicone resin than for the H44 one) is related to the polymer-to-ceramic conversion, leading in both cases to the formation of an amorphous silicon oxycarbide material [1]. The weight loss in the second temperature range is mainly due to the decomposition of organic moieties (methyl groups) with release of methane gas. The total weight loss (which depends on the degree of cross-linking) is  $\sim 16\%$  for the SOC-A35 silicone resin and  $\sim 20\%$  for the H44 silicone resin (that is the ceramic yield is  $\sim 84\%$  and  $\sim 80\%$  respectively), confirming the suitability of these silicone resins as high yield precursors for ceramic components.

The TGA analysis was performed also on a cross-linked microtube, co-extruded using SOC-A35 silicone resin and filler #2. The data are reported in Figure 26, together with the curve relative to the filler itself. It can be seen that the presence of the silicone resin does not change the decomposition behavior of the filler, nor the presence of the filler affects the decomposition behavior of the silicone resin, as hoped. The slight difference in the TGA curve of the silicone resin microtube in comparison to the one relative to cross-linked silicone resin powders (see Figure 25) can be attributed to the fact that the selected cross-linking procedure is well suited for thin layers of the silicone resin (i.e. cross-linking can occur in the whole mass of specimens of

this shape), while it is less effective for coarse powders. Thus, the core of the powders is not fully cross-linked hence there is an additional weight loss at low temperatures (in the range 200-400°C) that is not seen in the curve reported in Figure 26.

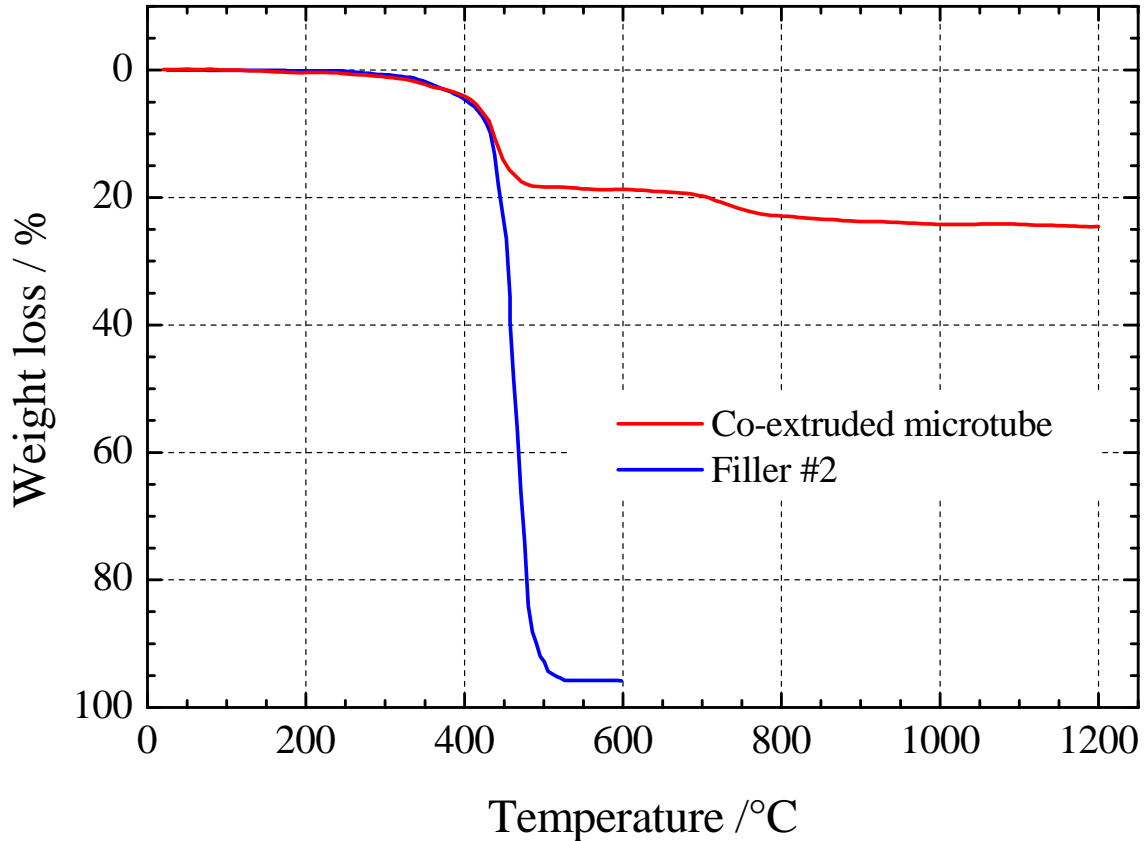


Figure 26. TGA curves for a co-extruded microtube and the filler used (#2)

It has to be noticed that the choice of using inert atmosphere for decomposing the sacrificial fillers is not required, unless the treatment is performed at temperatures higher than  $\sim 350^{\circ}\text{C}$  or preceramic polymers not containing oxygen in their backbone are used (such as polycarbosilanes or polysilazanes). What is necessary is maintaining some Si-R (where R can be  $-\text{CH}_3$ ,  $-\text{C}_2\text{H}_5$ ) moieties in the preceramic polymer, in order to produce a SiOC ceramic material (or a SiC or a SiNC if a ceramic material capable of reaching higher temperatures is needed) upon pyrolysis. In fact, it has been reported in the scientific literature, that silicon oxycarbide ( $\text{SiO}_x\text{C}_y$ ) glasses are amorphous materials in which the substitution of carbon for oxygen within the Si-O matrix greatly strengthens the molecular structure of the resulting glass network.  $\text{SiO}_x\text{C}_y$  glasses have tailorable physical properties that strongly depend on the microstructure (presence of phase separation and bonding state of carbon) and composition (carbon content), exhibiting remarkable mechanical properties (elastic modulus, bending strength, hardness), chemical durability (much superior to conventional silicate glasses in aggressive environments) and refractoriness (resistance to oxidation at high temperature, resistance to devitrification, creep resistance). These unique properties strongly correlate with the increase in the average coordination number in the

glass network [2-7]. The composition (C content) can be varied for instance changing the organic moieties attached to the Si-O backbone in silicone resins.

Experiments performed for a different project [8] demonstrated that SOC-A35 is capable to retain organic functionalities in its backbone after processing at  $\sim 350^{\circ}\text{C}$  in air, so this environment could be used as well for the decomposition of the fillers used to produce co-extruded microtubes. No particular difference in the residual content of decomposed fillers should be expected if air was used to burn them off instead of volatilizing them by thermal decomposition. However, using inert atmosphere is a convenient choice as it allows for a single heating step to be performed, which encompasses both the decomposition of the filler and the ceramization of the preceramic polymer.

### **2.3.2. Pyrolysis of the microtubes**

The samples, obtained using SOC-A35 and Filler #2, were pyrolyzed in a tube furnace, after cutting them into pieces approximately 5 cm long, by putting them in alumina boats. The limitation in size is related to the length of the region with uniform temperature in the furnace used. Based on the thermogravimetric analysis and on previous experiences, the pyrolysis schedule adopted was heating in inert atmosphere (nitrogen or argon gas) at the constant rate of  $2^{\circ}\text{C}/\text{min}$  up to a temperature of  $1200^{\circ}\text{C}$  (with a 1h dwelling time at final temperature). Some samples were also pyrolyzed at  $800$  or  $1000^{\circ}\text{C}$ , and they were found to be completely ceramized as well (only some difference in the relative density was observed – see later).

Alternatively, for instance when dealing with longer or thicker components (in which the amount of filler is higher) one could adopt a heating schedule which contemplates a dwelling step at a temperature within the range at which the filler decomposes, to allow for gas release. Another possibility is to reduce the heating rate in the same temperature range. For the samples we produced, it was not necessary to adopt these, longer, heating schedules.

After ceramization, the quality of the single-lumen microtubes fabricated by co-extrusion depended on various parameters, among which are (in terms of importance):

- a) the degree of cross-linking achieved before pyrolysis
- b) the quality of the produced microtube in the polymeric stage (e.g. presence of surface defects, presence of a permanent curvature/deviation from straightness)
- c) the layout of the samples in the refractory support boat.

In order to determine the best conditions for cross-linking, various combinations of temperature/time were used. When the cross-linking procedure was not optimized, defects in the microtube were generated. The following SEM images (Figures 27-30) report examples of what happened.

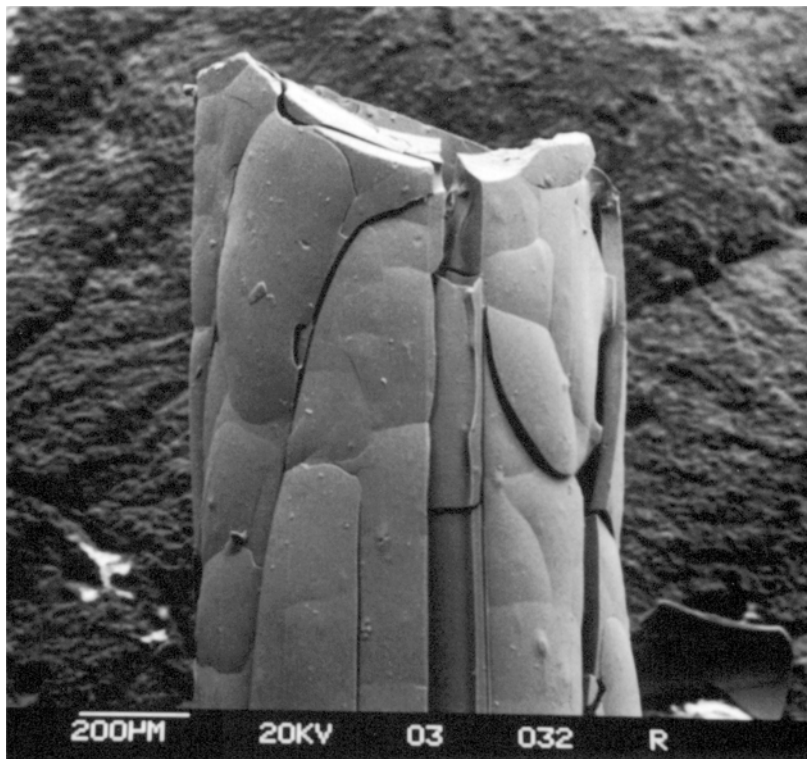


Figure 27. SEM image of a co-extruded microtube not well cross-linked, after pyrolysis (SOC-A35 and filler #2)



Figure 28. SEM image of a co-extruded microtube not well cross-linked, after pyrolysis (SOC-A35 and filler #2)

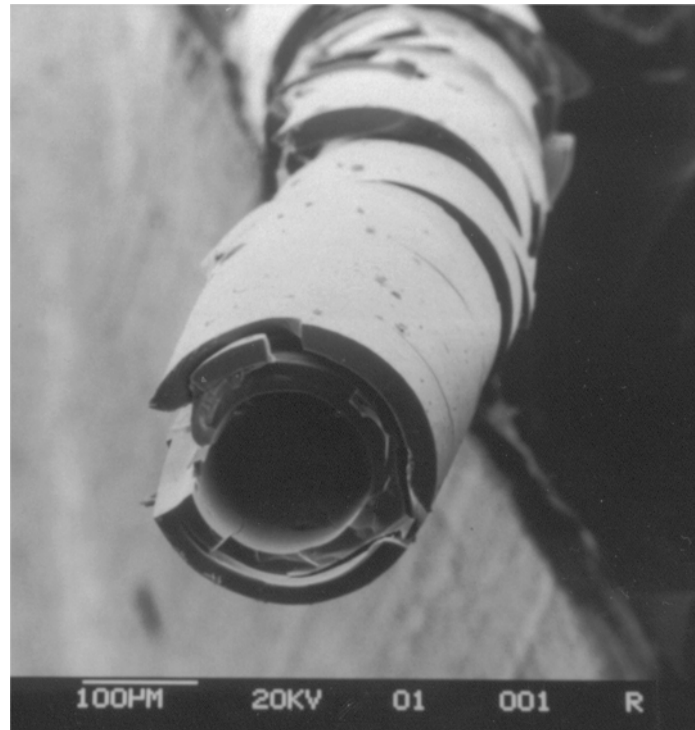


Figure 29. SEM image of a co-extruded microtube not well cross-linked, after pyrolysis (SOC-A35 and filler #2)

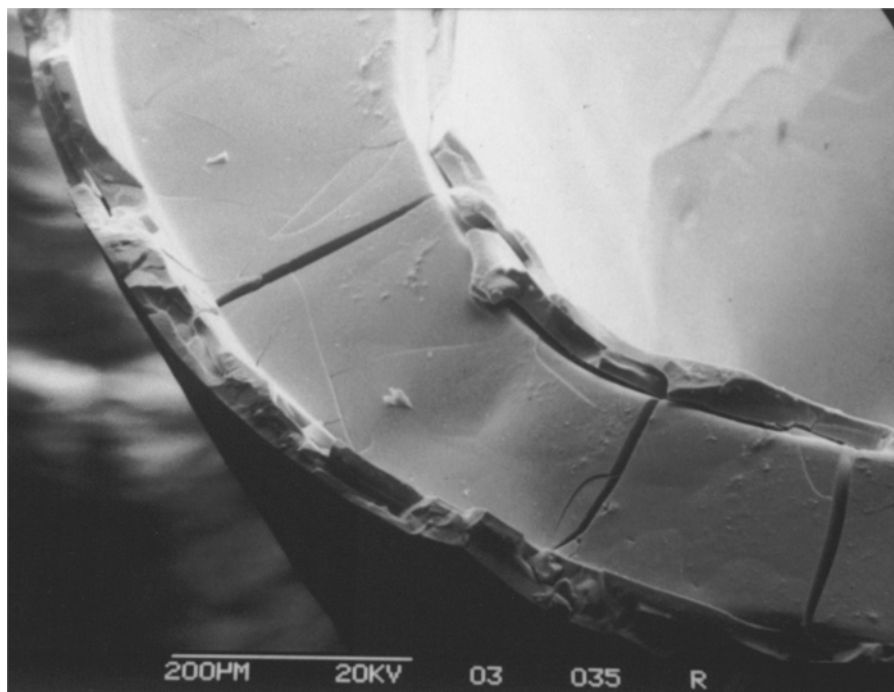


Figure 30. SEM image of a co-extruded microtube not well cross-linked, after pyrolysis (SOC-A35 and filler #2). This sample was cross-linked after manually extracting the filler fiber inside, hence the presence of a layer on both external and internal surface of the microtube.

As it can be seen, depending on the cross-linking conditions, some defects would be generated upon pyrolysis, including swelling (see Figure 27) and the presence of layers separated by cracks (see Figures 28 –30). Swelling is due to partial bloating/melting of the insufficiently cross-linked polymer upon pyrolysis, while the presence of layers is probably due to the fact that, if only the external surface of a preceramic polymer microtube is sufficiently cross-linked, one can expect a different behavior upon pyrolysis, leading to a differential shrinkage between external surface and the rest of the component. All these defects lead to cracks and unusable ceramic components.

It was found that, if the microtubes in the polymeric stage possessed already some curvature, this was enhanced by the pyrolysis process, sometime leading to heavily bent specimens. Moreover, it was noticed that sometimes specimens that were initially straight resulted deformed (with an unwanted curvature) after pyrolysis. This effect was attributed the fact that samples laid in the alumina refractory boats might experience a temperature gradient between the upper part (in contact with the flowing gas atmosphere) and the bottom part (in contact with the boat, possessing a certain thermal mass). Also, sometimes samples that were not well cross-linked stuck together when putting several of them inside the same alumina boat. To eliminate (or greatly reduce) this inconvenient, alumina powder was put in the alumina boats and the microtubes were laid on top of it, to favor a more uniform heating environment. Microtubes with suitable characteristics were thus produced (see later).

### 2.3.3. Morphological characterization of the pyrolyzed single-lumen microtubes

The pyrolyzed samples were characterized using digital photography, and optical or SEM microscopy. All the analysis reported here refer to samples obtained using SOC-A35 and Filler #2, pyrolyzed at 1200°C, as no morphological difference was observed among samples pyrolyzed at lower temperature (800 or 1000°C). In figures 31 and 32 are reported some images of pyrolyzed, single-lumen, co-extruded microtubes. Their black color is due to the fact that they're made of a silicon oxycarbide ceramic material (see later).

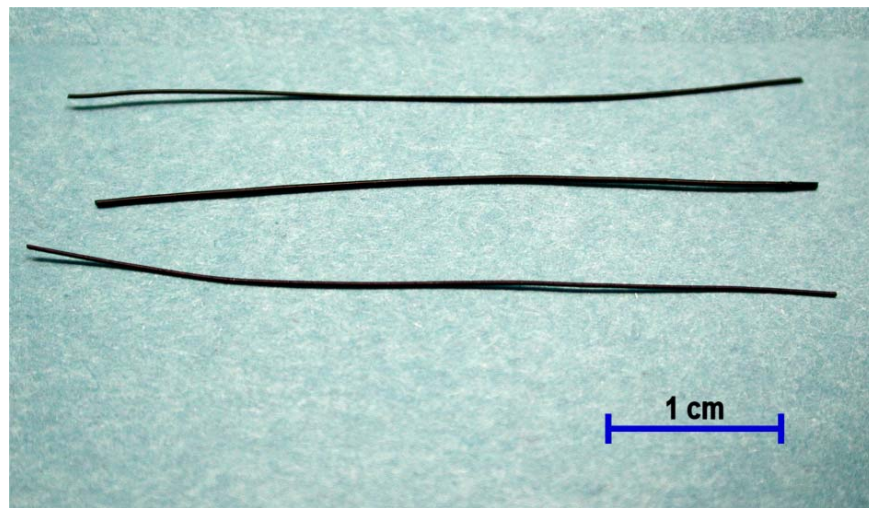


Figure 31. Digital picture of co-extruded single-lumen microtubes after pyrolysis (SOC-A35 and filler #2).

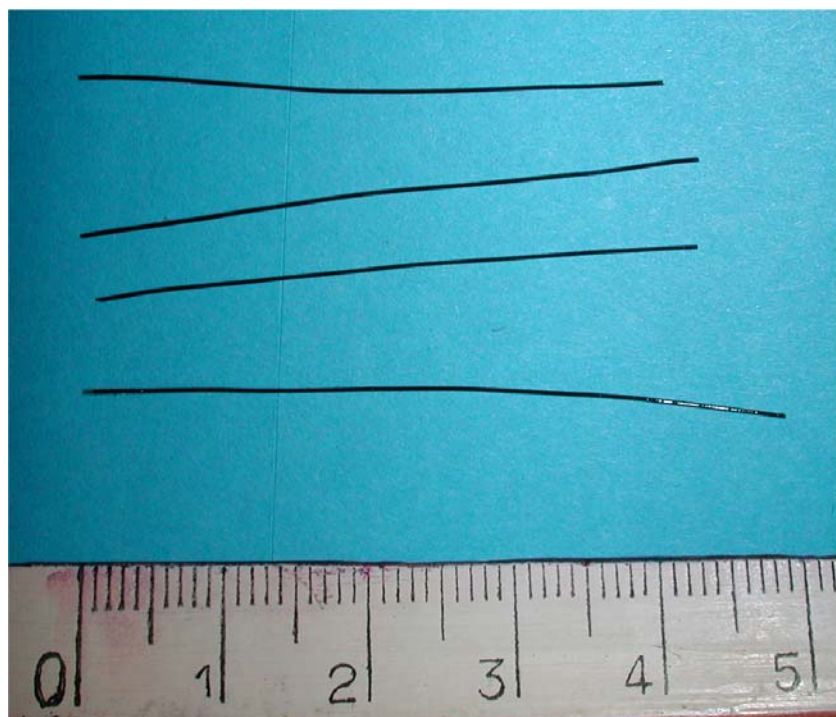


Figure 32. Digital picture of co-extruded single-lumen microtubes after pyrolysis (SOC-A35 and filler #2).

Optical (stereo)microscopy was used as a cheap and fast way of measuring the inner and outer diameter of the samples (see Figure 33), but because of its limited focusing depth it was not well suited for giving useful information concerning the general morphological characteristics of the microtubes.

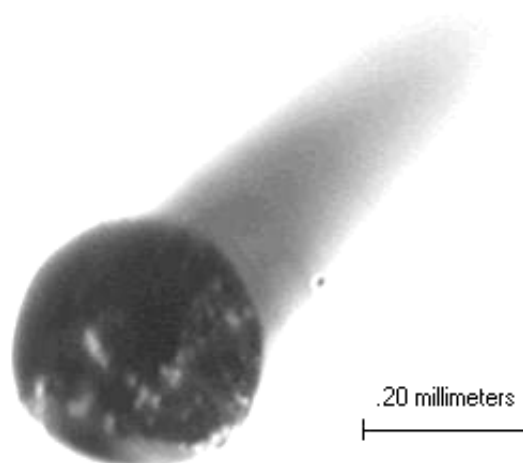


Figure 33. (Stereo-) optical microscopy image of a co-extruded single-lumen microtube after pyrolysis (SOC-A35 and filler #2).

In figures 34-43 are reported SEM images of co-extruded single-lumen microtubes after pyrolysis (produced using SOC-A35 and filler #2). All the images refer to fracture surfaces of samples freshly broken after pyrolysis. As reported earlier, it was not possible to produce samples using filler #1, and samples produced using other filler #2 did not survive the pyrolysis procedure without being always affected by numerous cracks (which were already present in the as-produced microtubes in the preceramic stage – see later). Attempts at producing microtubes using filler #4 were also unsuccessful (see later). These images are well representative of the kind of single-lumen specimens that was possible to produce using the co-extrusion of preceramic polymers.

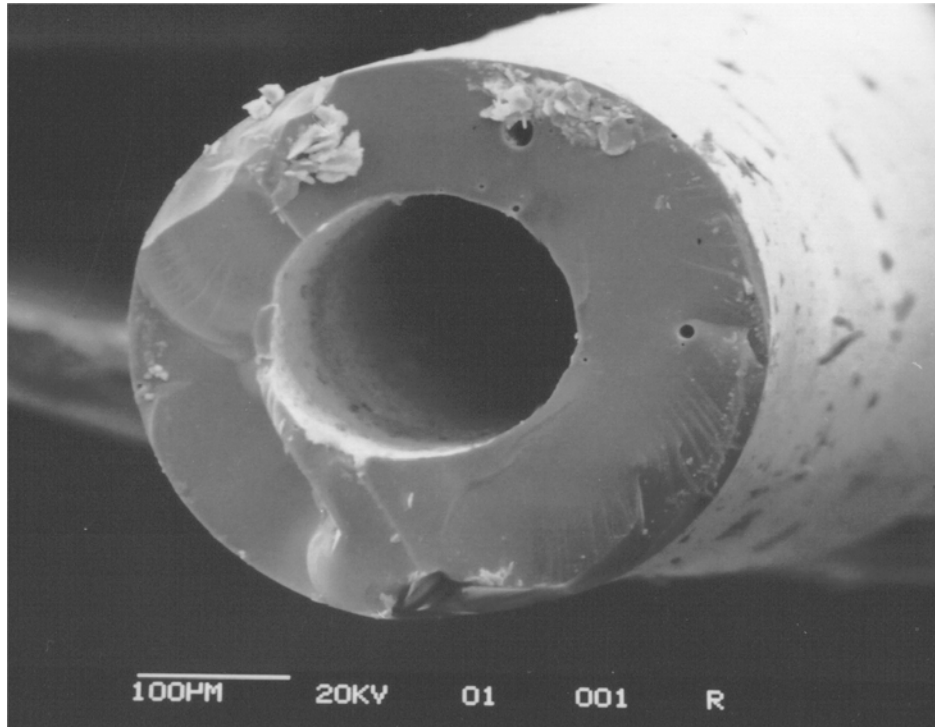


Figure 34. SEM image of a co-extruded single-lumen microtube after pyrolysis (SOC-A35 and filler #2).

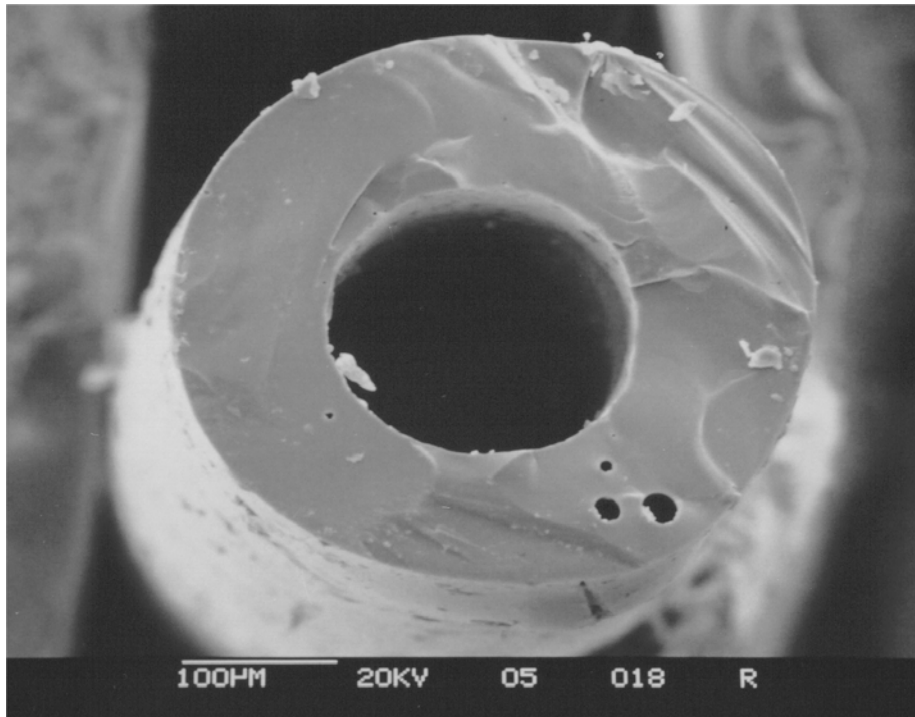


Figure 35. SEM image of a co-extruded single-lumen microtube after pyrolysis (SOC-A35 and filler #2).

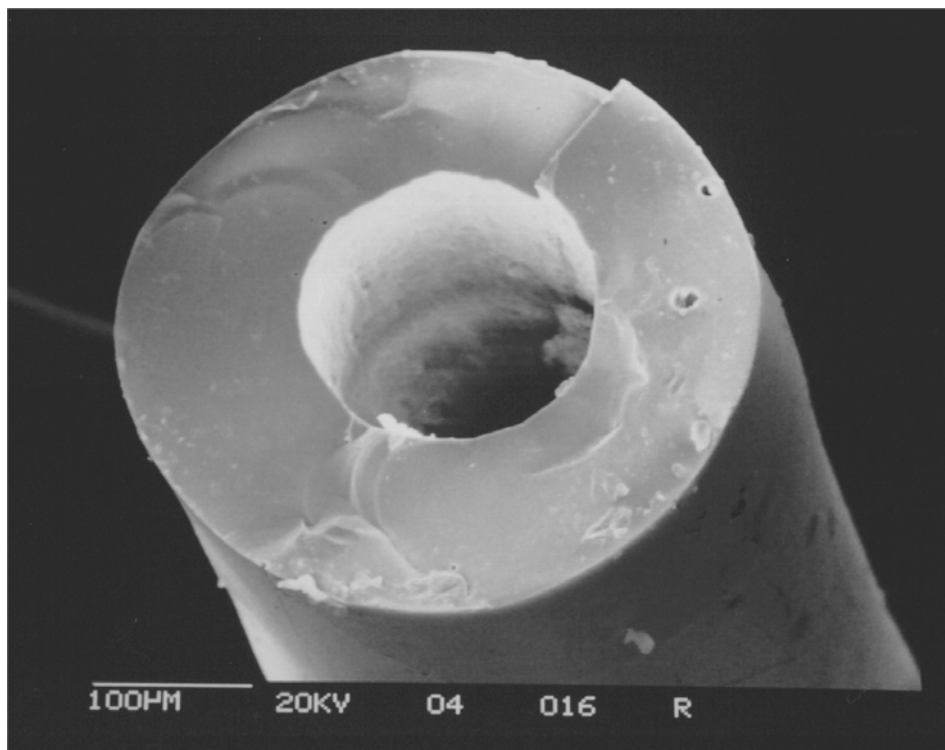


Figure 36. SEM image of a co-extruded single-lumen microtube after pyrolysis (SOC-A35 and filler #2).

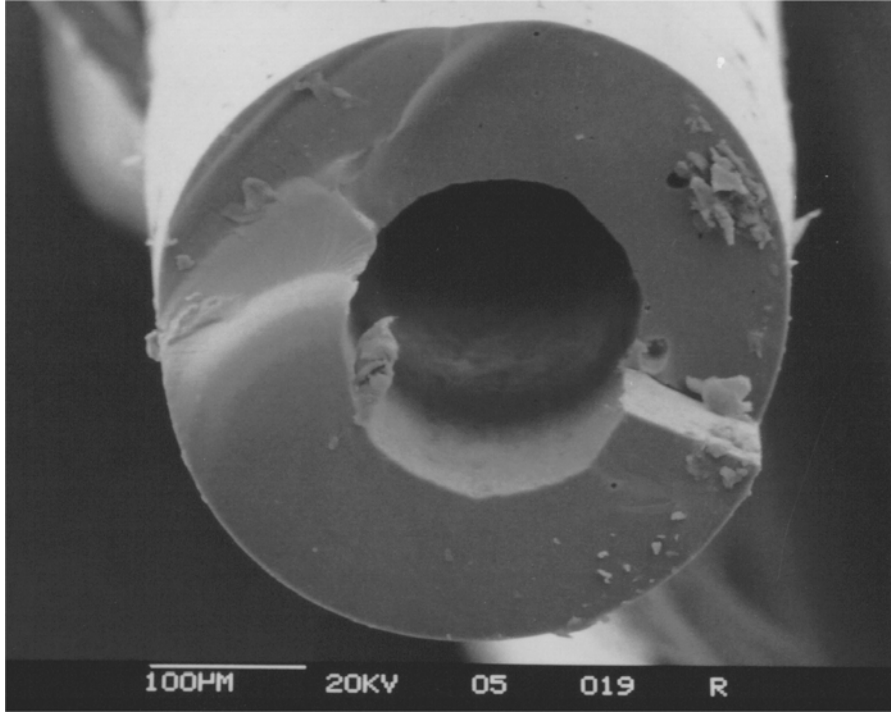


Figure 37. SEM image of a co-extruded single-lumen microtube after pyrolysis (SOC-A35 and filler #2).

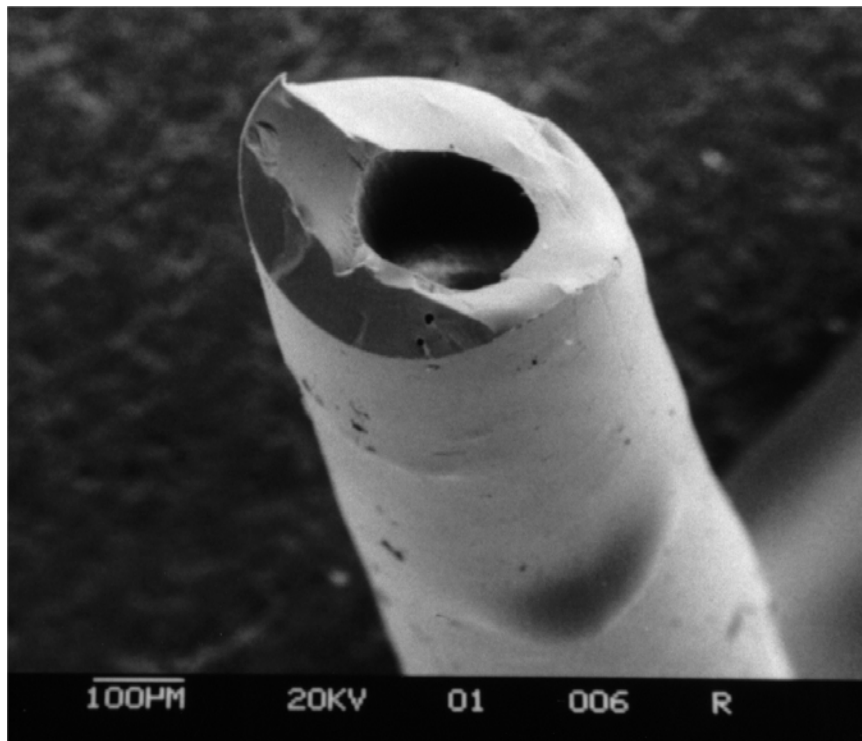


Figure 38. SEM image of a co-extruded single-lumen microtube after pyrolysis (SOC-A35 and filler #2).

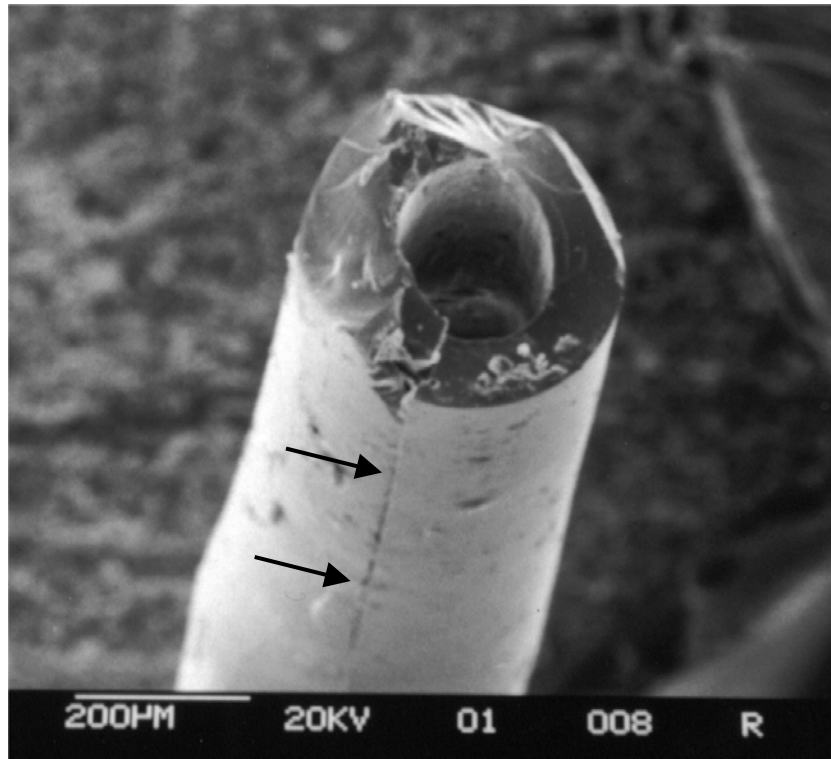


Figure 39. SEM image of a co-extruded single-lumen microtube after pyrolysis (SOC-A35 and filler #2).

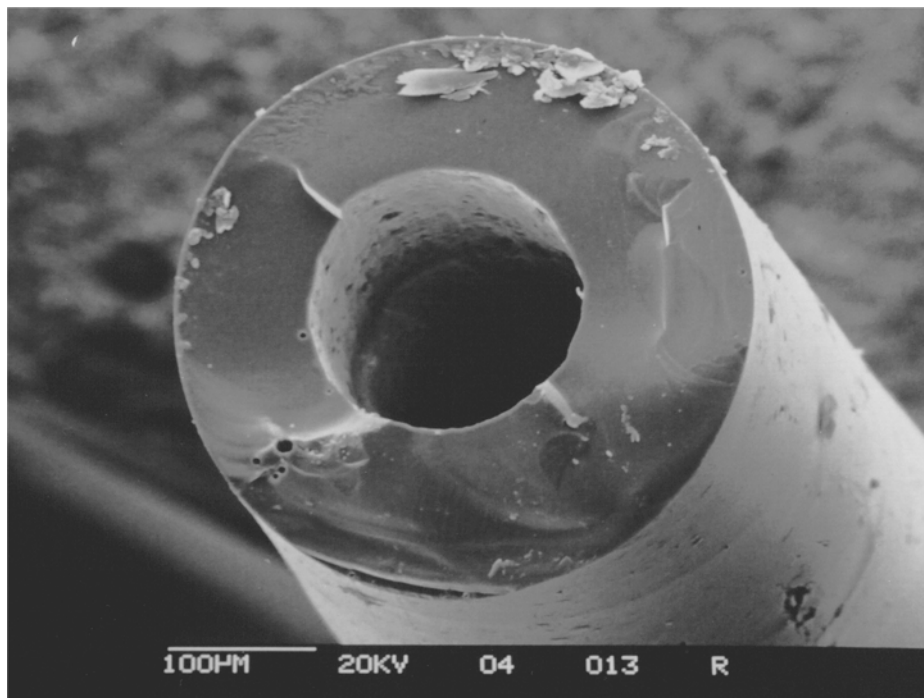


Figure 40. SEM image of a co-extruded single-lumen microtube after pyrolysis (SOC-A35 and filler #2).

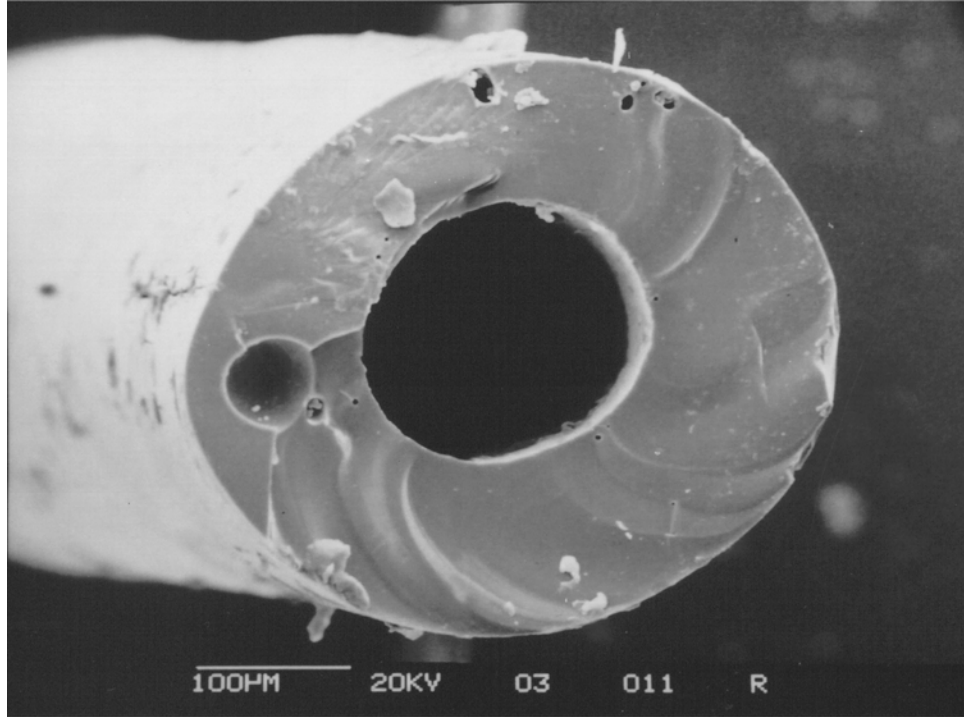


Figure 41. SEM image of a co-extruded single-lumen microtube after pyrolysis (SOC-A35 and filler #2).

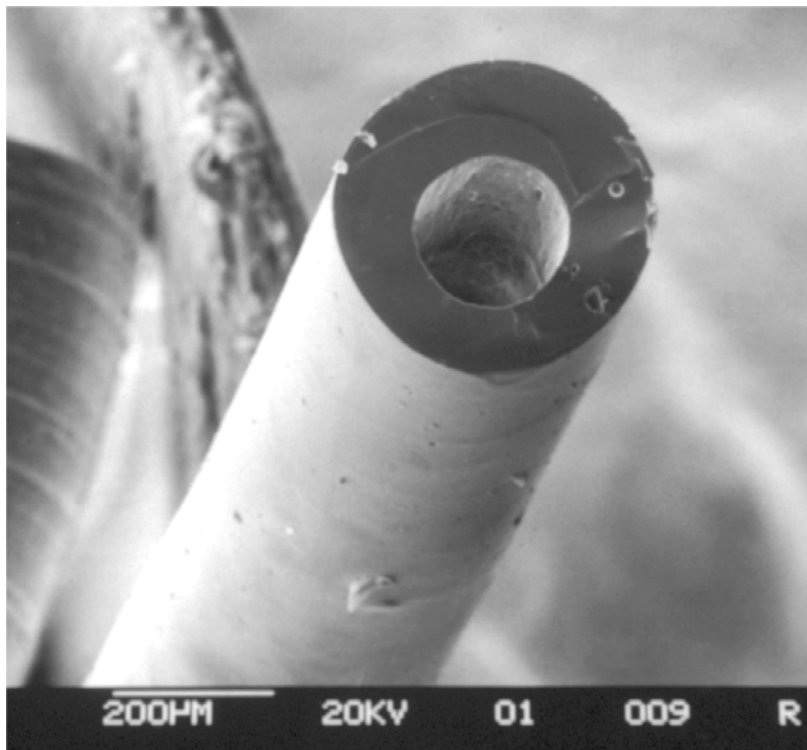


Figure 42. SEM image of a co-extruded single-lumen microtube after pyrolysis (SOC-A35 and filler #2).

The analysis of these images, showing the cross-section of pyrolyzed microtubes, allow to highlight some features typical of ceramic microtubes obtained by the pyrolysis of co-extruded preceramic polymer microtubes, namely:

- a) the process allows to produce ceramic microtubes with varying size (in the performed experiments the size ranged from ~180 to ~420  $\mu\text{m}$  for the outer diameter and from ~80 to 190  $\mu\text{m}$  for the inner diameter).
- b) when cross-linking is performed well, no loss of shape nor cracks are visible in the ceramized components. The morphological features of the microtubes in the preceramic state are accurately reproduced in the ceramized components.
- c) the process allows a good alignment of the central cavity along the main axis of the microtubes. Only occasionally central holes that were significantly off-center were produced, but it is believed that this could be corrected by a more careful control of the extrusion process.
- d) the microtubes are generally well-shaped (cylindrically shaped with a circular cross-section)
- e) the ceramic material appears compact and dense (at least at the scale of investigation)
- f) some voids are present in most cross-section areas, generally located away from the inner and outer surfaces of the microtube. These voids are a result of the presence of bubbles inside the preceramic material, probably caused by a condensation reaction with elimination of water during processing, as discussed earlier. Their size is usually  $< \sim 10 \mu\text{m}$ , although sometimes they can be larger (see Figure 41). The fact that the voids are mostly contained within the bulk of the material and are not located at the surface is certainly advantageous from a mechanical properties point of view, as their presence would not alter the surface flaw population of the ceramic material.
- g) the fracture surface is smooth, being the material an amorphous ceramic (see later), and sometimes displays the typical features of glassy, brittle fracture (see for example Figures 35 and 41).

The quality of the outer surface of the specimens was generally very good, with a very limited presence of debris and scarring (see in particular Figure 43, but also Figures 42 and above).

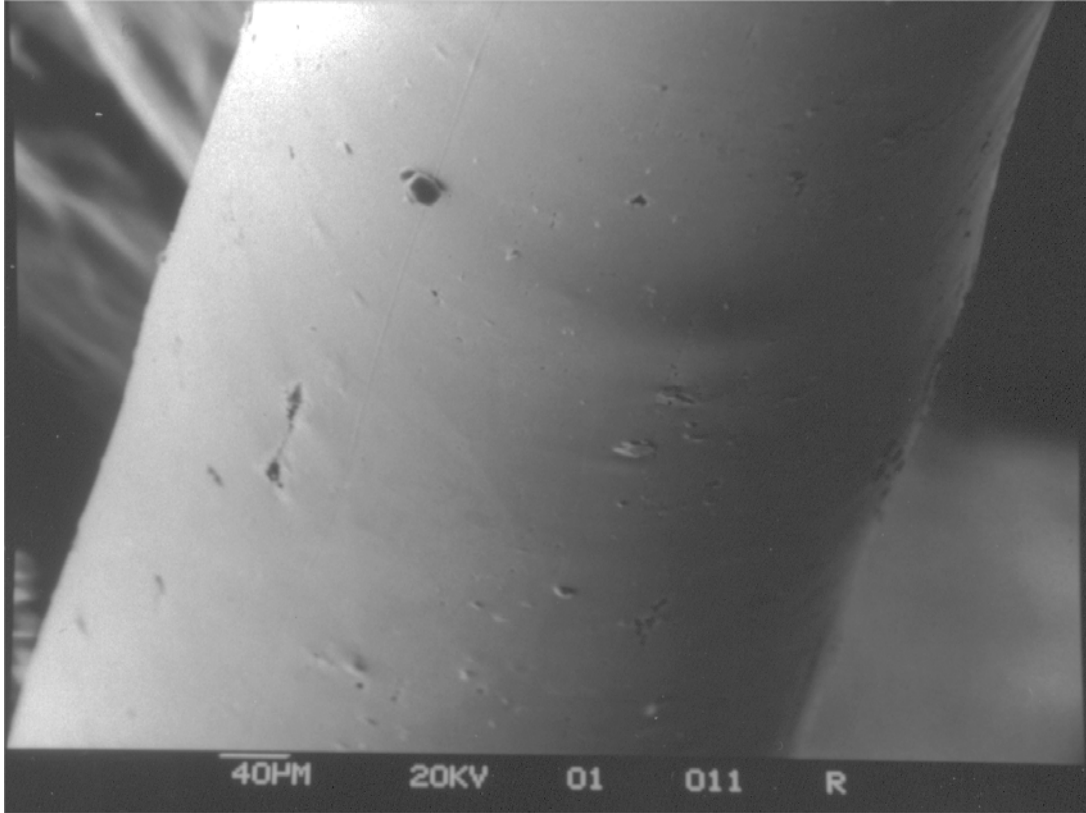


Figure 43. SEM image of a co-extruded single-lumen microtube after pyrolysis (SOC-A35 and filler #2), showing the good quality of the outer surface.

However, sometimes some macro-defects could be observed, which manifest themselves as longitudinal lines along the main axis of the microtubes (see the arrows in Figure 43 and also in Figure 39). These are attributable to the extrusion process, and are present only in a very limited set of specimens.

Sometimes, a deformation in the shape of the microtubes was found (see Figure 45), but this can be attributed to a transient instability of the micro-extrusion process that does not occur with great frequency.

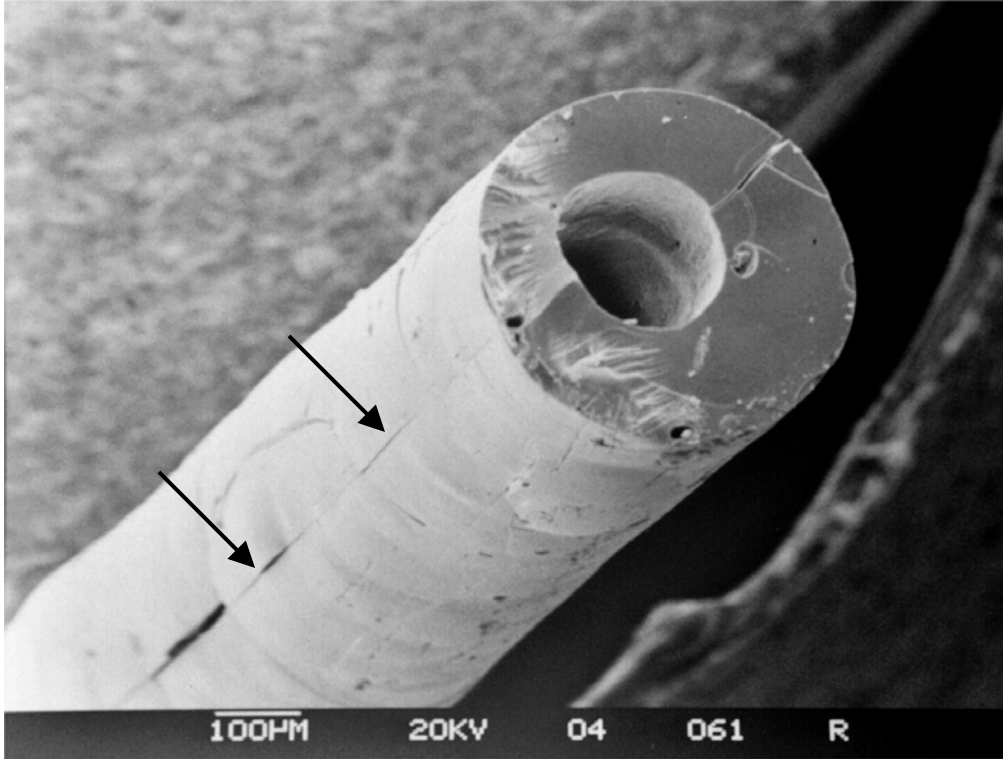


Figure 44. SEM image of a co-extruded single-lumen microtube after pyrolysis (SOC-A35 and filler #2), showing the presence of a longitudinal defect.

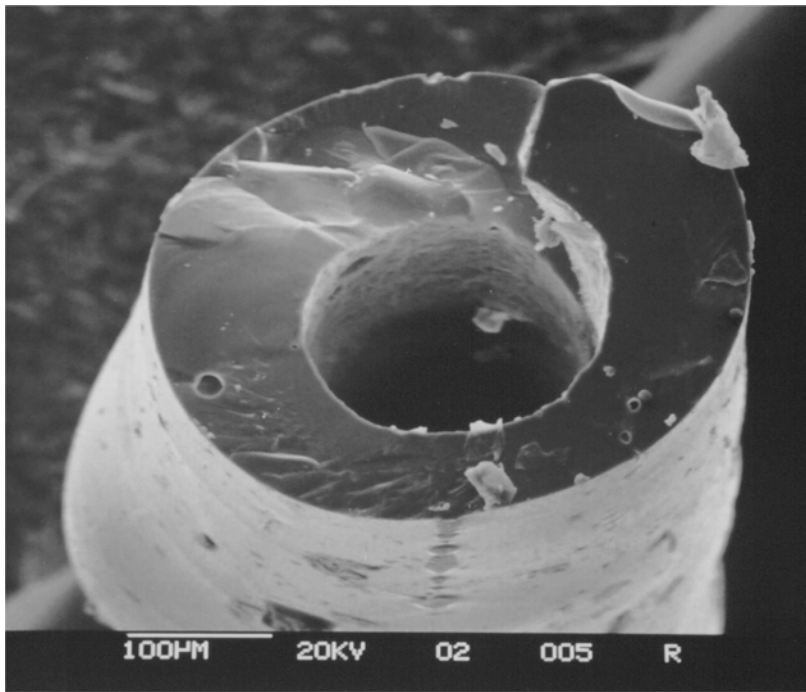


Figure 45. SEM image of a co-extruded single-lumen microtube after pyrolysis (SOC-A35 and filler #2), showing a deformation in the shape of the component.

The inner surface of the microtube (the surface of the axial central hole) was generally rougher than the outside one (see Figure 46), probably due to the mismatch of physical characteristics between the preceramic polymer and the filler (as noted already in the microtubes in the polymeric stage – see Figures 14 and 15). This indicates, again, that because of the good cross-linking achieved in the as-produced preceramic microtubes, the characteristics of the components in the polymeric stage were very accurately – at least at the micrometric level - reproduced in the ceramic component. Thus, no (partial) melting of the preceramic microtubes occurred during the heat treatment. Furthermore, this data suggest that the shrinkage that occurs during the polymer-to-ceramic conversion (which can be quite significant, as high as 30% linear) is isotropic, thus allowing the retention of the shape and aspect ratios of the ceramized components. Of course, both of these factors are of extreme importance for successfully producing ceramic components from preceramic polymers.

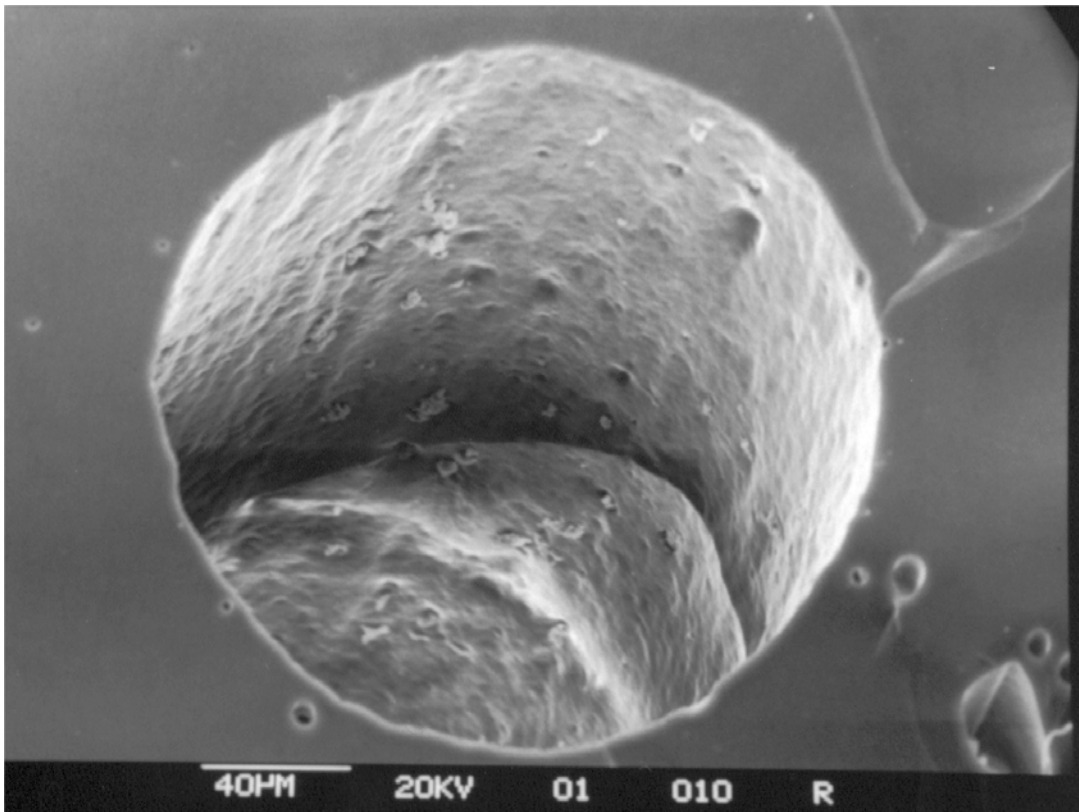


Figure 46. SEM image of a co-extruded single-lumen microtube after pyrolysis (SOC-A35 and filler #2), showing the inner surface (the surface of the axial central hole).

#### 2.3.4. Microstructural characterization of the pyrolyzed microtubes

The pyrolyzed microtubes, obtained from silicone resin SOC-A35, were comprised of a silicon oxycarbide amorphous ceramic, as expected [1, 8]. In figures 47 and 48 are reported the X-ray diffraction patterns and the FTIR spectra for samples pyrolyzed at 800, 1000 and 1200°C.

The XRD data show that the ceramic material is completely amorphous; only after pyrolysis at 1200°C, the presence of a limited amount of nano-sized C (turbostratic graphite) as well as  $\beta$ -SiC become evident. If the material would be heated at higher temperatures (in inert atmosphere), than phase separation and carbothermal reduction reactions would occur, leading to a larger presence of SiC crystallites in the amorphous matrix [1]. This behavior is typical for SiOC ceramic materials, and has been extensively reported in the scientific literature [1-8].

The FTIR data show that the organic moieties (Si-CH<sub>3</sub> bonds; C-H bonds) that were present in the silicone resin in the as-manufactured stage disappear because of the polymer-to-ceramic conversion. As expected [1], the ceramization was already completed after a pyrolysis temperature of 800°C.

The only significant change that occurs in the 800 to 1200°C temperature range is the increase in density of the pyrolyzed ceramic material, as reported in Table I (data obtained using a gas pycnometer), which occurs with loss of H<sub>2</sub> gas (at T < ~1000°C H atoms are still bonded to the “free” turbostratic C regions, which originated from the decomposition of the organic moieties). In the scientific literature, an optimal pyrolysis temperature in the range 1000 to 1200°C is often chosen to produce stable, dense SiOC amorphous ceramic materials. As an useful reference for engineering design, we mention that the typical coefficient of thermal expansion of a SiOC ceramic (after pyrolysis at 1000-1200°C) is in the range 3.5-4.1 x 10<sup>-6</sup> K<sup>-1</sup>. Due to their small size, it was impossible to directly measure the coefficient of thermal expansion on the pyrolyzed microtubes.

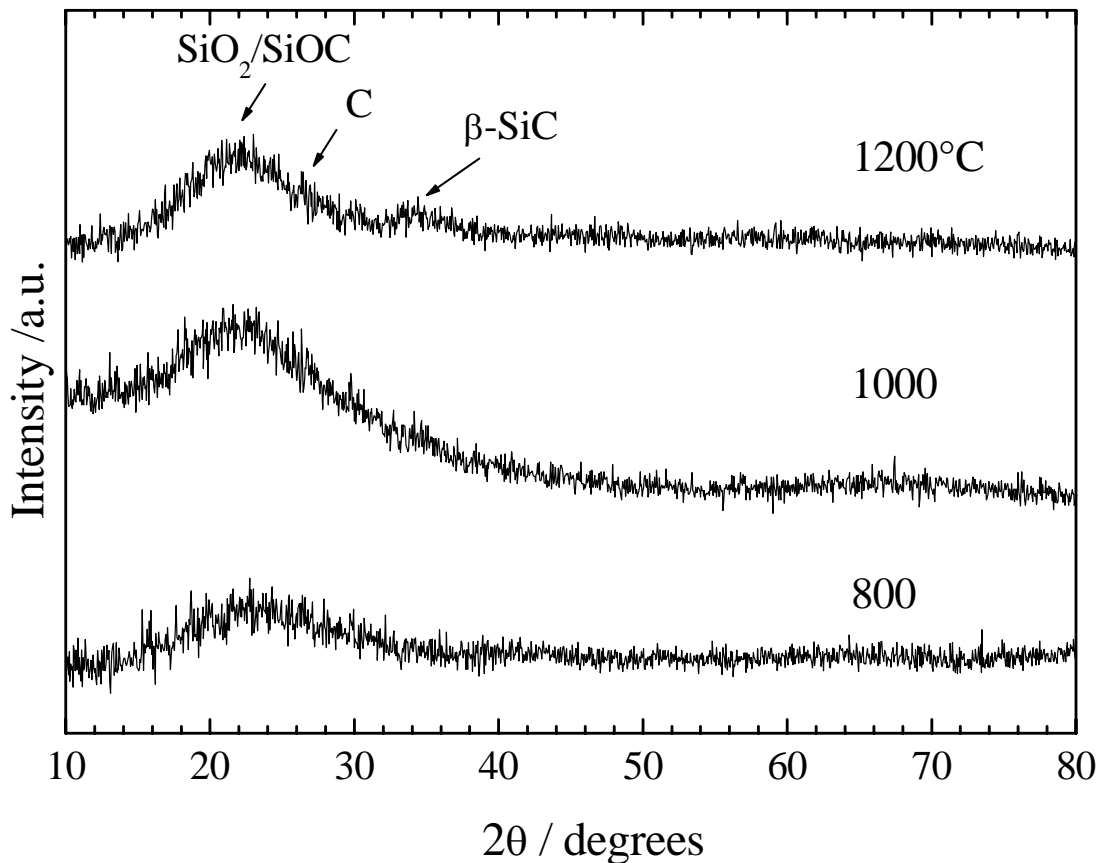


Figure 47. XRD patterns of co-extruded single-lumen microtubes after pyrolysis (SOC-A35) at various temperatures.

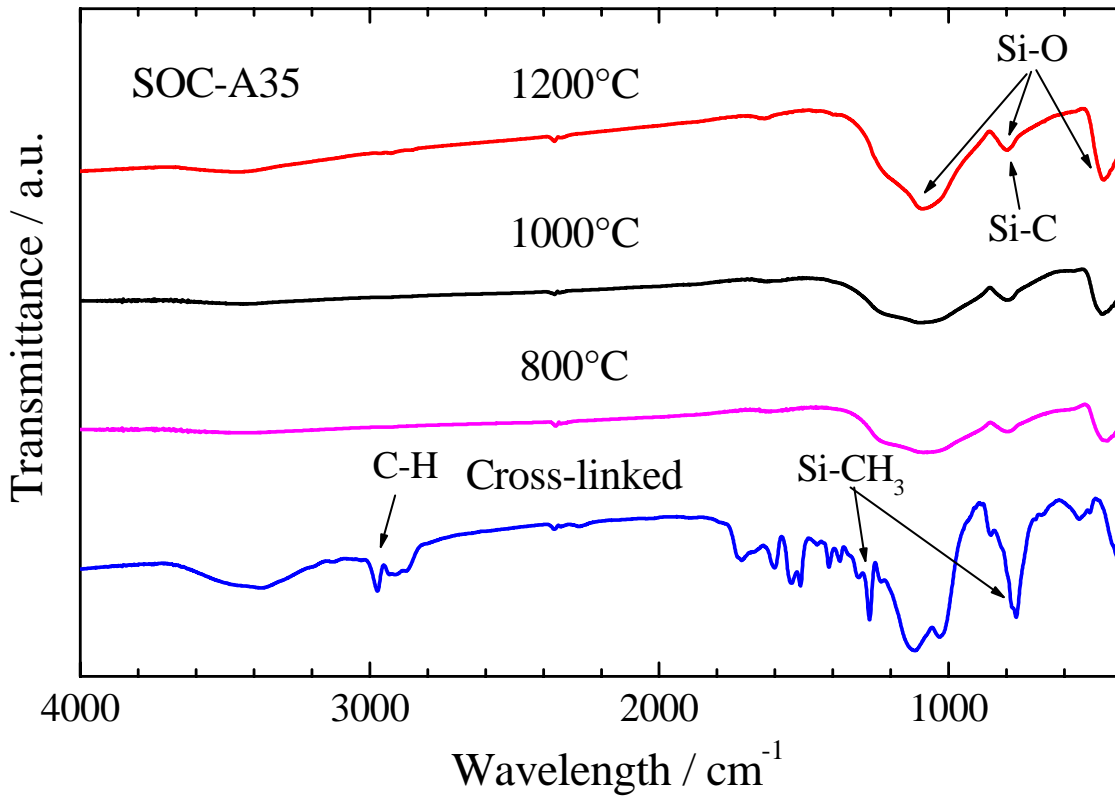


Figure 48. FTIR spectra of co-extruded single-lumen microtubes after pyrolysis (SOC-A35) at various temperatures.

Table I. Density values of co-extruded single-lumen microtubes after pyrolysis (SOC-A35) at various temperatures.

Pyrolysis temperature (°C)	Average density (g/cm <sup>3</sup> )
SOC-A35 (as received)	1.08 ± 0.05
800	1.85 ± 0.05
1000	2.01 ± 0.04
1200	2.21 ± 0.03

### 2.3.5. Mechanical properties of pyrolyzed microtubes

The mechanical properties of the single-lumen microtubes, obtained by the co-extrusion of SOC-A35 silicone resin and filler #2, were measured in various ways. An Instron 1121 UTM machine was used; cross-head speed was 0.5 mm/min in all tests). Only samples pyrolyzed at the optimal temperature of 1200°C were tested, and a limited set of samples was used because mechanical testing requires a very time-consuming procedure. Only the samples with a rather large diameter size were tested, as they were easier to handle without introducing defects. In

order to quantify the results, each sample was analyzed for determining its outer diameter – OD - (using a digital caliper as well as optical microscopy) and its inner diameter – ID - (using optical microscopy). It is quite probable that samples pyrolyzed at lower temperatures would possess lower strength values, because of their lower density.

First of all, a tensile test was attempted. The specimens were glued to a sample holder and then gripped in hydraulic clamps; however, because of the high strength of the components, it was impossible to break the samples in this way, as their tensile strength was higher than the maximum stress allowable (500 g) in the loading cell (which is commonly applied to the testing of fibers).

Thus, we decided to measure the strength of the ceramized microtubes by using 4-pt bending, using a specially designed fixture (see figure 49). The loading cell maximum allowable stress was 500 g;  $S_1$ - $S_2$  was about 4.5 mm.

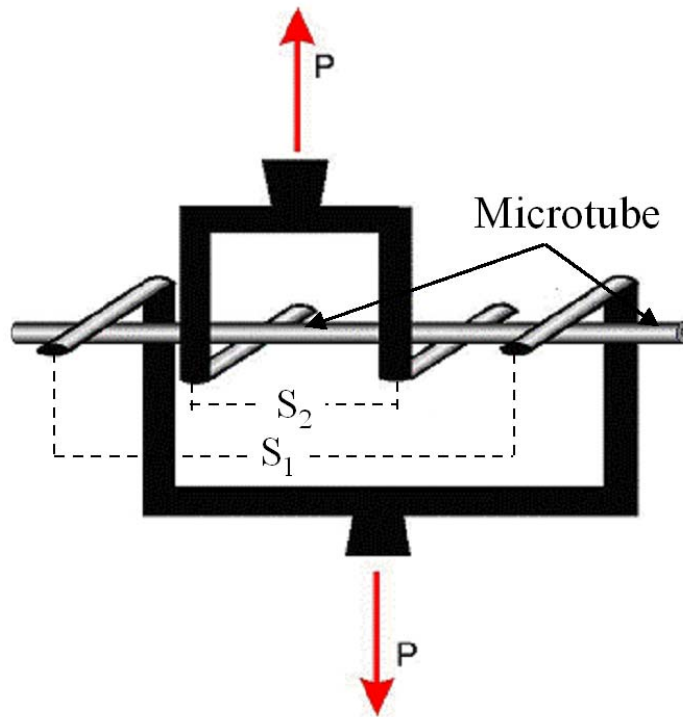


Fig. 49. Detail of the loading fixture used for the determination of the bending strength of the pyrolyzed single-lumen microtubes.

For the determination of the 4-point bending strength we followed the procedure outlined below:

- 1) we computed the bending moment:

$$M_f = \frac{P}{4} * (S_1 - S_2) \quad (\text{eq. 1})$$

where:

$M_f$  = bending moment;

$P$  = applied load;

$S_1, S_2 =$  distance between the loading points.

2) we computed the fracture stress:

$$\sigma_{rott} = \frac{M_f * Y_{max}}{J} \quad (\text{eq. 2})$$

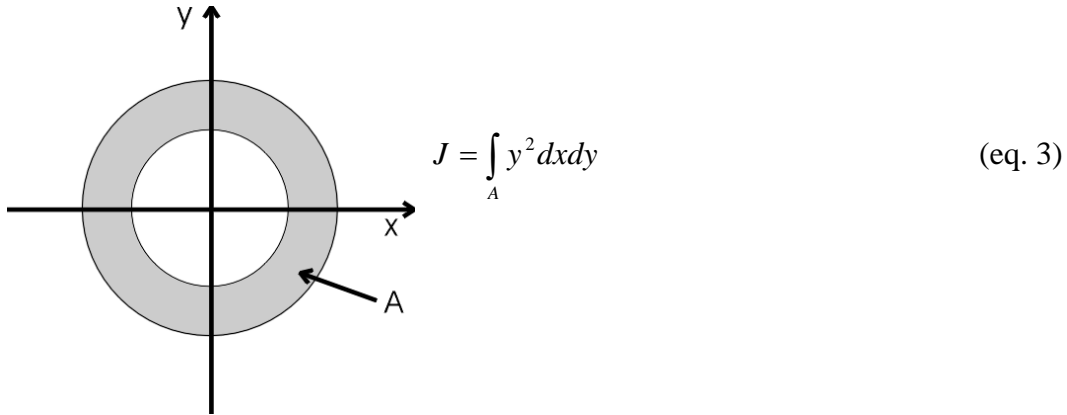
where:

$M_f =$  bending moment (from eq. 1);

$Y_{max} =$  maximum distance from the neutral axis (in our case  $Y_{max} = r_{est}$  where  $r_{est} = 1/2$  of the OD of the microtube);

$J =$  moment of inertia for the fracture area

3) We computed the moment of inertia relative to the area A, according to eq. 3:



$$J = \int_A y^2 dx dy \quad (\text{eq. 3})$$

and then, going to polar coordinates ( $x = r * \sin(\theta)$ ;  $y = r * \cos(\theta)$ ):

$$\begin{aligned} J &= \int_A r^2 \cdot \sin^2(\theta) \cdot r \cdot dr d\theta = \left( \int_{r_{int}}^{r_{est}} r^3 dr \right) \cdot \int_0^{2\pi} \sin^2(\theta) d\theta = \\ &= \left( \frac{r_{est}^4 - r_{int}^4}{4} \right) \cdot \int_0^{2\pi} \sin^2(\theta) d\theta = \left( \frac{r_{est}^4 - r_{int}^4}{4} \right) \cdot \int_0^{2\pi} \left( \frac{1}{2} - \frac{\cos(2\theta)}{2} \right) \cdot d\theta = \\ &= \left( \frac{r_{est}^4 - r_{int}^4}{4} \right) \cdot \left[ \frac{1}{2} \cdot \theta - \frac{1}{4} \cdot \sin(2\theta) \right]_0^{2\pi} \\ &= \pi \cdot \left( \frac{r_{est}^4 - r_{int}^4}{4} \right) \end{aligned}$$

4) thus, for our microtubes with a tubular geometry, the 4-point bending strength was:

$$\sigma_{rott} = \frac{\frac{P_{rott}}{4} \cdot (S_1 - S_2) \cdot r_{est}}{\frac{\pi}{4} \cdot (r_{est}^4 - r_{int}^4)} =$$

(eq. 4)

$$= \frac{P_{rott} \cdot (S_1 - S_2) \cdot r_{est}}{\pi \cdot (r_{est}^4 - r_{int}^4)}$$

where:

$P_{rott}$  = fracture load [N];

$r_{est}, r_{int}$  = external and internal radius (= 1/2 OD and 1/2 ID, respectively) [mm];

$S_1, S_2$  = distance between loading points [mm];

$\sigma_{rott}$  = fracture stress [MPa].

We have to point out, however, that we over-simplified the reality, as often the microtubes did not have a perfectly centered axial hole. This should be taken into account for each sample (as it directly influences the value for the moment of inertia) in order to accurately determine the bending strength of the tubular samples.

In Figure 50, as an example, is shown a typical stress-strain curve for a single-lumen ceramic microtube.

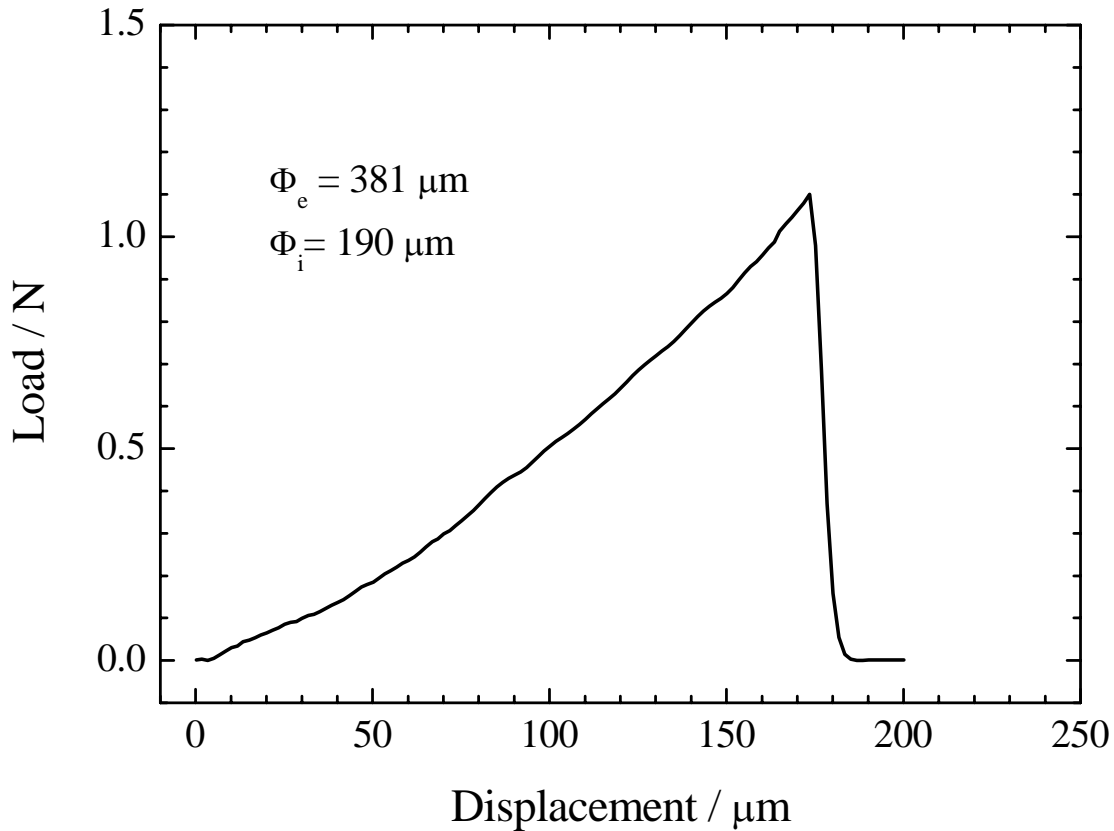


Figure 50. Typical stress-strain curve for a single-lumen ceramic microtube tested in 4-pt bending.

In Table II are reported the bending strength data for the various microtubes tested.

<b>Sample #</b>	<b>OD (μm)</b>	<b>ID (μm)</b>	<b>Load (N)</b>	<b>Fracture stress (MPa)</b>
1	354	174	0.97	245.8
2	384	184	0.50	98.3
3	375	173	1.73	360.8
4	396	189	1.89	338.3
5	391	181	0.68	127.0
6	407	209	0.45	75.3
7	403	187	0.83	139.2
8	401	193	1.43	246.4
9	378	179	1.43	295.2
10	381	190	1.12	228.4
11	403	187	0.92	155.6
12	387	169	1.42	267.7
13	379	179	0.84	171.3
14	381	180	0.41	83.4
15	394	190	1.74	317.9
16	379	183	0.78	160.6
17	420	193	0.93	137.7
18	408	186	0.64	104.5
19	413	199	0.61	97.0
20	392	187	0.86	159.5

In Figure 51 the data are plotted as a function of the microtubes' external diameter. As it can be seen the data are quite scattered, due to the various factors influencing the measured values (such as the actual position of the axial hole along the microtube's axis; the possible presence of defects on the surface of the microtubes; the possible lack of uniformity in thickness along the axial direction; the possible variation in diameter along the axial direction). However, a trend of increasing strength with decreasing diameter can be discerned, and certainly expected in analogy with data for glass fibers. In fact, decreasing the size of the component decreases the critical flaw dimension that can exist on the surface and hence increases the measured flexural strength of the component.

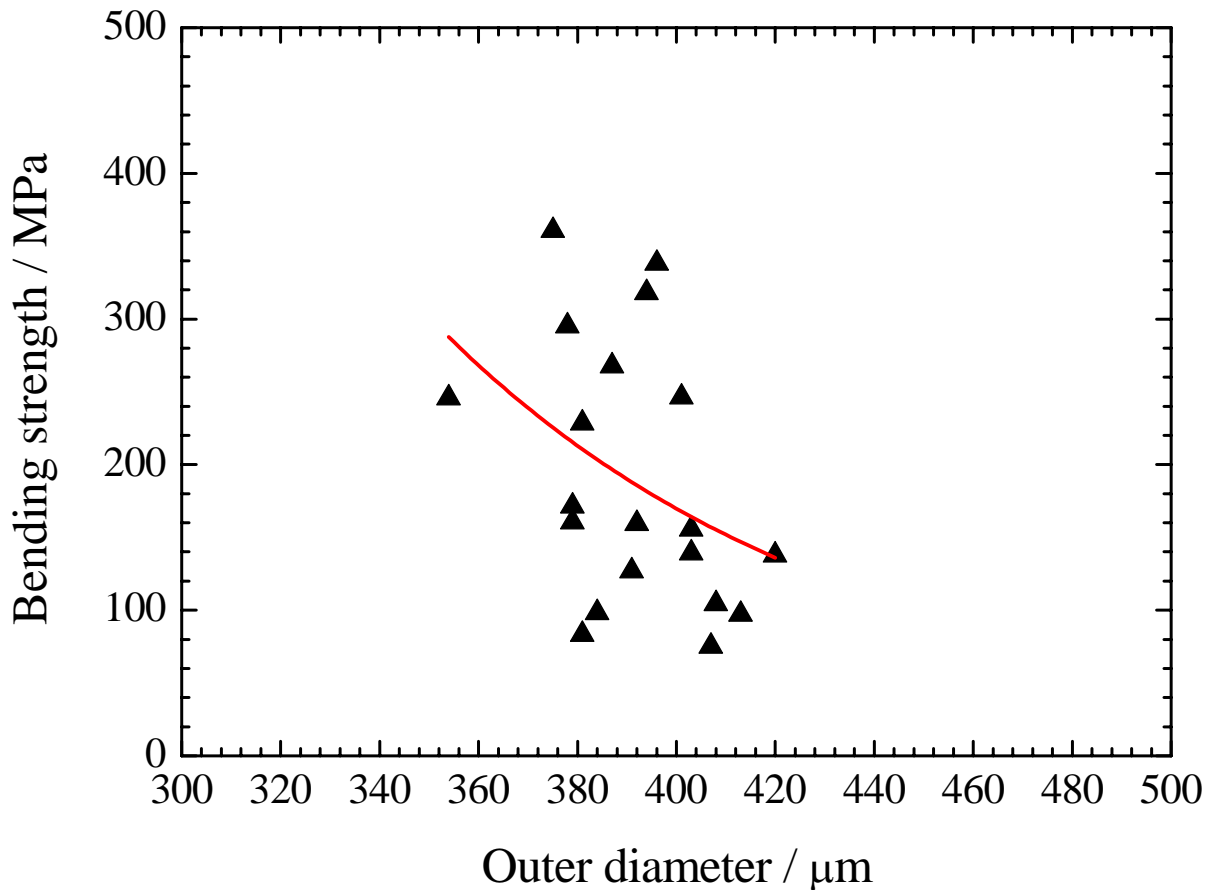


Figure 51. Bending strength of ceramic microtubes as a function of the OD.

### 3.1. Modification of the extruder heads

An extruder head capable of producing multilumen microtubes from preceramic polymers (silicone resins) was fabricated modifying commercially available components. The design included devising suitable pathways for uniformly distributing the molten resins and the sacrificial filler within the equipment.

With this head, a structure comprised of 9 cores made by a sacrificial filler surrounded by the silicone resin can be formed (see Figure 52). It was chosen to fabricate multilumen microtubes with such a large number of sacrificial filaments / channels, as we wanted to fully assess the feasibility of the microextrusion technique for the fabrication of samples of some practical interest, and a lower number of lumens (say 5) was deemed of much lower significance. Of course, this choice meant that we are probably working at the upper end of what the technology might allow to produce. It is noteworthy to mention, also, that a single extruder head can only produce a single number of lumens, and to fabricate more heads with a different number of lumens would have taken us outside the allotted budget.

Once again (see Figures 1-3), the assembled equipment that was used for the production of ceramic microtubes (Model TR 12/24 LD, Gimac, Castronno (VA), Italy) is constituted by:

- two loading trays, for the introduction of granulated or powdered materials
  - two extruder cylinders (fitted with three thermocouples each), containing the extruding screws
- the extruder's head, where the two material fluxes are mixed and the microtubes are formed

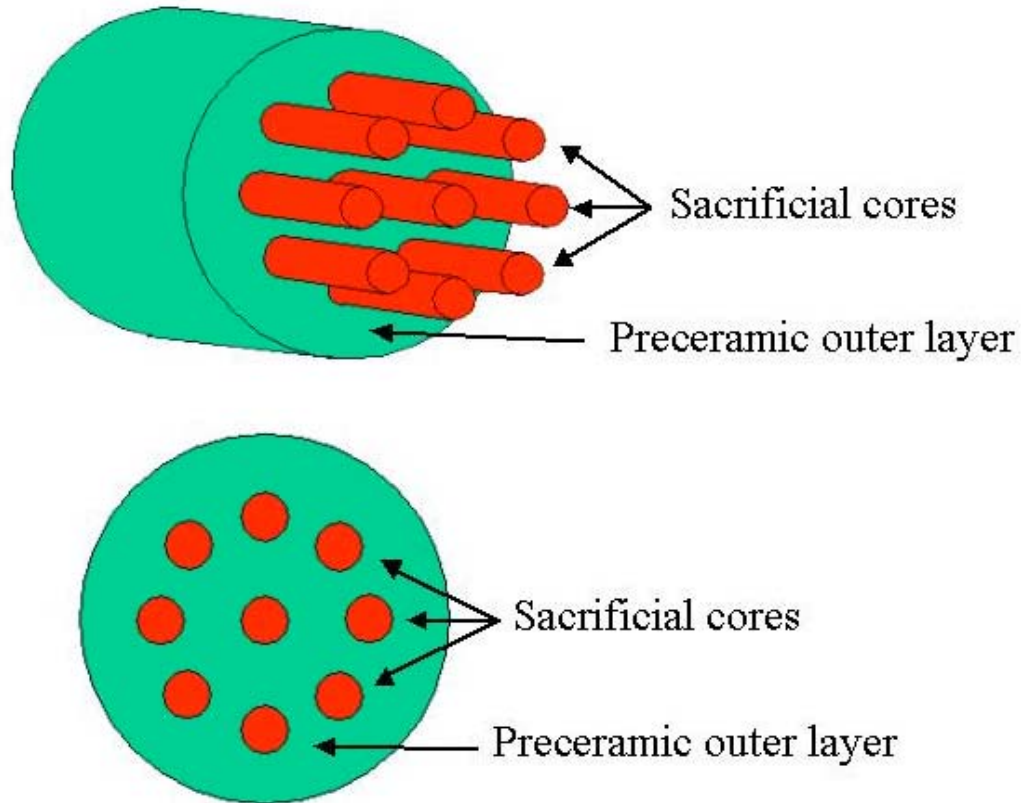


Figure 52. Schematic concept for the realization of a multilumen ceramic microtube from a preceramic polymer (in green) and a filler material (sacrificial cores, in red) by co-extrusion.

### 3.2. Fabrication of preceramic-polymer-based multilumen microtubes by co-extrusion

For the fabrication of multilumen microtubes from silicone resins, the same general considerations expressed in paragraph 1.3 still apply, with the added comment that a particularly critical aspect would probably be the maintaining of fully separated molten filler streams within the microtube section during forming, and the possible problems that the simultaneous release of decomposition gases from several areas within the same cross-section could cause.

The silicone resins employed were SOC-A35 (a methyl-silicone resin; Starfire Systems, Malta, NY) and H44 (a methyl-phenyl silicone resin; Wacker Chemie, München, Germany), all successfully previously employed for the fabrication of single-lumen microtubes. The H44 preceramic polymer is also sold in powder form (suitable for directly loading the extruder), it is not hazardous, has a glass transition temperature of about 50°C and a softening temperature in the range of 50-90°C. It crosslinks via condensation reactions of Si-OH and C<sub>2</sub>H<sub>5</sub>OH groups

(about 3% total), and upon heating in inert atmosphere it forms an amorphous silicon oxycarbide (SiOC) ceramic material, with a ceramic yield of about 80 wt% - see paragraph 2.4.1.

We chose to employ Filler #2 for most of the experiments, but Filler #3 was also used. In fact, the thermal compatibility with the silicone resins was good for both filler materials used (#2 and #3), allowing the production of single-lumen microtubes in the preceramic stage – see paragraphs 1.3 and 2.2. Another reason why we tested Filler #3 for the production of multilumen microtubes is that we hoped that the distribution of the filler material in several parallel thin strands might reduce the problems earlier observed when producing single-lumen microtubes. Namely, cracks perpendicular to the drawing axis which were attributed to different mechanical and thermal (coefficient of thermal expansion) properties between the silicone resins and the filler material.

In the first set of experiments, Filler #2 was used to fabricate the inner cores, and the extrusion was carried out by processing the SOC-A35 silicone resin at a temperature of about 90-110°C, while the Filler #2 reached temperatures in the range of 160-180°C. In this case, successful co-extrusion was achieved, as demonstrated by the images shown in Figures 53-57, which refer to samples in which the silicone resin was as received or cross-linked, but in any case before pyrolysis. The sacrificial inner cores are thus still present.

Differently from before, when the filler used was homogeneously pink in color (see for example Figures 9-12) because when purchased it also contained a coloring agent, these tests were conducted using a filler with the exactly the same composition but without coloring agent. We added a small amount of coloring agent ourselves (red or blue-purple), in order to better differentiate among various samples depending on the processing conditions (e.g. drawing speed). This, however, not always led to a homogeneously colored set of filler filaments embedded within the silicone resins (see later).

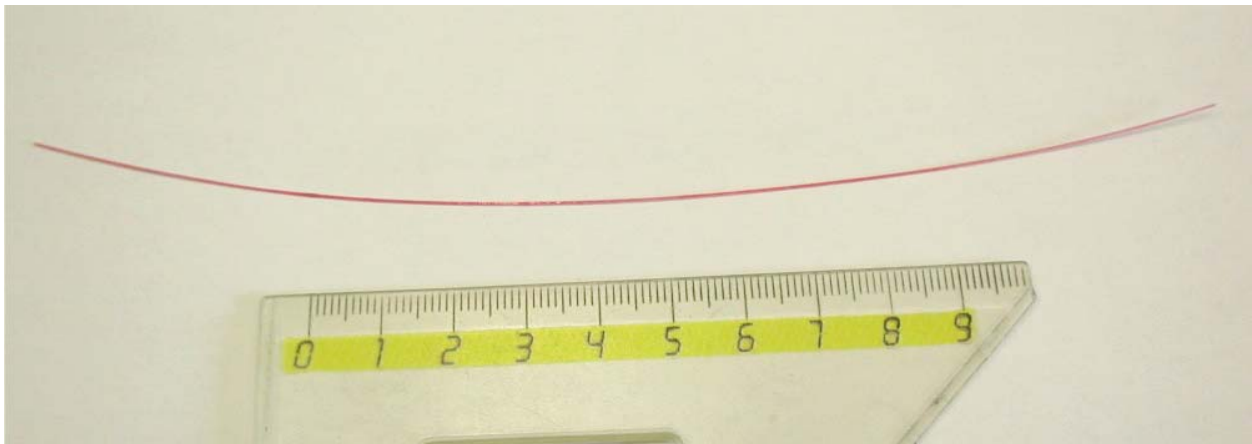


Figure 53. Photographic image of a multilumen preceramic silicone resin microtube (SOC-A35, Filler #2, red coloring agent) before cross-linking

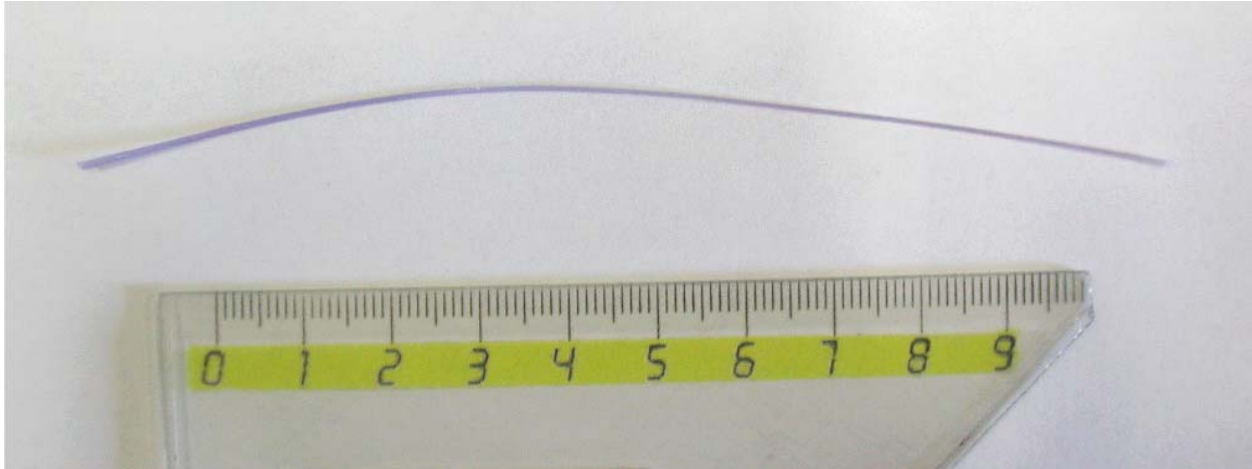


Figure 54. Photographic image of a multilumen preceramic silicone resin microtube (SOC-A35, Filler #2, blue coloring agent) before cross-linking

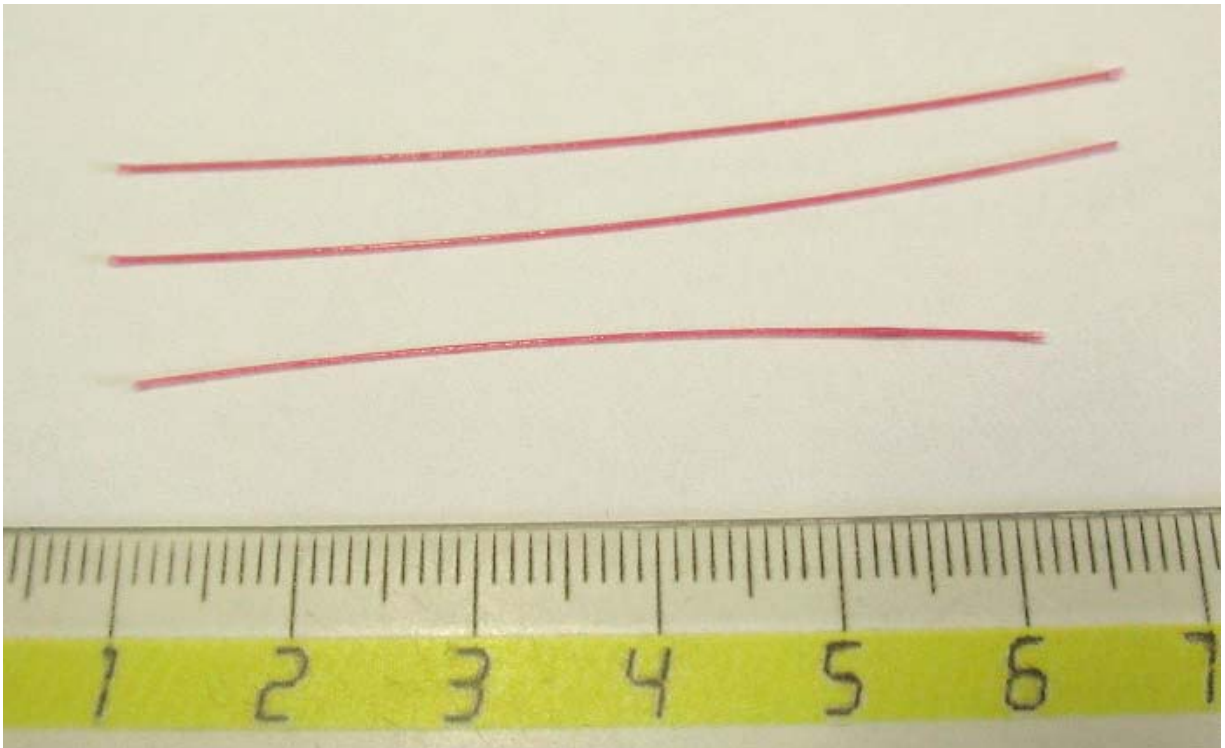


Figure 55. Photographic image of a multilumen preceramic silicone resin microtube (SOC-A35, Filler #2, red coloring agent) before cross-linking

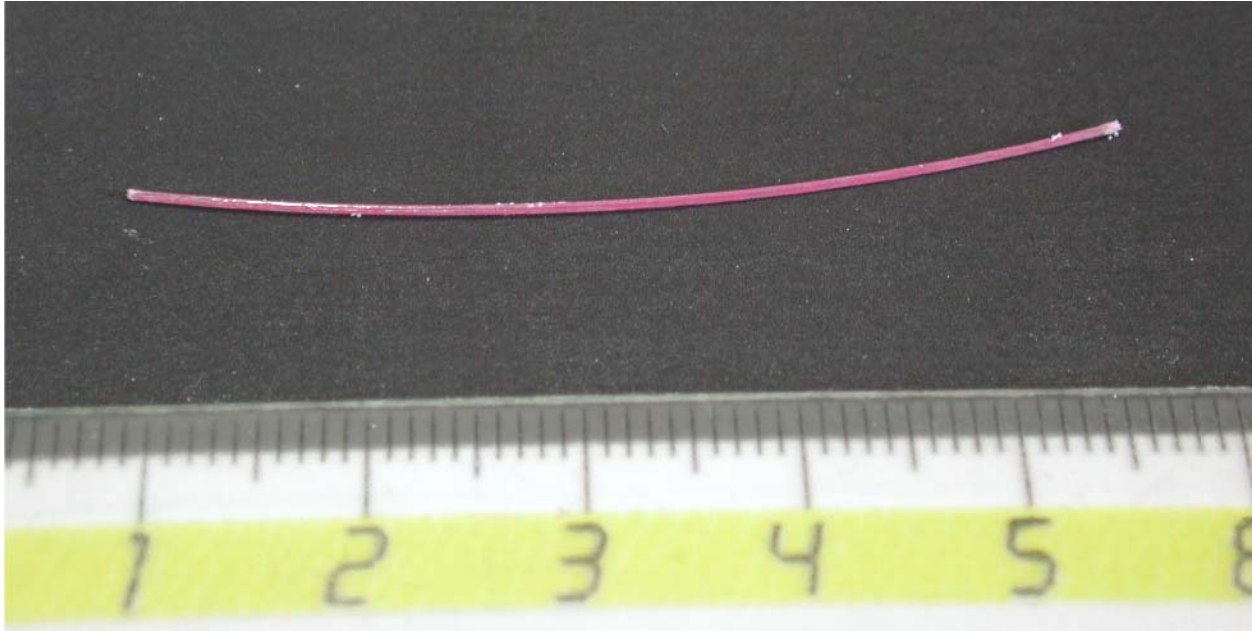


Figure 56. Photographic image of a multilumen preceramic silicone resin microtube (SOC-A35, Filler #2, red coloring agent) after cross-linking

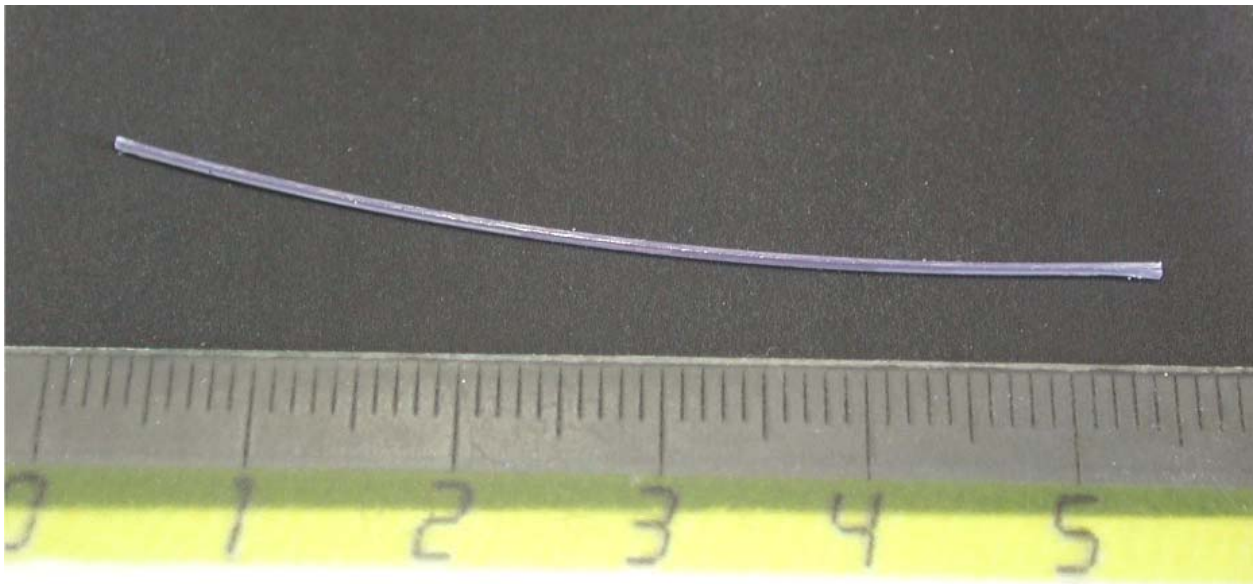


Figure 57. Photographic image of a multilumen preceramic silicone resin microtube (SOC-A35, Filler #2, blue coloring agent) after cross-linking

From the above images one can see that microtubes of a good quality, homogeneous appearance and suitable length can be fabricated (the microtubes were cut to that length – ~4-12 cm - for transportation, handling and further processing purposes), albeit with some deviation from linearity. The fact that tubes are not completely straight can be attributed to several factors, including the direction of drawing, the distribution of the filler strands within the silicone resin, the difference in thermo-mechanical characteristics between the filler and the preceramic

polymer and possibly the cooling rate. However, as it can be seen in Figure 55, when cut in shorter dimensions, the microtubes are reasonably straight.

The effect of cross-linking on the look of the microtubes can once again be noticed, especially in Figure 57, with the silicone resin becoming opaque (see Figure 23). This effect is not noticeable under the strong lighting conditions used in the stereo-optical microscope.

Because of difficulties in obtaining meaningful images at somewhat high magnification, because of the large number of filler strands, it was chosen to investigate the morphology of the preceramic microtubes, after cross-linking, mainly by stereo-microscopy. Samples were prepared by cutting them using a sharp blade, at room temperature. Some images of fresh fracture/cut surfaces are reported in the following figures. In some of the shown samples, the silicone resin part of the microtube was broken to reveal the embedded filaments. Due to the fact that at room temperature the preceramic polymer is below its glass transition temperature, and thus behaves like a brittle solid, it was possible to clearly separate the two components. Moreover, the limited amount of silicone debris that remains attached to the sacrificial filler filaments after removal (see for instance Figure 59, 60 and 61), clearly indicates the suitability of filler #2 for this processing approach (no mixing, adhesion or reaction between the chosen sacrificial filler and preceramic polymer).

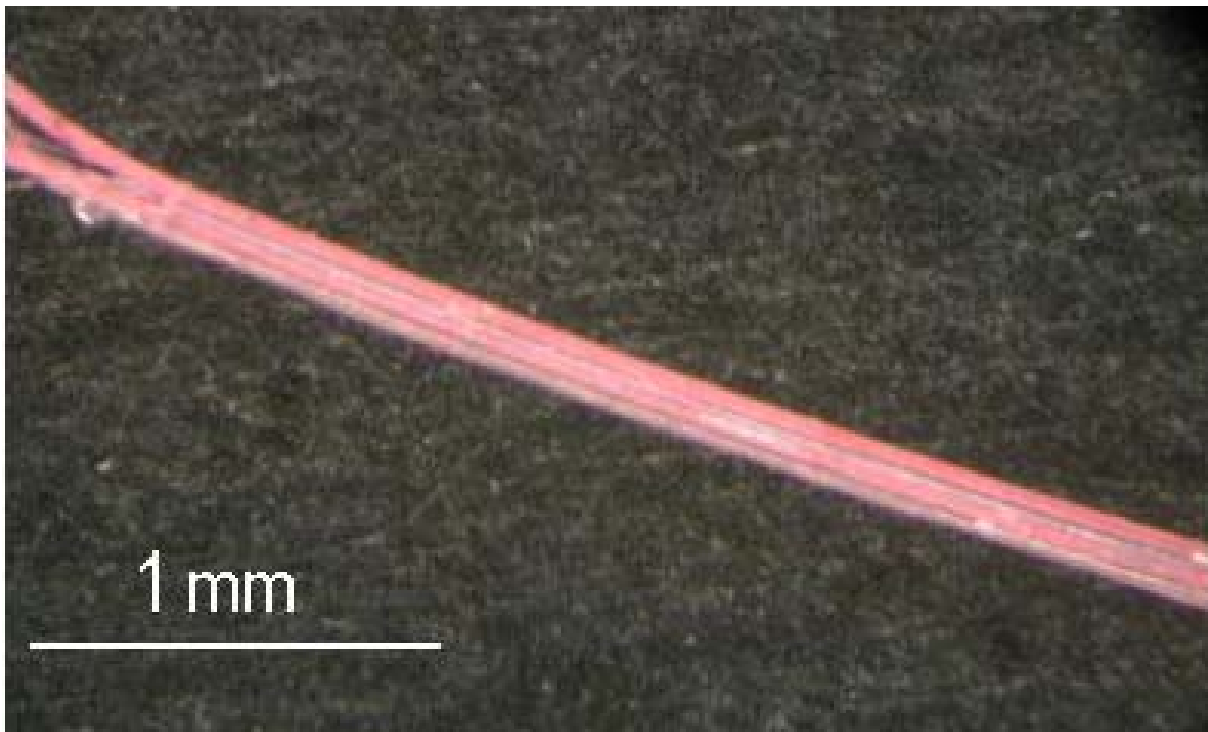


Figure 58. Optical stereo-microscopy image of a multilumen preceramic silicone resin microtube (SOC-A35, Filler #2, red coloring agent)

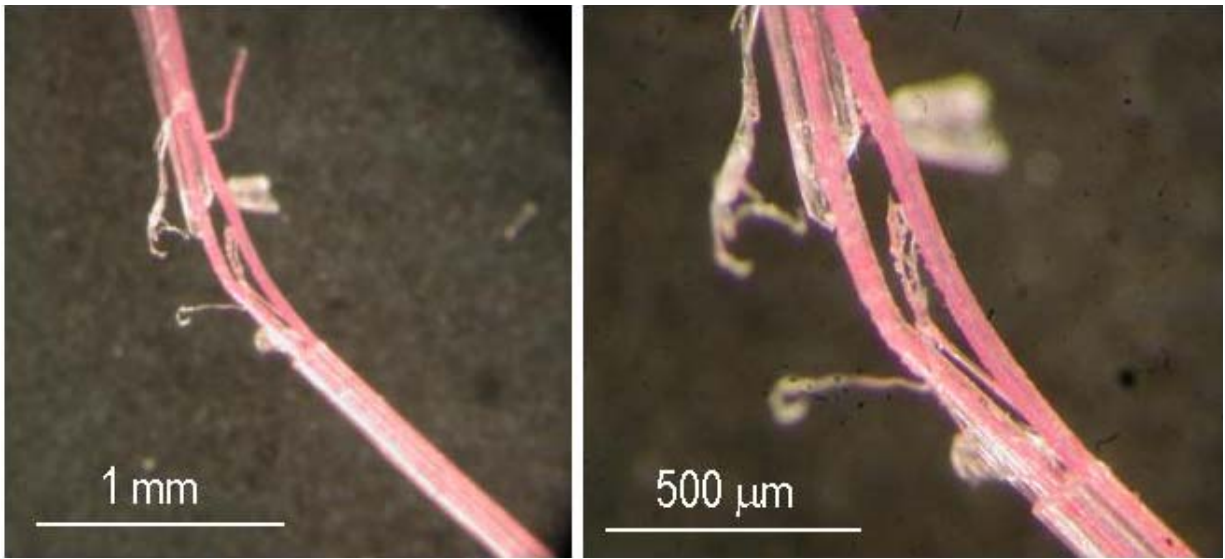


Figure 59. Optical stereo-microscopy image of a multilumen preceramic silicone resin microtube (SOC-A35, Filler #2, red coloring agent). Same sample, at different magnification.

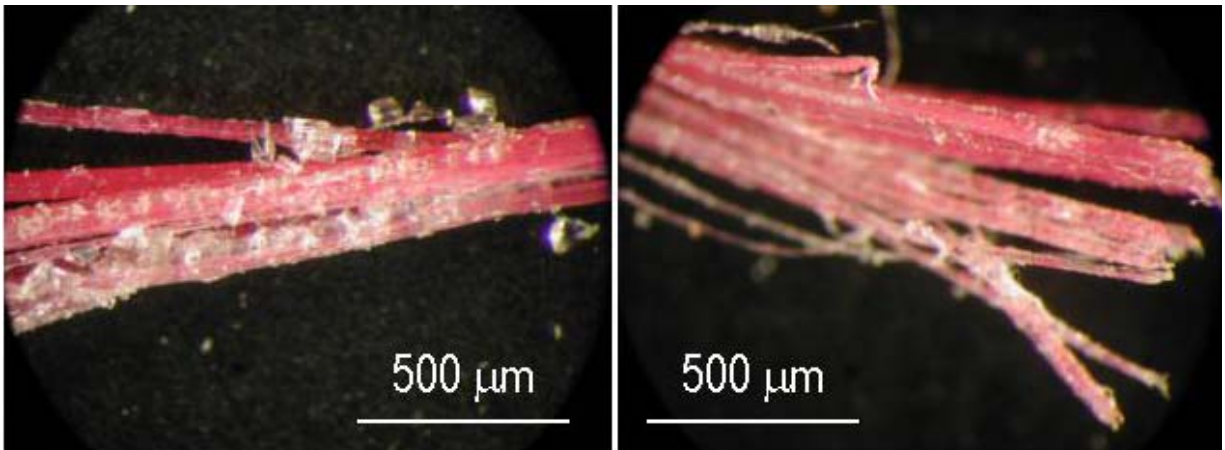


Figure 60. Optical stereo-microscopy image of two different multilumen preceramic silicone resin microtubes (SOC-A35, Filler #2, red coloring agent)

From these images, it is clearly possible to see how the sacrificial filler filaments are embedded within the silicone resin, as desired. However, in some samples, when breaking apart the preceramic component of the microtube (the transparent material) some of the filaments seem to be joined together, or at least not completely separable from each other (see for example Fig. 59: that microtube should contain 9 independent filaments, but in the micrograph only 2 separate strands seem to be visible). In Figure 60, several independent strands are instead noticeable, but they seem to have different sizes, possibly indicating that some of them contain more than one original filament.



Figure 61. Optical stereo-microscopy image of a multilumen preceramic silicone resin microtube (SOC-A35, Filler #2, red coloring agent)

In this image, it is possible to distinguish 9 separate, individual sacrificial filler filaments embedded in the silicone resin microtube. The filaments appear to have a similar thickness, of about 30-50  $\mu\text{m}$ . The overall thickness of the microtubes, before pyrolysis, appears to be in the ~400-600  $\mu\text{m}$  range.

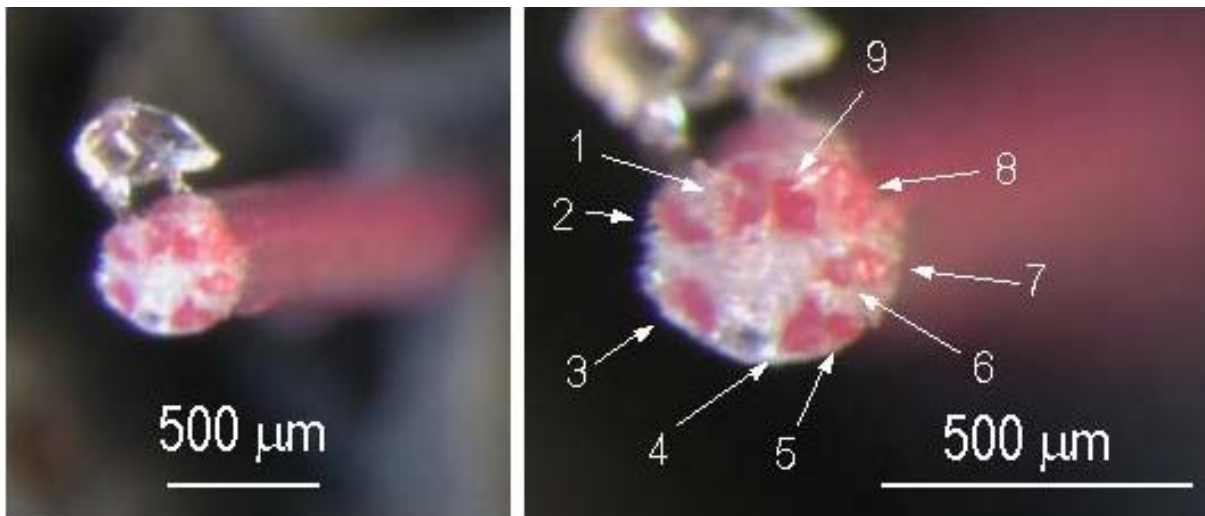


Figure 62. Optical stereo-microscopy image of a multilumen preceramic silicone resin microtube (SOC-A35, Filler #2, red coloring agent). Images of the same sample, but with different viewing angle and magnification.

In Figure 62, which refers to the cross-section of another sample, it is again possible to distinguish 9 separate, individual sacrificial filler filaments embedded in the silicone resin material comprising the microtube. The filaments appear to have a thickness in the range of 30-60  $\mu\text{m}$ . Most of the filler filaments have a round cross-section, and some appear to be touching, or at least to be separated by a very limited amount of silicone resin (see for example filaments # 4 and 5, 6 and 7, 1 and 9). It can also be noticed that their distribution within the cross-section of the microtube is not completely homogeneous; in particular the central filament – see Figure 52 – is shifted from its expected middle position. The sacrificial filaments, also, appear to be quite close to the edge of the microtube (a small portion of the silicone resin has probably been removed from the top part of the cross-section during cutting, as suggested by the flake still attached to the microtube).

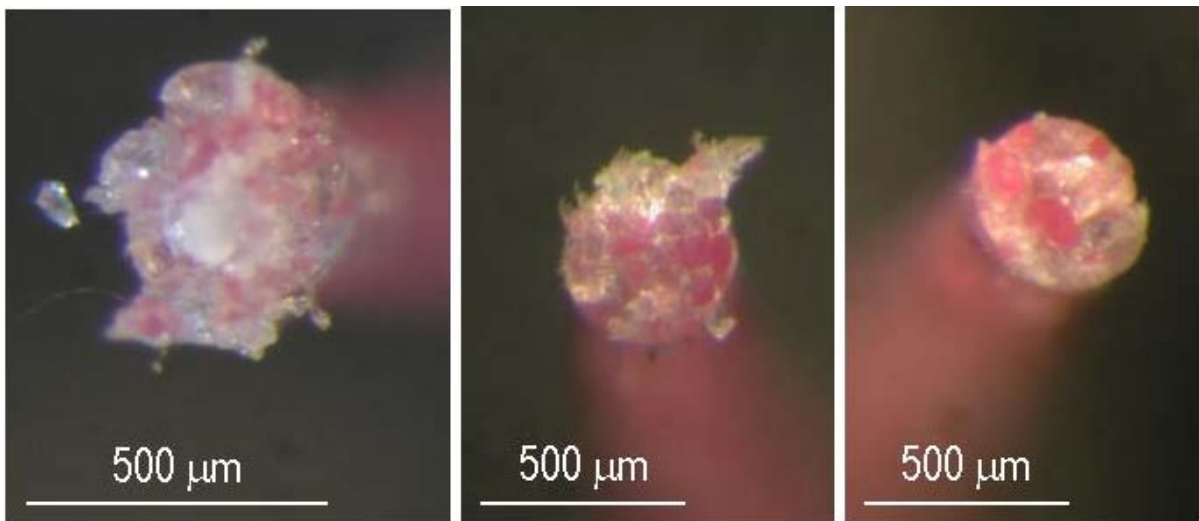


Figure 63. Optical stereo-microscopy image of multilumen preceramic silicone resin microtubes (SOC-A35, Filler #2, red coloring agent)

In other samples (see Figure 63) it was not possible to clearly distinguish all of the sacrificial filaments, either because of optical effects (artifacts in the images due to the high light reflectivity from the silicone resin) or because of how the samples were cut by the blade, or maybe because they were fused together during processing.

There can be several reasons for this partial lack of homogeneity in the spatial distribution of the sacrificial filler filaments within the microtube's cross-section. In particular, the drawing conditions and the amount of sacrificial filler that enters the extruder's head would influence both the size and the distribution of the individual strands. As an example, Figure 64 shows microtubes made using Filler #2 colored in blue/purple (to indicate slightly different processing conditions): in this case it seems that most of the filaments are bonded together and occupy a large volume of space within the cross-section.

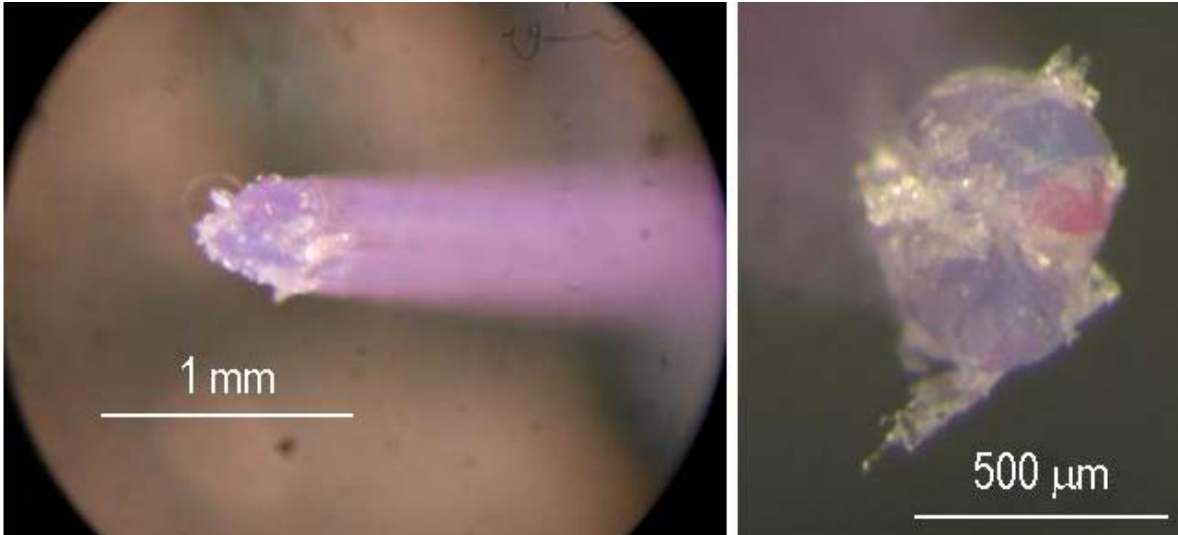


Figure 64. Optical stereo-microscopy image of multilumen preceramic silicone resin microtubes (SOC-A35, Filler #2, blue coloring agent)

Finally, even if it is not trivial to distinguish what actually occurs in the samples and what appears as an artifact of the investigating method chose (stereo-optical-microscopy), we can say that in some samples some debris (filler #2 particles) are embedded within the silicone resin (see Figure 65). The debris were not previously observed when analyzing single-lumen microtubes, and in our opinion they are more probably due to the fact that in these experiments we mixed ourselves the coloring agent with the filler (not always achieving a homogeneous mixture) rather than being due to the presence of multiple sacrificial filler strands. Further experiments employing an optimized mixing procedure will help clarifying this point.

The presence of bubbles was noted before (see Figures 10 - 12), and attributed to cross-linking of the silicone resin.

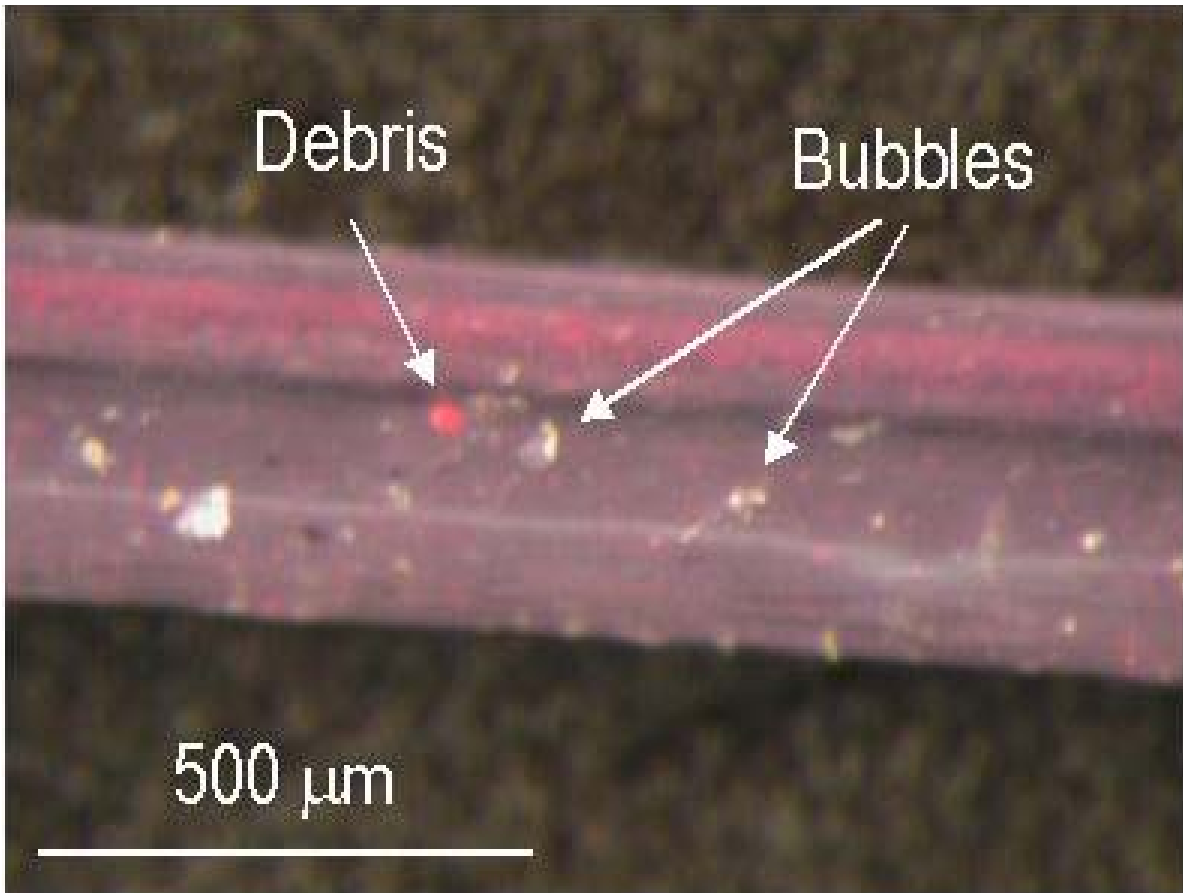


Figure 65. Optical stereo-microscopy image of a multilumen preceramic silicone resin microtube (SOC-A35, Filler #2, red coloring agent)

In a second set of experiments, Filler #2 was used to fabricate the inner cores, and the extrusion was carried out by processing the H44 silicone resin at a temperature of about 60-100°C, while the Filler #2 reached temperatures in the range of 160-180°C. Also in this case, successful co-extrusion was achieved, as demonstrated by the images shown in Figures 66-71, which again refer to samples in which the silicone resin was as received or cross-linked, but in any case before pyrolysis. The sacrificial inner cores are thus still present.

Figure 66 shows how microtubes containing several filaments of the sacrificial filler (Filler #2) were indeed fabricated using the H44 silicone resin. Again, in some cases it appears that some of the strands are partially joined together (see for example Figure 66, left, one of the bottom strands appears to have a size larger than the other filaments).



Figure 66. Optical stereo-microscopy image of multilumen preceramic silicone resin microtubes (H44, Filler #2, no coloring agent)

Some filler debris and bubbles are present in these samples too (see Figure 67), suggesting that the H44 preceramic polymer has a similar behavior to the SOC-A35 one. The external surface of the microtubes appears to be somewhat rougher than observed for the specimens produced by the SOC-A35 resin, probably due to the different rheological characteristics of the two preceramic polymers.

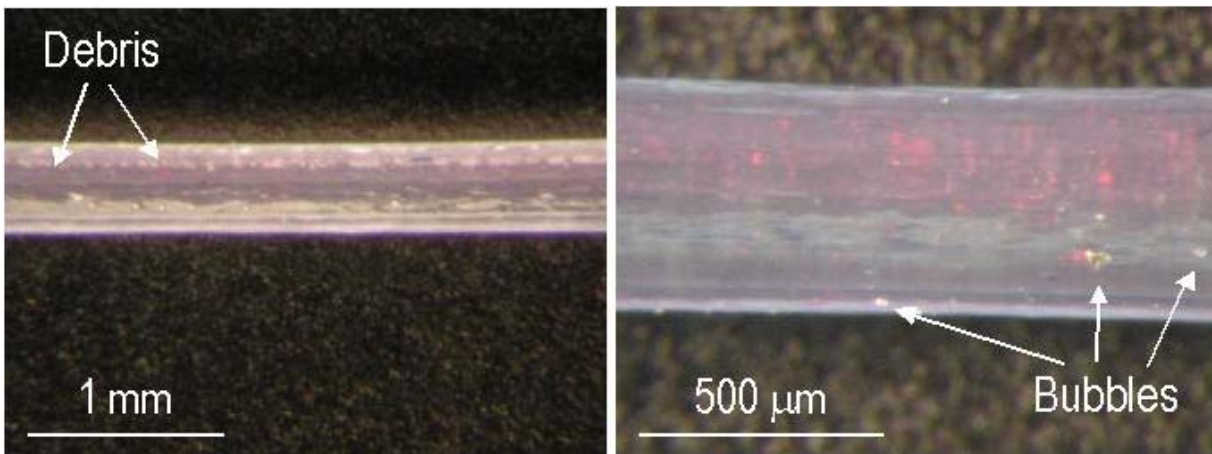


Figure 67. Optical stereo-microscopy image of multilumen preceramic silicone resin microtubes (H44, Filler #2, pink coloring agent)

Also for H44-derived specimens, in some cases the filler strands joined together during co-extrusion and it was difficult to distinguish them clearly (see Figure 68).

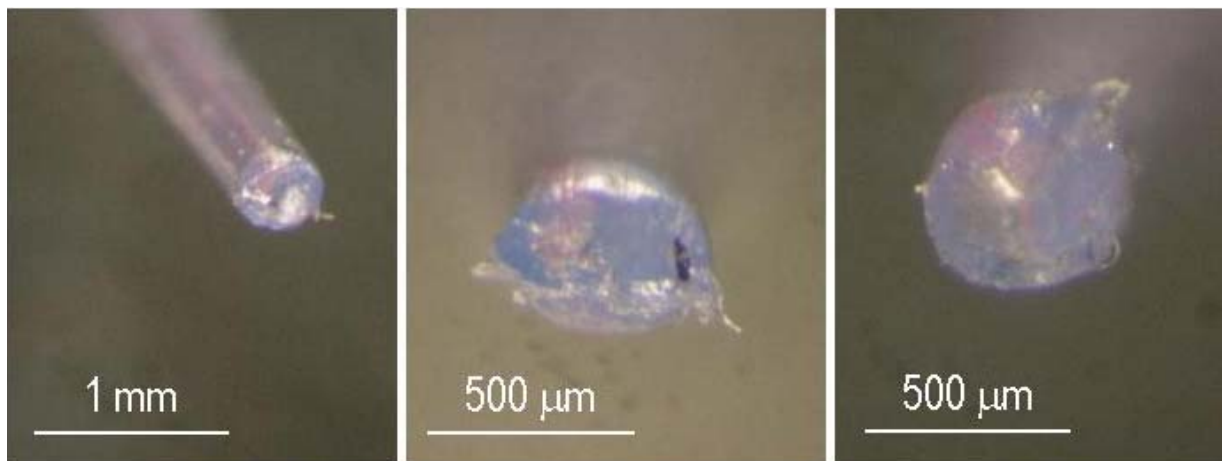


Figure 68. Optical stereo-microscopy image of multilumen preceramic silicone resin microtubes (H44, Filler #2, blue coloring agent)

However, using the H44 preceramic polymer and Filler #2 it was also possible to produce microtubes in which the different filaments of sacrificial filler were not only reasonably well separated, but also quite homogeneously placed within the microtubes' cross-section (see Figures 69 and 70) In particular in Figure 69, center, and Figure 70, left, it is possible to clearly distinguish 9 separate filaments (albeit some seem to be touching). The difference in color among some of the filaments is due to a non homogeneous distribution of the coloring agent within the sacrificial filler. The filaments appear to have a similar thickness, of about 50-90  $\mu\text{m}$ . The overall thickness of the microtubes, before pyrolysis, appears again to be in the  $\sim 450\text{-}600$   $\mu\text{m}$  range.

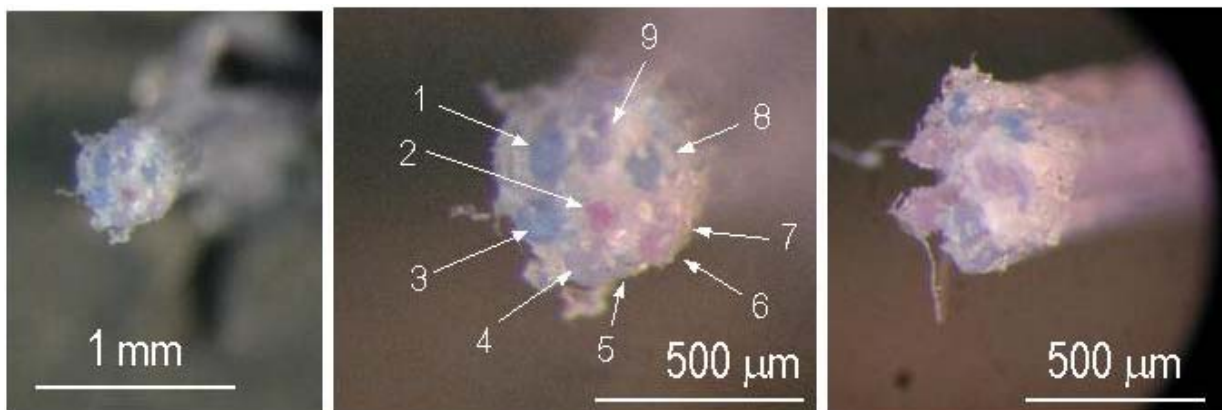


Figure 69. Optical stereo-microscopy image of multilumen preceramic silicone resin microtubes (H44, Filler #2, blue coloring agent)

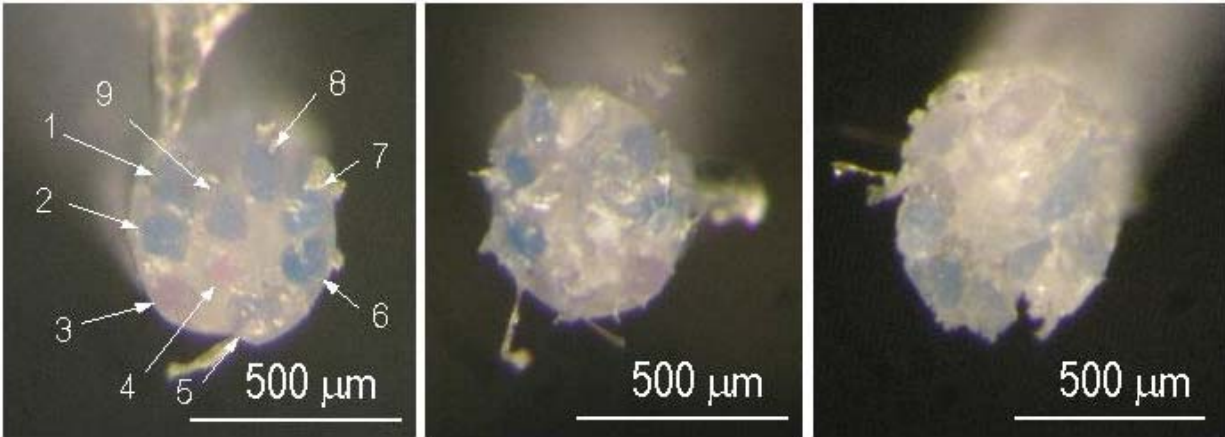


Figure 70. Optical stereo-microscopy image of multilumen preceramic silicone resin microtubes (H44, Filler #2, blue coloring agent)

In other samples (see Figure 71), individual filaments are visible within the microtubes' cross-section, but their distribution is less homogenous, as observed before for some samples produced using the SOC-A35 preceramic polymer (see Figure 63).

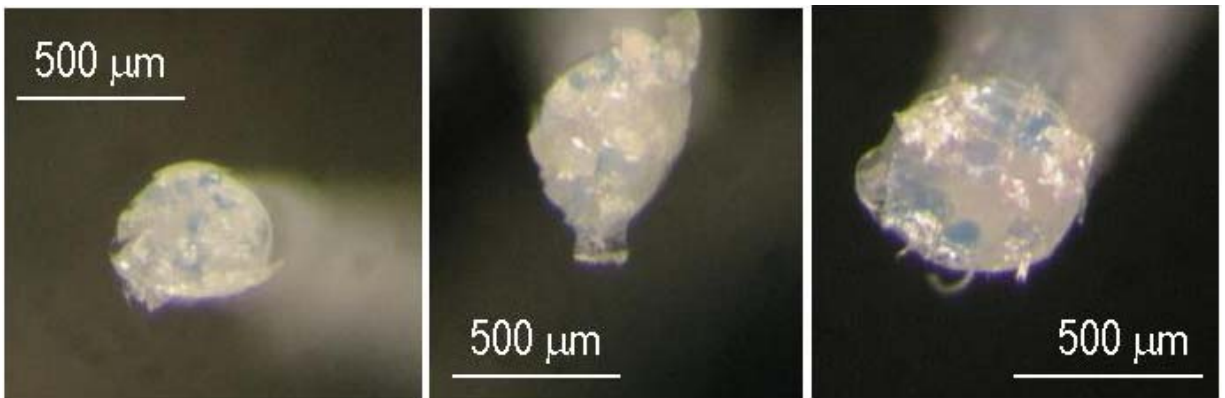


Figure 71. Optical stereo-microscopy image of multilumen preceramic silicone resin microtubes (H44, Filler #2, blue coloring agent)

In a third set of experiments, Filler #3 was used to fabricate the inner cores, and the extrusion was carried out by processing the SOC-A35 silicone resin at a temperature of about 90-110°C, while the Filler #3 reached temperatures in the range of 100 to 130°C. No coloring agent was added for this filler. Also in this case, successful co-extrusion was achieved, as demonstrated by the images shown in Figures 72-75 referring to samples in which the silicone resin was as received or cross-linked, but in any case before pyrolysis. However, optical microscopy analysis reveals the presence of cracks in most samples, as observed previously when processing single-lumen microtubes (see Figures 19 and 20). This was attributed to the different mechanical properties of the preceramic polymer and the filler, and the images demonstrate that the problem is not eliminated when reducing the size of the sacrificial core. At this stage of the investigation it is not clear why a few samples did not have cracks, having been produced in the same identical

processing conditions as the cracked samples. In any case, we can state that Filler #3 is also not suitable for the production of multi-lumen microtubes.

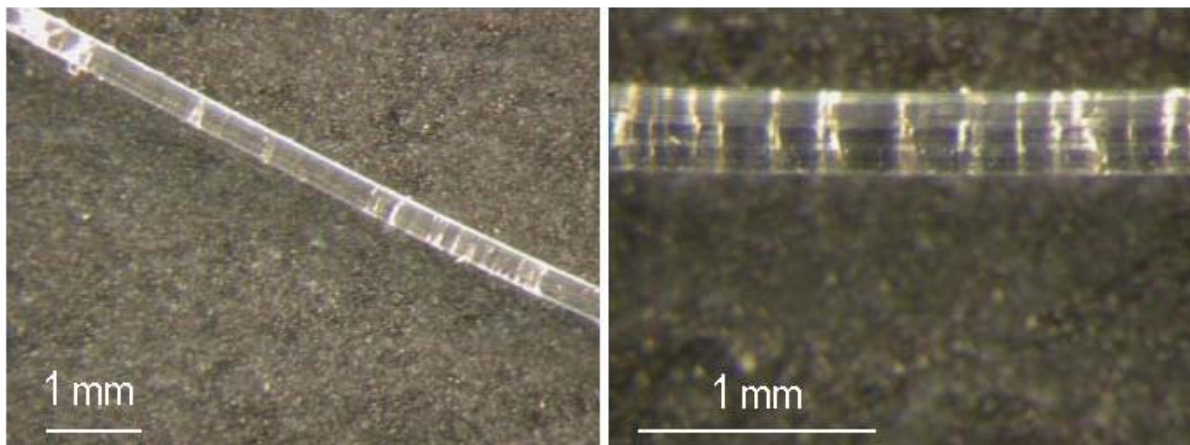


Figure 72. Optical stereo-microscopy image of multilumen preceramic silicone resin microtubes (SOC-A35, Filler #3). Samples were cross-linked. Note the presence of cracks, especially in the sample on the right.

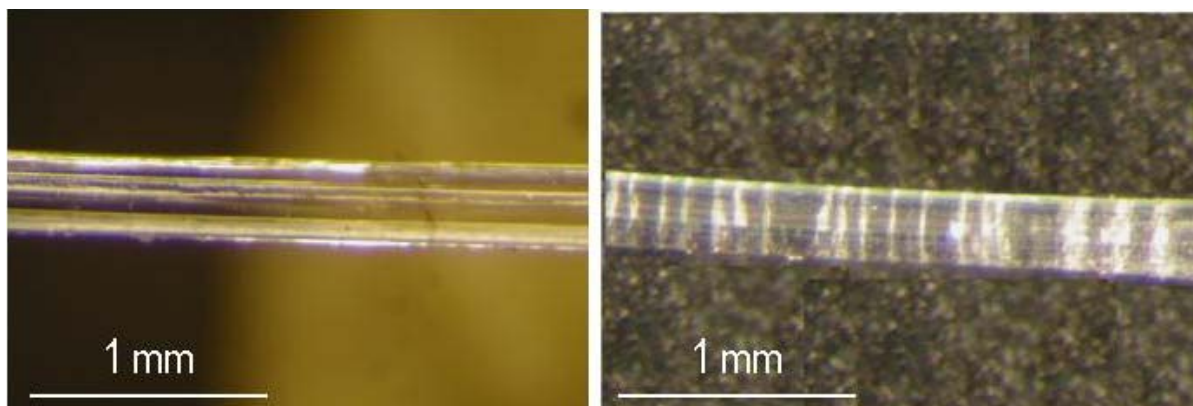


Figure 73. Optical stereo-microscopy image of a multilumen preceramic silicone resin microtube (SOC-A35, Filler #3). Samples were cross-linked. Sample on the left did not appear to have cracks; sample on the right was cracked (processing of both samples was identical).

The attempt of cutting the edge of a microtube in order to assess the position of the sacrificial filler strands did not prove successful (see Figure 74, left) due to the elastomeric nature of Filler #3. Upon removing part of the preceramic polymer, it was possible to see the individual strands (see Figure 74, right, and Figure 75). However, again because of the characteristics of the filler, this operation probably modified the size of the filaments, due to stretching by the blade.

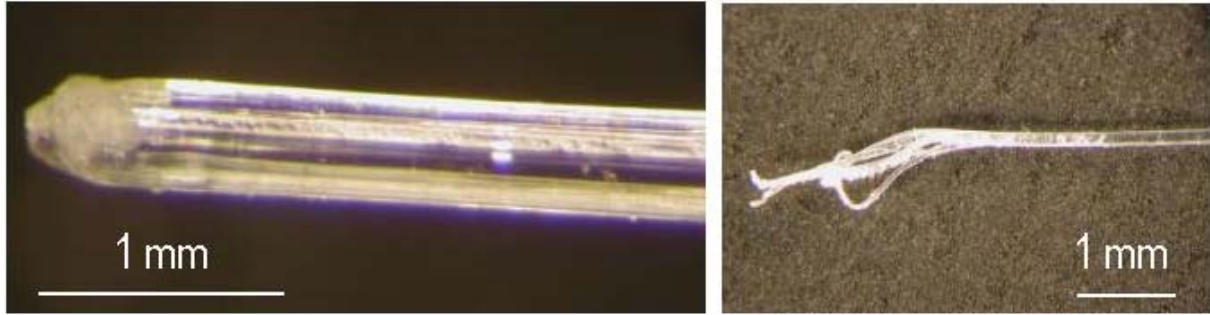


Figure 74. Optical stereo-microscopy image of a multilumen preceramic silicone resin microtube (SOC-A35, Filler #3). Samples were cross-linked.

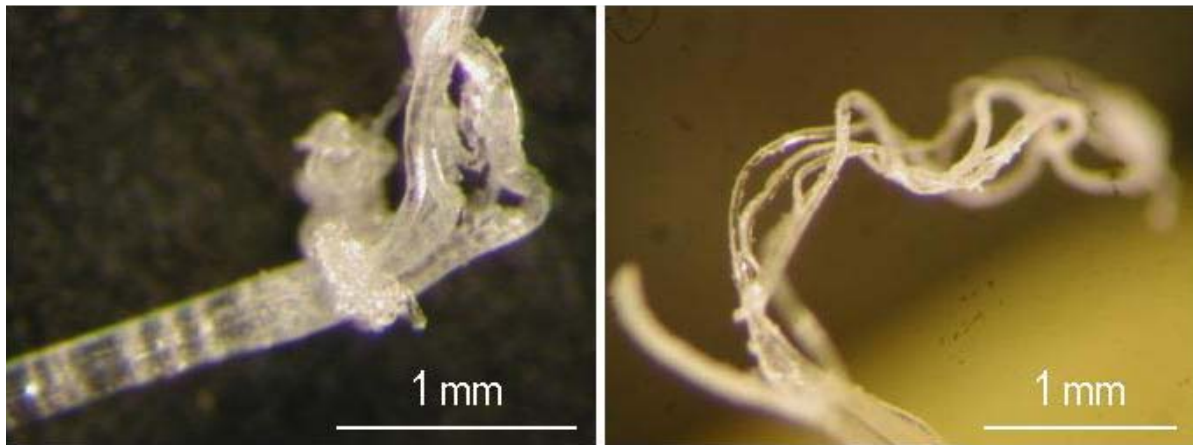


Figure 75. Optical stereo-microscopy image of multilumen preceramic silicone resin microtubes (SOC-A35, Filler #3). Samples were cross-linked.

As mentioned before, SEM analysis was also used for investigating the produced microtubes; as an example in Figure 76 is shown the outer surface of a microtube, in which some defects seems to be present (in particular a non perfectly circular shape, possibly due to the presence of several filler filaments within the cross-section and to the nature of the sacrificial filler – Filler #3).

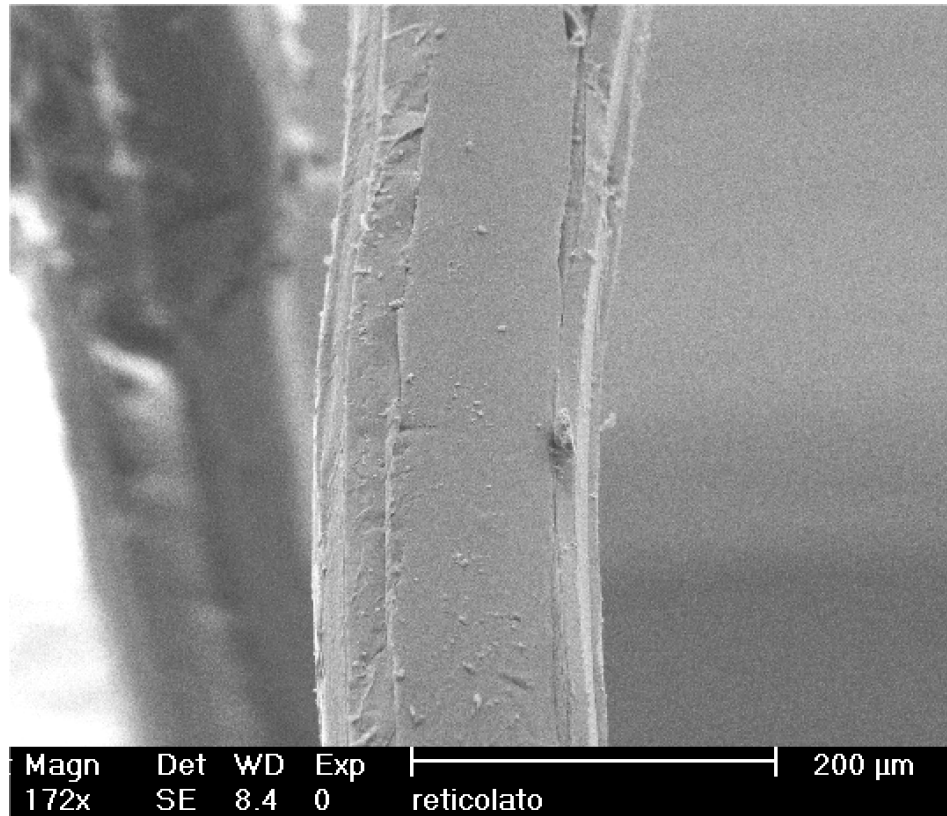


Figure 76. SEM image of a multilumen preceramic silicone resin microtube (SOC-A35, Filler #3). Sample was cross-linked.

In Figure 77 is shown an image of the end of a multilumen microtube produced using Filler #3, in which it was attempted to remove the silicone resin to expose the various filler filaments. The number of filaments does not seem to be 9, as expected, but this is probably due to the fact that some of them joined together during processing. In fact, the diameter of the single filaments is of the order of 40  $\mu\text{m}$ , but some of the strands are larger than what they should be, evidently because they're not comprised of single, individual filaments. The presence of some silicone resin debris attached to the filler strands, noticeable in Figure 77, indicates an interaction between Filler #3 and the preceramic polymer (more probably due to the chemical nature of the two components, as the processing temperature for Filler #3 was lower than that for Filler #2), adding to the non suitability of this filler material for the production of multilumen microtubes, at least in the processing conditions employed in these experiments.

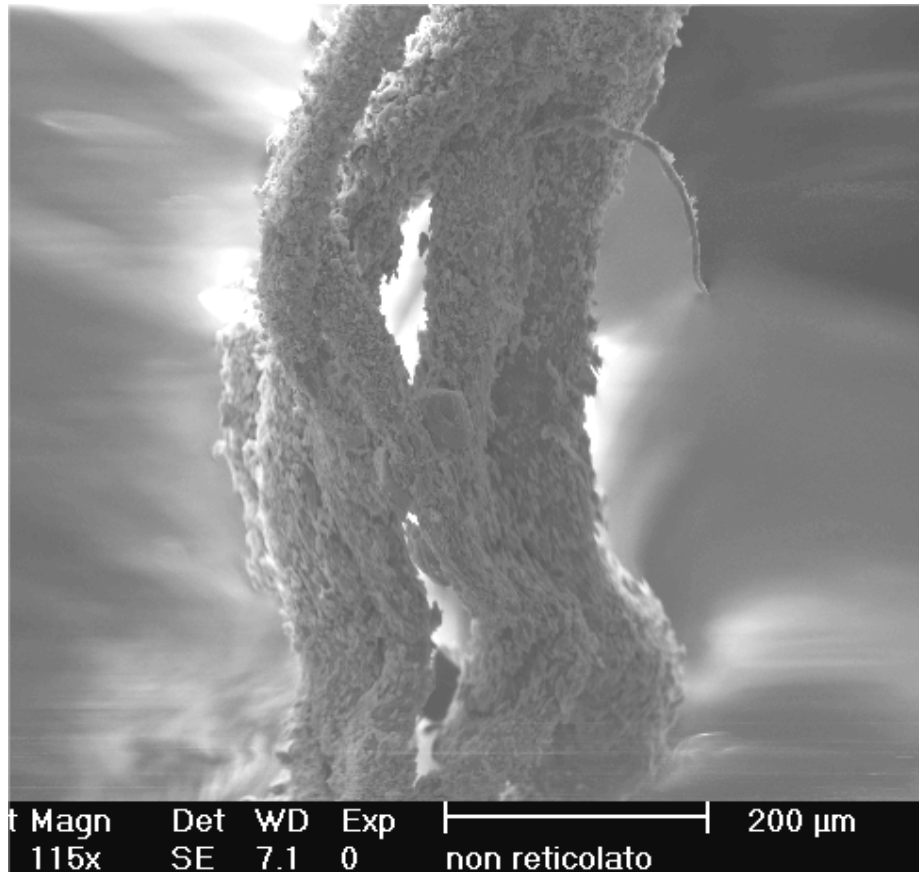


Figure 77. SEM image of a multilumen preceramic silicone resin microtube (SOC-A35, Filler #3). Sample was not cross-linked

#### 4.1. Further experimentation for the fabrication of multi-lumen microtubes

Further experimentation was carried out using the SOC-A35 and H44 silicone resins and Filler #2, with the aim of improving the morphology of the multi-lumen microtubes before pyrolysis. In particular, we modified the flow rate of the sacrificial filler within the extruder's head (which is related to the amount of filler ending up embedded in the silicone resin microtube) with the hope to increase the amount of silicone resin within the cross-section as well as to obtain a more homogeneous distribution of the sacrificial filler filaments in the same cross-section.

However, all the tests we performed varying different parameters (flow rate, temperature, drawing rate) did not prove successful, leading often to samples with a less homogeneous morphology than before, as illustrated by an example shown in Figure 78-80. A blue die was added to the filler for improved clarity, and the pictures of samples were taken after the cross-linking step.

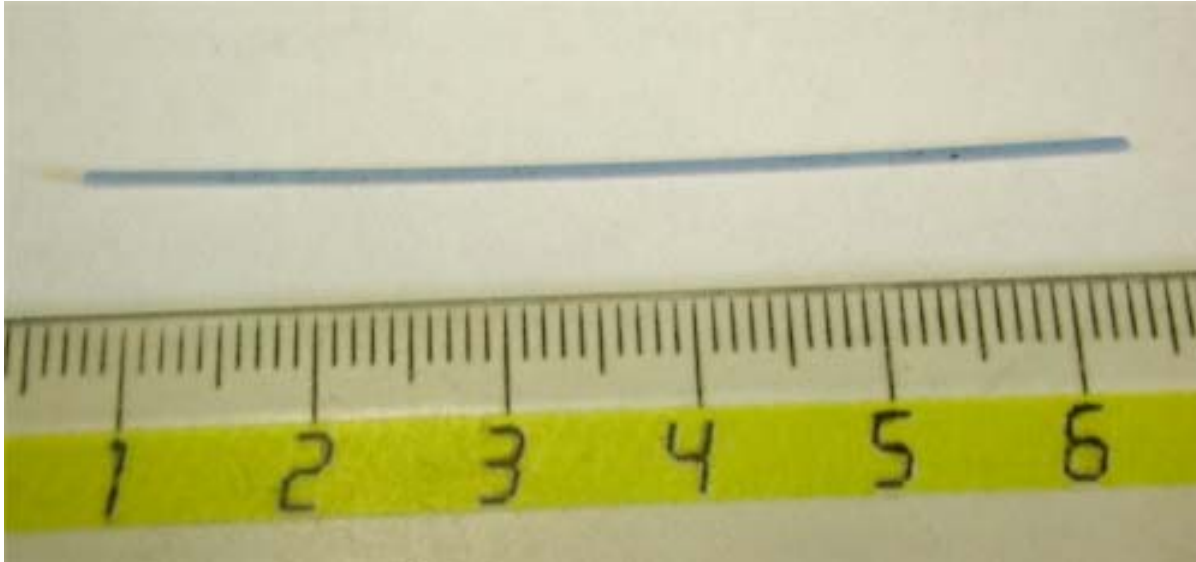


Figure 78. Digital image of multilumen preceramic silicone resin microtubes (SOC-A35, Filler #2, blue coloring agent)

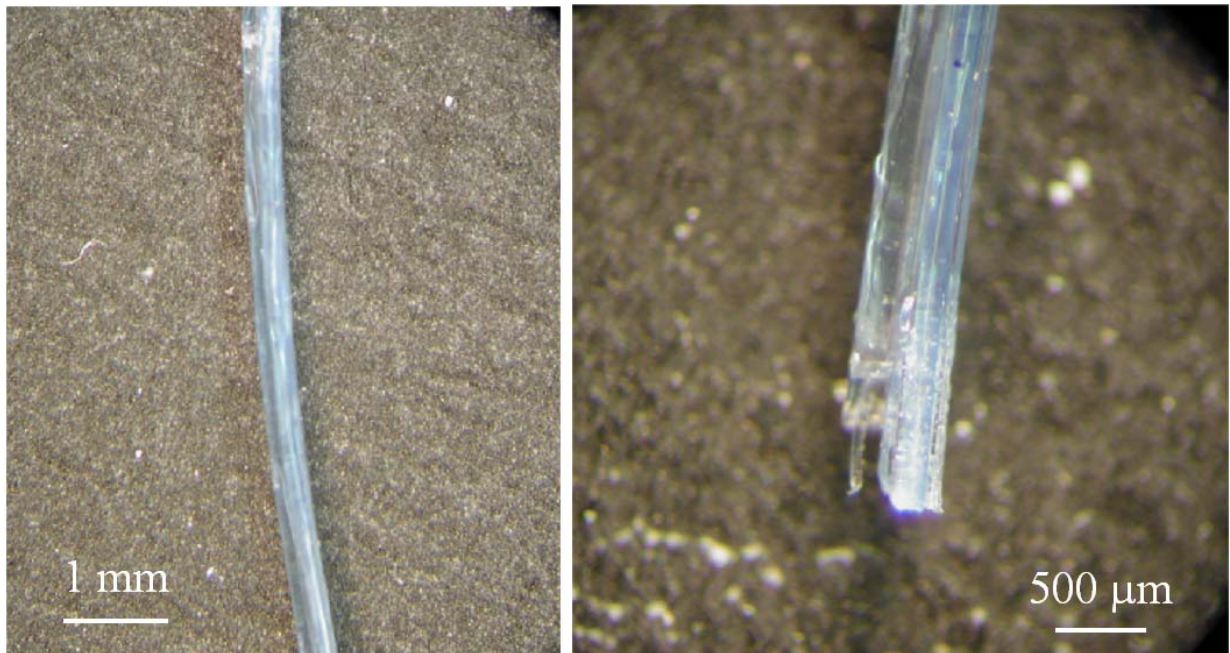


Figure 79. Optical stereo-microscopy image of multilumen preceramic silicone resin microtubes (SOC-A35, Filler #2, blue coloring agent)

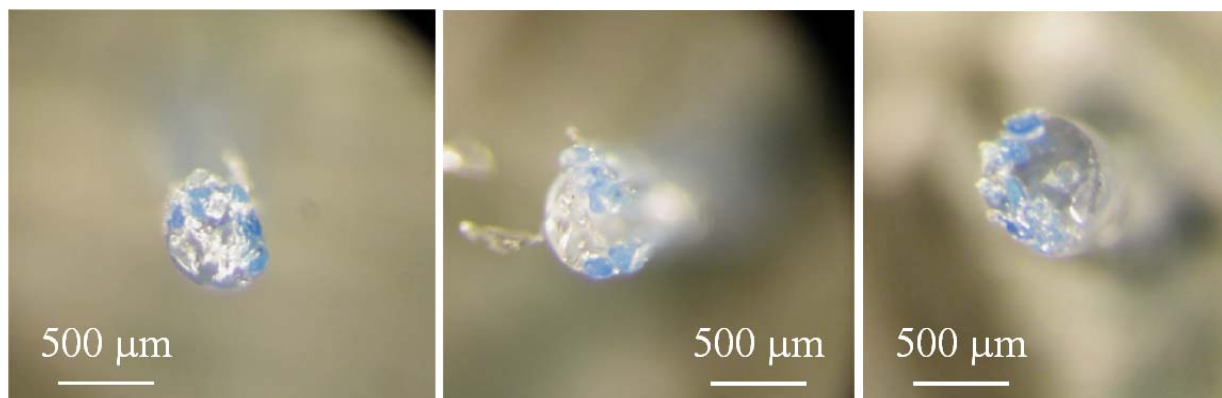


Figure 80. Optical stereo-microscopy image of multilumen preceramic silicone resin microtubes (SOC-A35 and H44 – sample at the right hand side, Filler #2, blue coloring agent)

As it can be seen, the produced samples did not have significant defects along the main axis, but the obtained distribution of the sacrificial filler filaments within the cross-section was not optimal, with the different strands grouped together either on a side of the microtube, or separated into two groups. Moreover, the thickness of the individual filaments do not appear to be significantly smaller than that of the strands in microtubes obtained in previous experiments (see Figures 69-71).

These findings point out on one side to the great sensitivity of the morphology of the multi-lumen microtubes to the processing conditions (small variations in the processing conditions lead to a non satisfying cross-section morphology), and on the other side to the complexity of the inter-relationship among the different processing variables (among them: the flow rate of the silicone resin and the sacrificial filler, the temperature profile in the extruder's head, the drawing rate). A separate study of the effect of the various parameters on the morphology, in which a single parameter is changed at any given time, should be conducted, but this lies outside the scope of the present work.

#### 4.2. Ceramization of the multi-lumen, co-extruded microtubes

The samples, obtained using SOC-A35 or H44 silicone resins and Filler #2, were pyrolyzed in a tube furnace, after cutting them into pieces approximately 5 cm long, by putting them in alumina boats. Following what was previously done for single-lumen microtubes, the pyrolysis schedule adopted comprised heating in inert atmosphere (nitrogen gas) at the constant rate of 2°C/min up to a temperature of 1200°C (with a 1h dwelling time at final temperature).

Similarly to the previous experiments concerning single-lumen microtubes, the quality of the multi-lumen microtubes fabricated by co-extrusion, after ceramization, depended on various parameters, including the degree of cross-linking achieved before pyrolysis, the quality of the produced microtubes in the polymeric stage (e.g. presence of surface defects, presence of a permanent curvature/deviation from straightness) and the layout of the samples in the refractory support boat.

Because we built on the experience of previous tests and were thus able to select the appropriate cross-linking and pyrolysis conditions, we never experienced problems related to partial melting of the microtubes (due to partial cross-linking of the silicone resin) or incomplete ceramization of the specimens.

Moreover, despite the presence of a relatively large amount of sacrificial filler filaments within the cross-section of each microtube, we also did not observe the presence of defects attributable to the release of gas coming from the decomposition of the sacrificial filler upon pyrolysis (the samples never fractured into several small pieces, as it would occur if a build-up of internal pressure would form, leading to an “explosive” release of gas). This is likely due both to the fact that we pyrolyzed relatively short specimens (< ~5 cm) and that during the polymer-to-ceramic transition a significant transient porosity forms because of the transformations occurring in the preceramic polymer. This porosity, which is open and interconnected, develops in a range of temperatures (approximately 350-650°C) at which the fillers decompose (the fillers were chosen specifically for this reason), allowing both for the release of the decomposition gas and for the production of dense ceramic components, when continuing the pyrolysis treatment at higher temperatures. Moreover, the heating rate was appropriately chosen to be very slow, allowing for the continuous formation and release of gas upon pyrolysis in the polymer-to-ceramic transformation temperature range.

However, some samples did break into fragments during the heat treatment, but SEM investigations seemed to indicate that the reason for the breakage was related to the specific morphology of the specimens (see later), instead of being associated to the decomposition of the filler filaments.

In Figures 81-83 are shown digital images of the pyrolyzed multi-lumen microtubes, obtained both using SOC-A35 or H44 silicone resin and Filler #2.

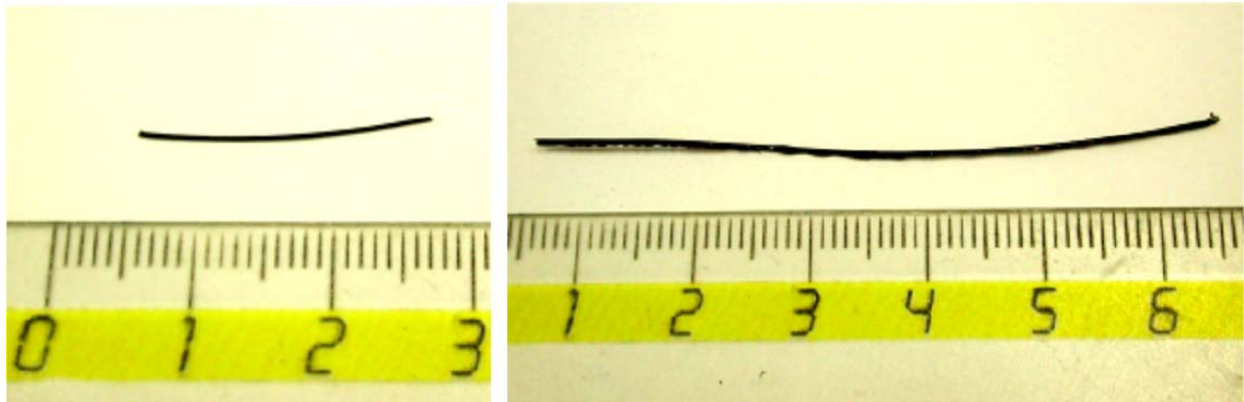


Figure 81. Digital image of pyrolyzed multilumen preceramic silicone resin microtubes (SOC-A35 - left; H44 – right; Filler #2)

The produced samples in some cases were of good quality (see Figure 81), while in other they displayed a large deflection from linearity (see Figure 82). The distortion in shape upon pyrolysis can be attributed to both a preexisting partial curvature in the samples as well as to a non homogeneous distribution of the filler filaments within the cross-section of the microtube. However, if the samples were cut into smaller segments (~ 1 cm long) before pyrolysis, they remained straight after the heat treatment (see Figure 83).

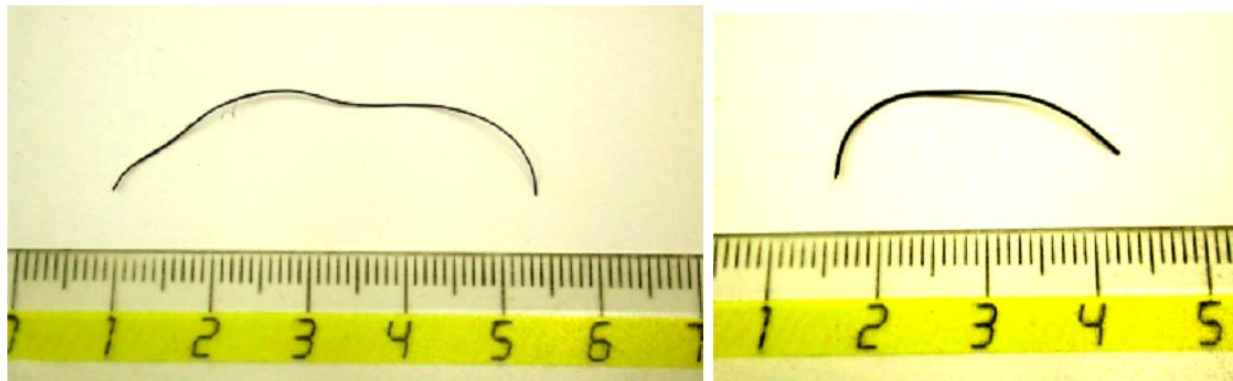


Figure 82. Digital image of pyrolyzed multilumen preceramic silicone resin microtubes (SOC-A35 - left; H44 – right; Filler #2)

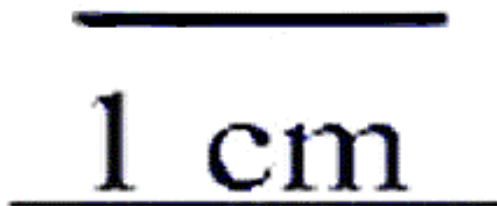


Figure 83. Digital image of a pyrolyzed multilumen preceramic silicone resin microtube (SOC-A35; Filler #2)

We did not observe significant differences when pyrolysing samples obtained from the two different silicone resins, in accordance with the fact that their behavior upon ceramization is similar (see paragraph 2.3).

#### 4.3. Morphological characterization of the pyrolyzed multi-lumen microtubes

The morphology of the pyrolyzed samples was characterized using SEM microscopy. The analysis reported here refer to samples obtained using SOC-A35 or H44 silicone resins and Filler #2, after pyrolysis at 1200°C. Differences in the morphology of the cross-section can be attributable to the difference in rheological behavior between the two silicone resins, and not to other factors such as the decomposition behavior or possible variation in the coefficient of thermal expansion between the two preceramic polymers.

In Figure 84-91 are shown SEM micrographs of the multi-lumen microtubes produced by co-extrusion using SOC-A35 silicone resin and Filler #2 (see paragraph 3.2).

Using this silicone resin it was possible to fabricate samples which did not break upon pyrolysis and were not curved (see Figure 84), even if some surface defects were present in some samples (see for example a longitudinal crack along the main axis of the microtube in Figure 84). This is probably not related to the handling of the microtubes prior to the analysis but rather to some intrinsic defect originated by the presence of the sacrificial filler filaments.

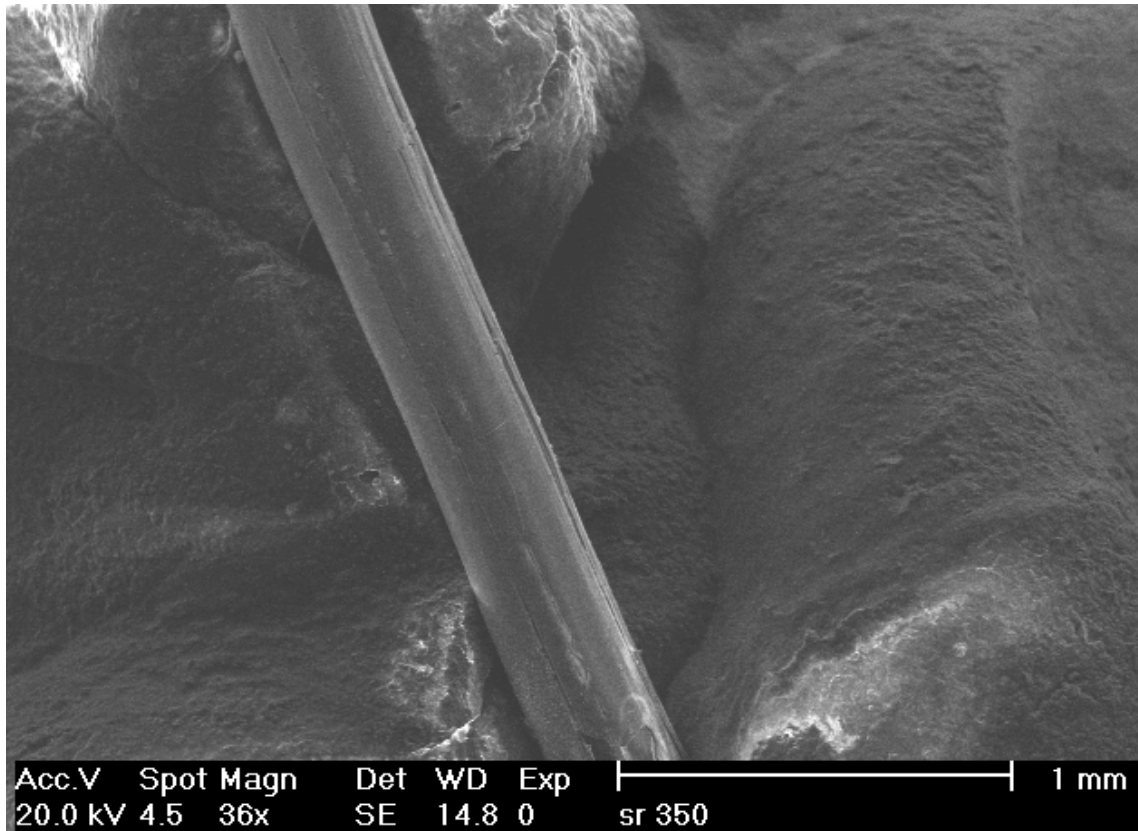


Figure 84. SEM image of a co-extruded multi-lumen microtube, after pyrolysis (SOC-A35 and filler #2)

As it can be seen in the following images, using the SOC-A35 silicone often did not lead to multi-lumen microtubes with a suitable morphology, as discussed previously in paragraph 3.2. In particular, the axial holes left by the sacrificial filaments appear in some instances to be grouped together, or to have different sizes and shapes or to be non evenly spaced within the cross-section. This led, in some instances, to the formation of cracks in the specimens, especially when the sacrificial filament(s) was very close to the edge of the microtube's cross-section; in fact during the heat treatment, either the gas escaping from the material or, more probably, the differential shrinkage between filler and silicone resin caused the ceramic material to fracture, leaving a inhomogeneous cross-section.

Of course, one cannot rule out that the cracks formed during the handling of the specimens, particularly considering that in some cases only a very thin (a few microns) layer of SiOC ceramic separates the axial hole from the outside, but it seems more probable that the fractures formed during pyrolysis (considering also that in some cases some cracks appear to be present along a good part of the main axis - see Figure 84, as discussed previously, thus likely ruling out accidental damage). Another example of damages (longitudinal cracks) on the surface of a pyrolyzed multi-lumen microtube is reported in Figure 85.

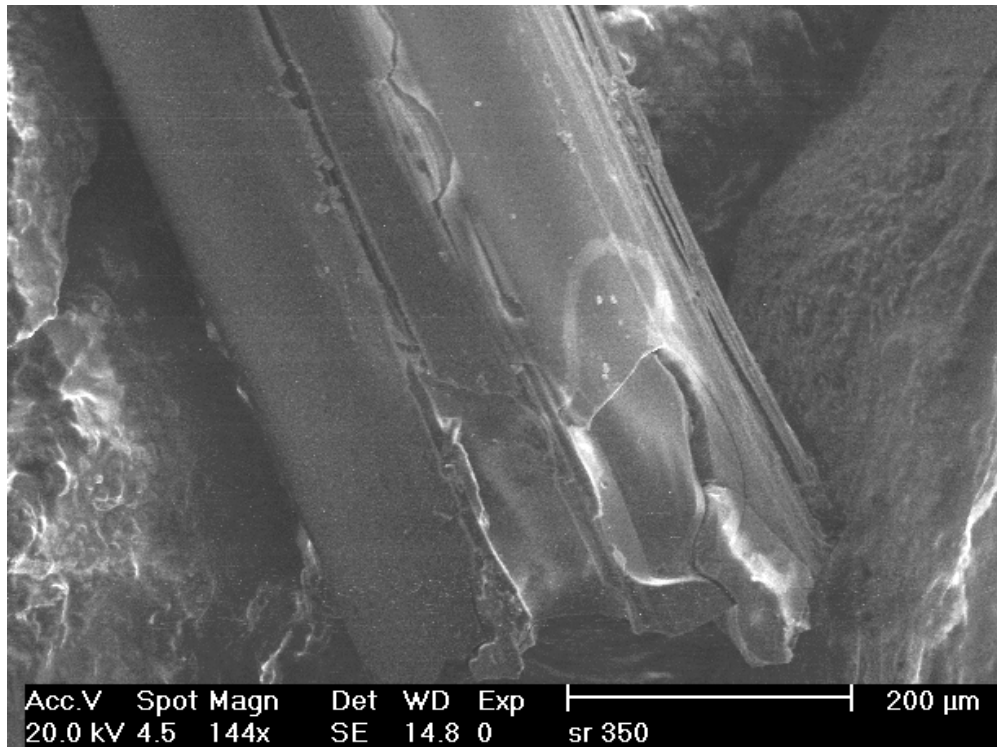


Figure 85. SEM image of a co-extruded multi-lumen microtube, after pyrolysis (SOC-A35 and filler #2)

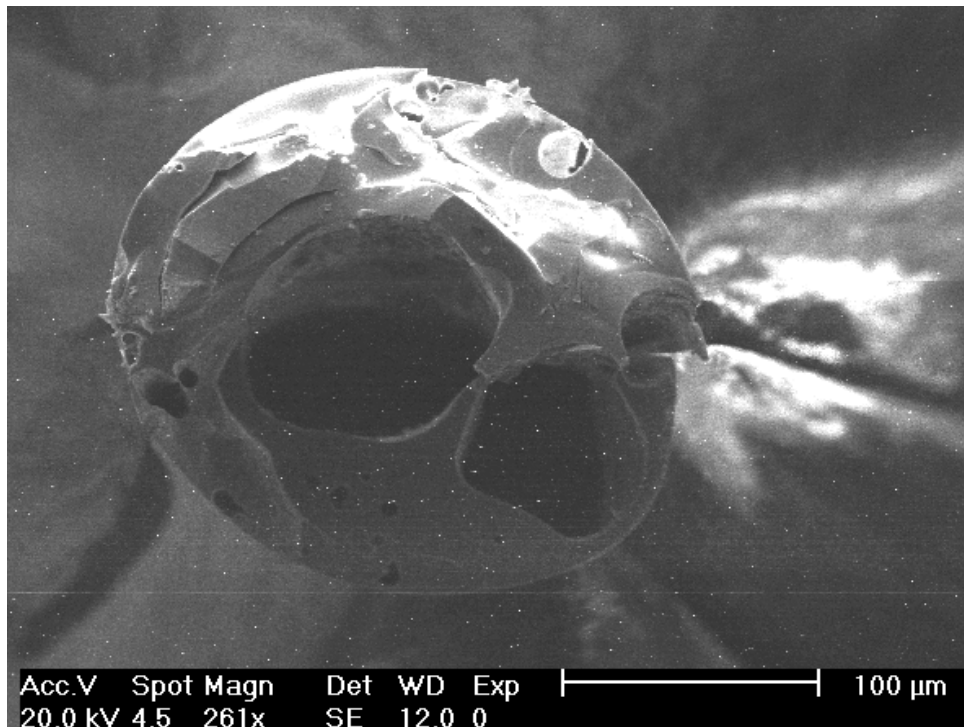


Figure 86. SEM image of a co-extruded multi-lumen microtube, after pyrolysis (SOC-A35 and filler #2)

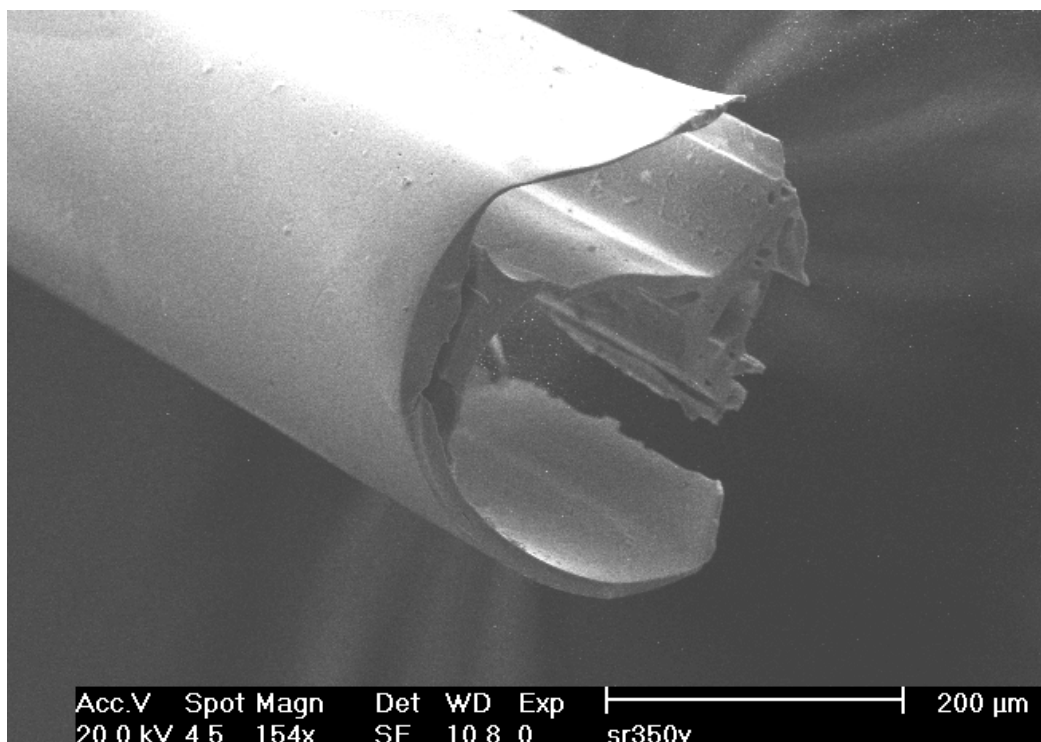


Figure 87. SEM image of a co-extruded multi-lumen microtube, after pyrolysis (SOC-A35 and filler #2)

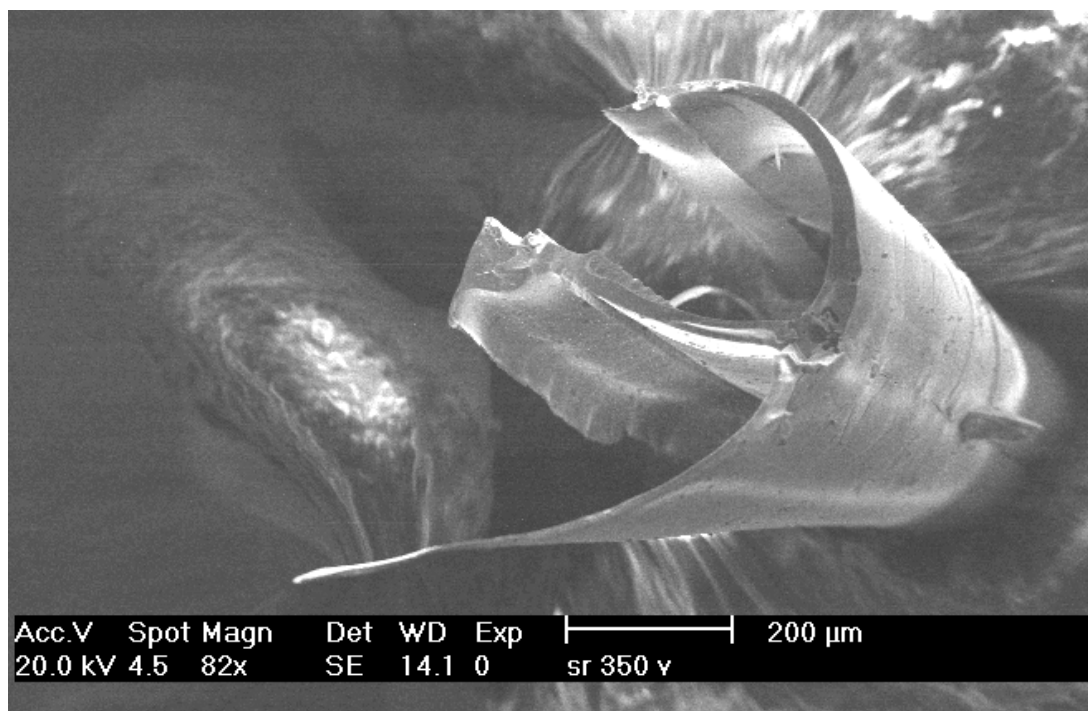


Figure 88. SEM image of a co-extruded multi-lumen microtube, after pyrolysis (SOC-A35 and filler #2)

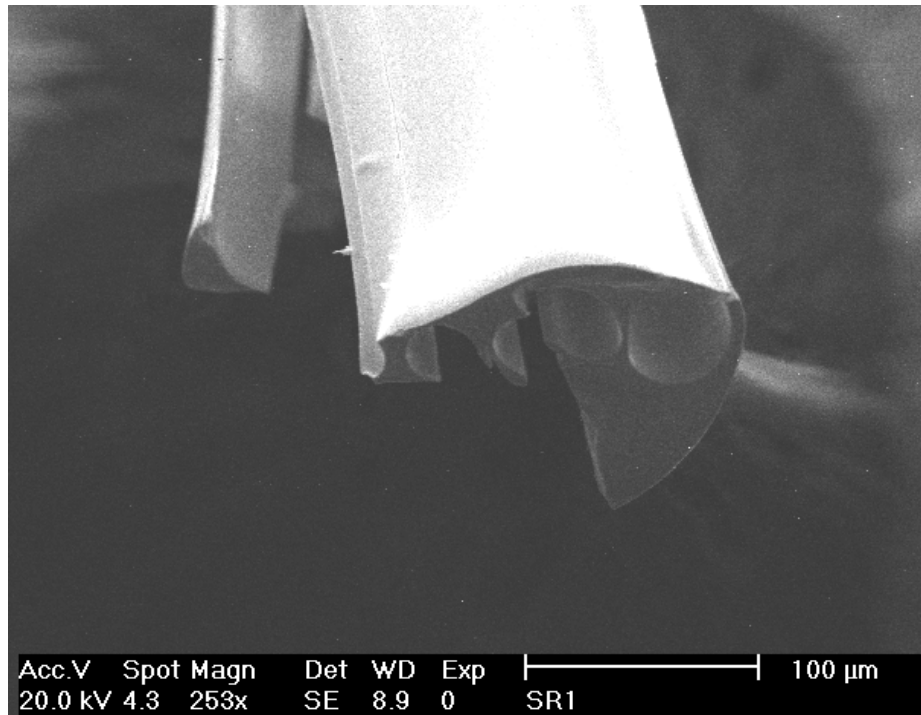


Figure 89. SEM image of a co-extruded multi-lumen microtube, after pyrolysis (SOC-A35 and filler #2)

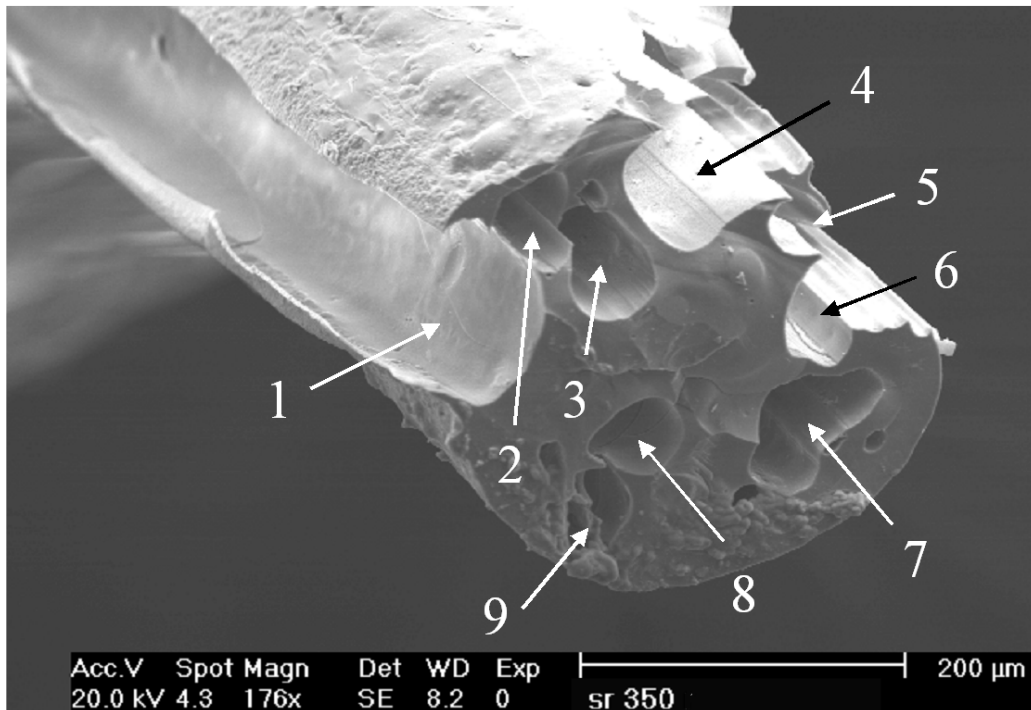


Figure 90. SEM image of a co-extruded multi-lumen microtube, after pyrolysis (SOC-A35 and filler #2)

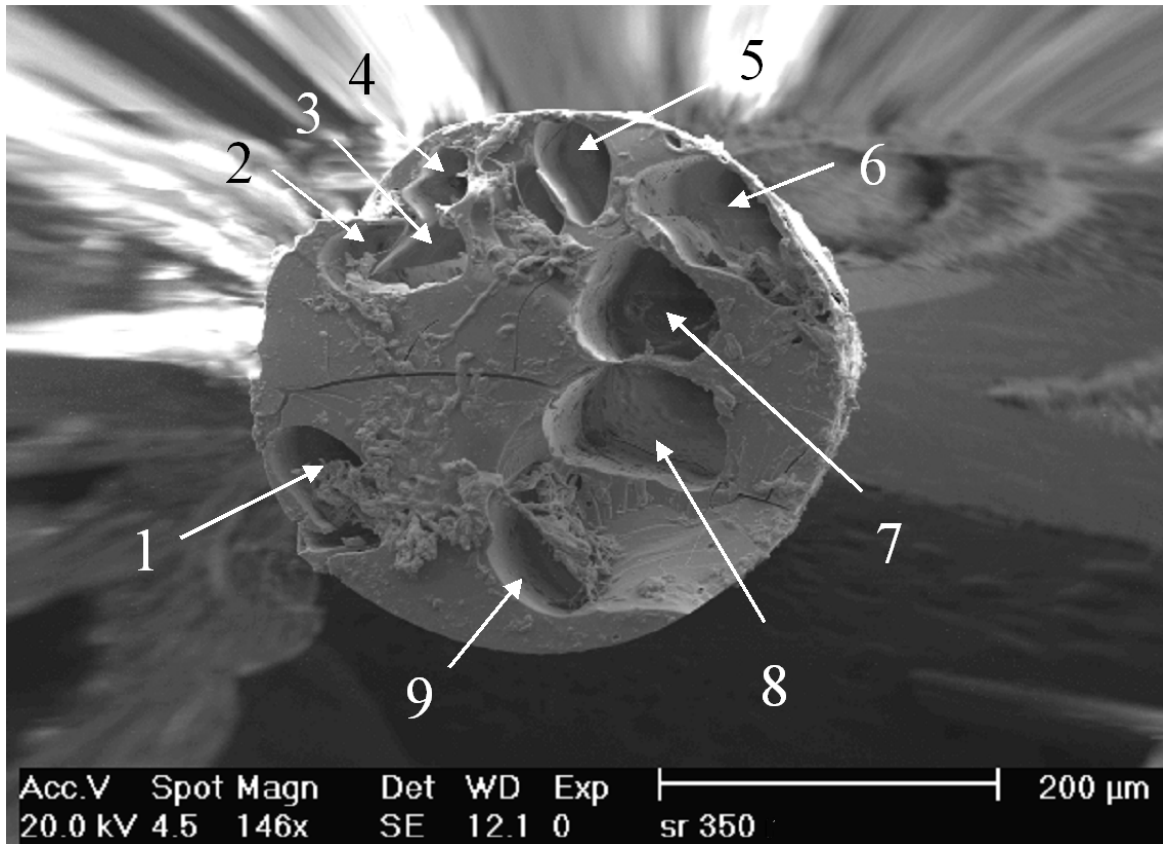


Figure 91. SEM image of a co-extruded multi-lumen microtube, after pyrolysis (SOC-A35 and filler #2)

Figure 86 shows an example of a microtube in which the sacrificial filler filaments grouped together during extrusion, leaving only two major cavities and another individual cavity instead of nine separate holes. Figure 87 and 88 show again a similar example, but in this case very little ceramic material is left at the edge of the cross-sections, indicating that the silicone resin outside layer was very thin. In our opinion, the reason why the microtubes appear to be fractured in the axial direction is precisely that only a thin layer of silicone resin was present in those areas after co-extrusion, and during pyrolysis it fractured, probably due to the CTE mismatch between the preceramic polymer and the sacrificial filler. Figure 89 and 90 show examples of microtubes in which the distribution of voids in the cross-section is not homogeneous; in Figure 90 in particular it can be seen that when the holes left by the decomposition of the filaments are too close to the edge of the microtube, then the surface tends to fracture. In the same cross-section some voids deriving from the presence of bubbles in the preceramic microtube are also evident. Figure 91 shows an example of a microtube which did not fracture upon pyrolysis; however the size and the shape of the holes left by the decomposition of the sacrificial filaments are not homogeneous, and some of the voids are very close to the edge of the microtube.

Using the H44 preceramic polymer gave somewhat better results in terms of the morphology of the ceramic multi-lumen microtubes produced, as observed already earlier in the preceramic stage (see paragraph 3.2). This difference in our opinion is related mainly, as pointed out

previously, to the difference in rheological behavior of the two preceramic polymers, allowing for a better distribution of the sacrificial filaments upon co-extrusion. This difference in the rheological behavior should be quantified using viscometric measurements, and will be the subject of further studies; however it should be pointed out that the rheological properties of these silicone resins depend not only on their chemical structure and composition but also on the age of the batch where they come from. In fact, cross-linking reactions through condensation of Si-OH groups occur at ambient temperature, and thus the same preceramic polymer can exhibit a different viscosity/temperature curve depending on how old it is in relation to its synthesis date.

In Figure 92-102 are shown SEM micrographs of the multi-lumen microtubes produced by co-extrusion using H44 silicone resin and Filler #2 (see paragraph 3.2). Again, a variety of morphologies was observed, depending on the individual sample examined.

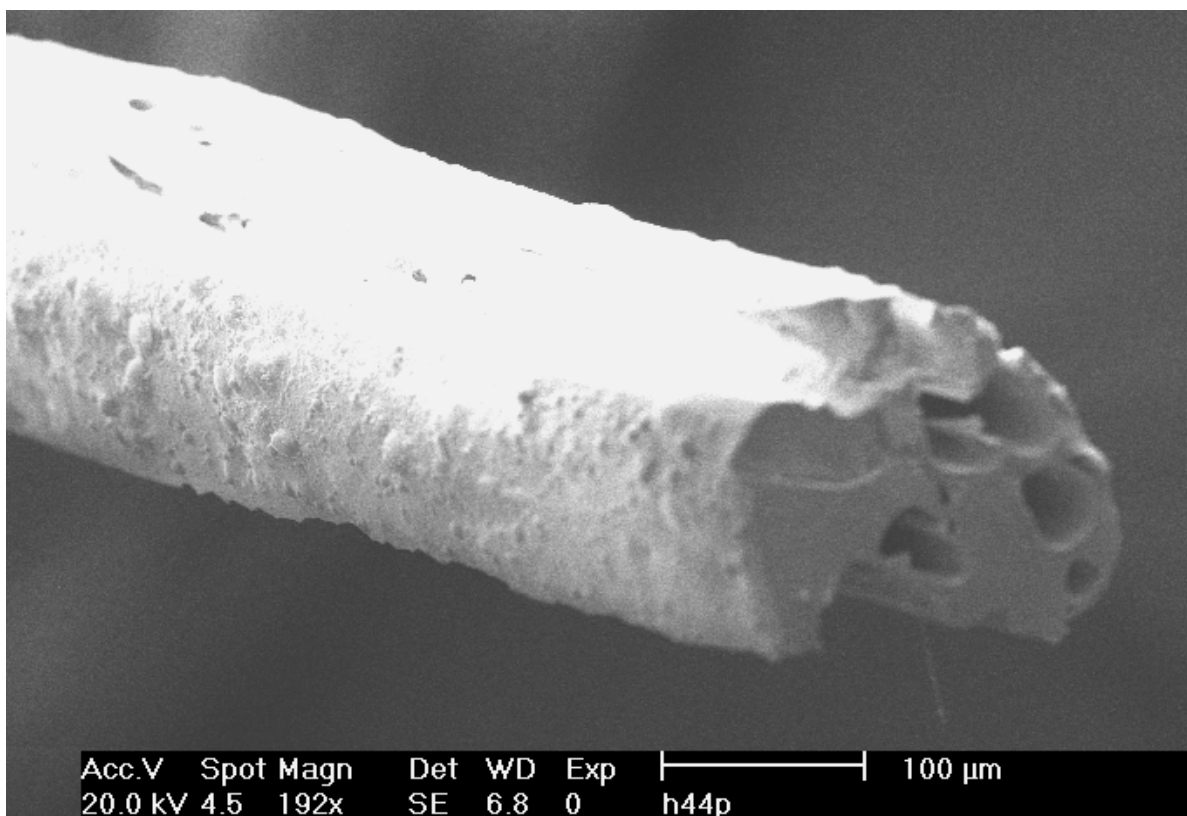


Figure 92. SEM image of a co-extruded multi-lumen microtube, after pyrolysis (H44 and filler #2)



Figure 93. SEM image of a co-extruded multi-lumen microtube, after pyrolysis (H44 and filler #2)



Figure 94. SEM image of a co-extruded multi-lumen microtube, after pyrolysis (H44 and filler #2)

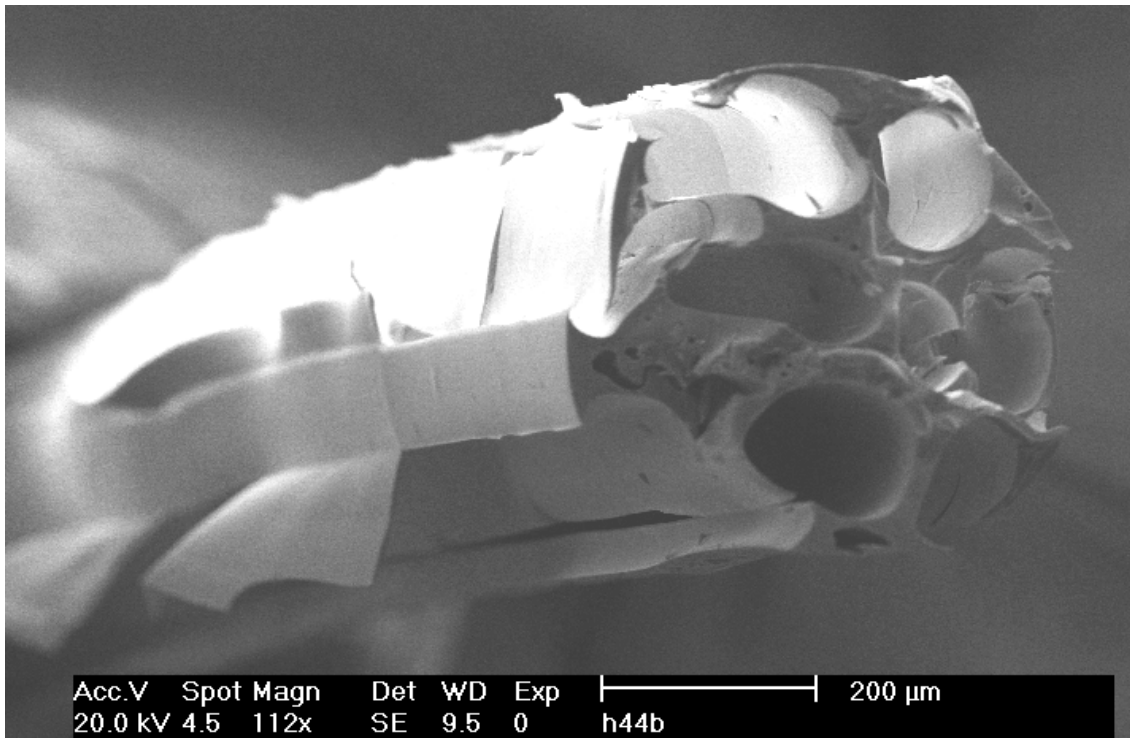


Figure 95. SEM image of a co-extruded multi-lumen microtube, after pyrolysis (H44 and filler #2)

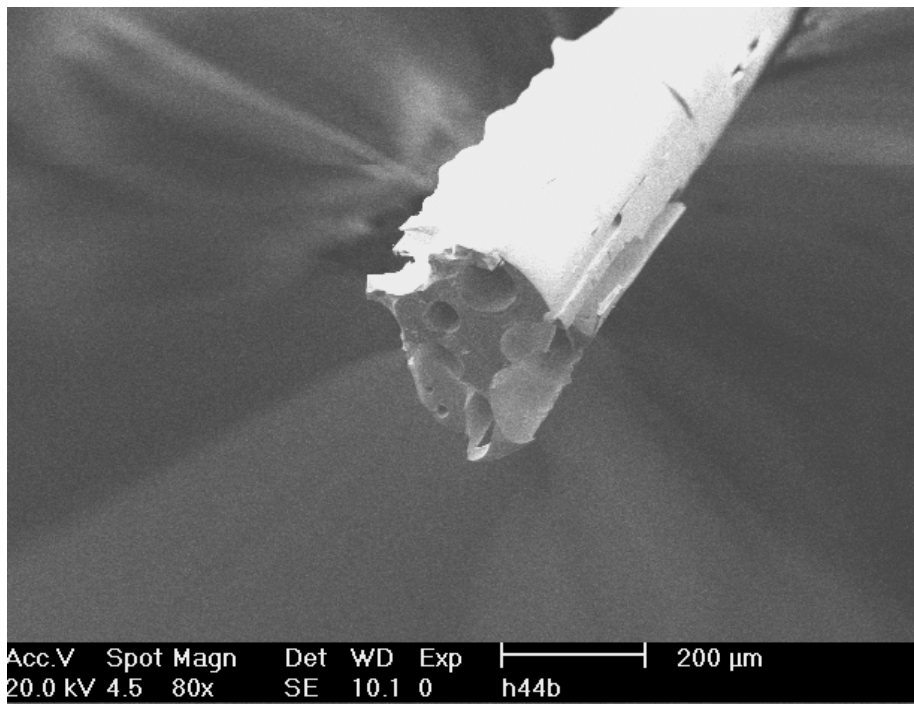


Figure 96. SEM image of a co-extruded multi-lumen microtube, after pyrolysis (H44 and filler #2)

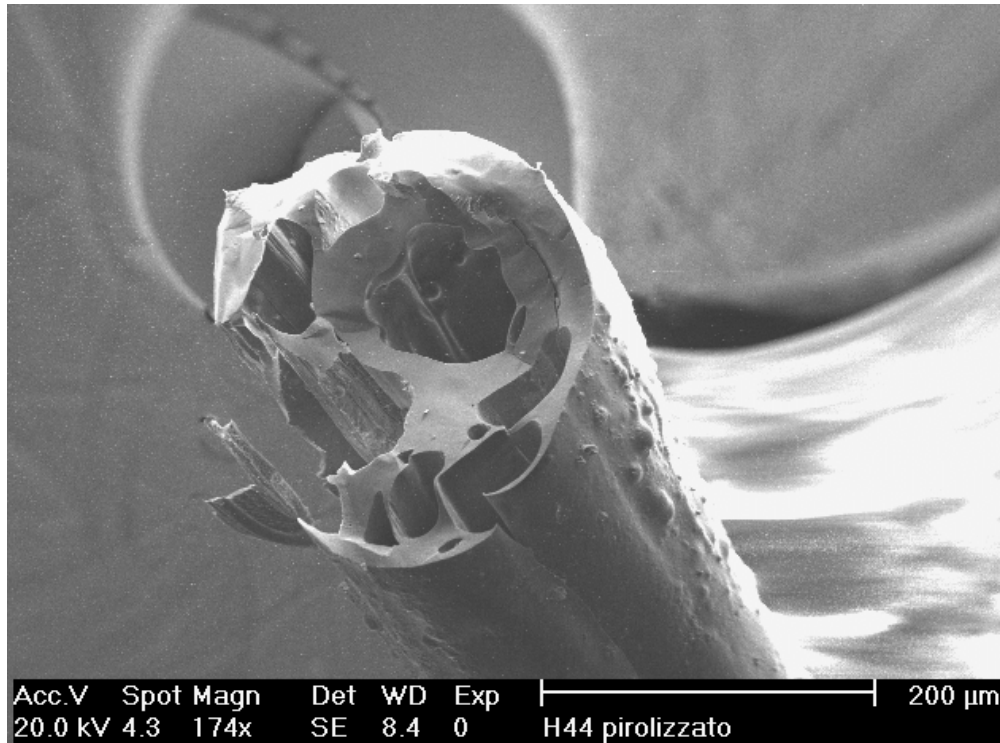


Figure 97. SEM image of a co-extruded multi-lumen microtube, after pyrolysis (H44 and filler #2)

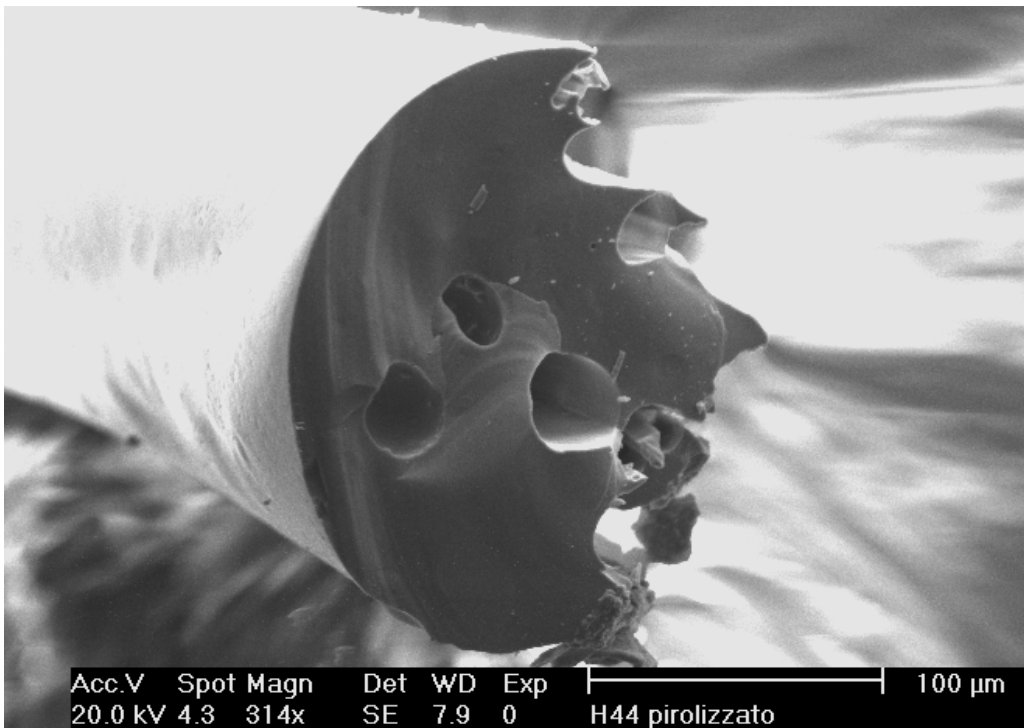


Figure 97. SEM image of a co-extruded multi-lumen microtube, after pyrolysis (H44 and filler #2 – sample obtained in a later series of experiments, see paragraph 4.1)

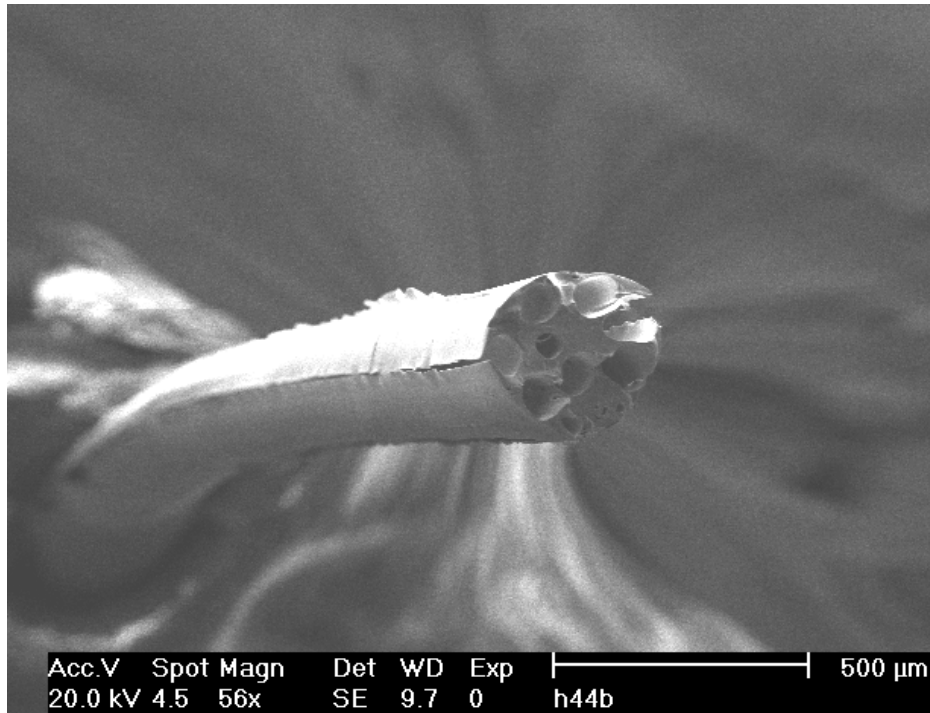


Figure 99. SEM image of a co-extruded multi-lumen microtube, after pyrolysis (H44 and filler #2)

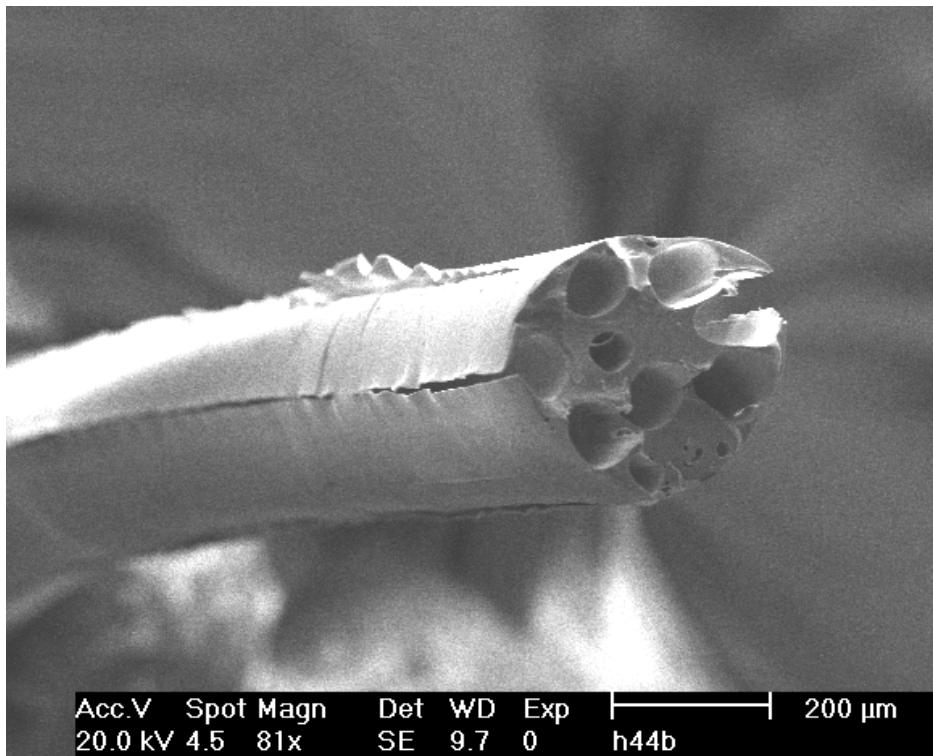


Figure 100. SEM image of a co-extruded multi-lumen microtube, after pyrolysis (H44 and filler #2). Same sample as Figure 99, but with a magnified view

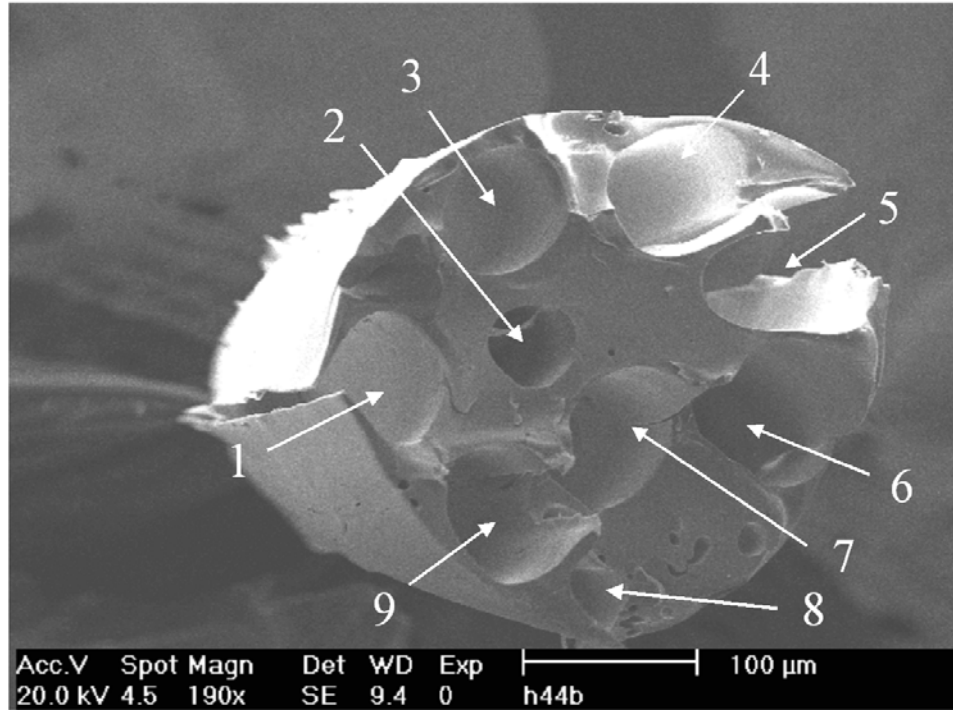


Figure 101. SEM image of a co-extruded multi-lumen microtube, after pyrolysis (H44 and filler #2) – same sample as Figures 99 and 100 but with a different view

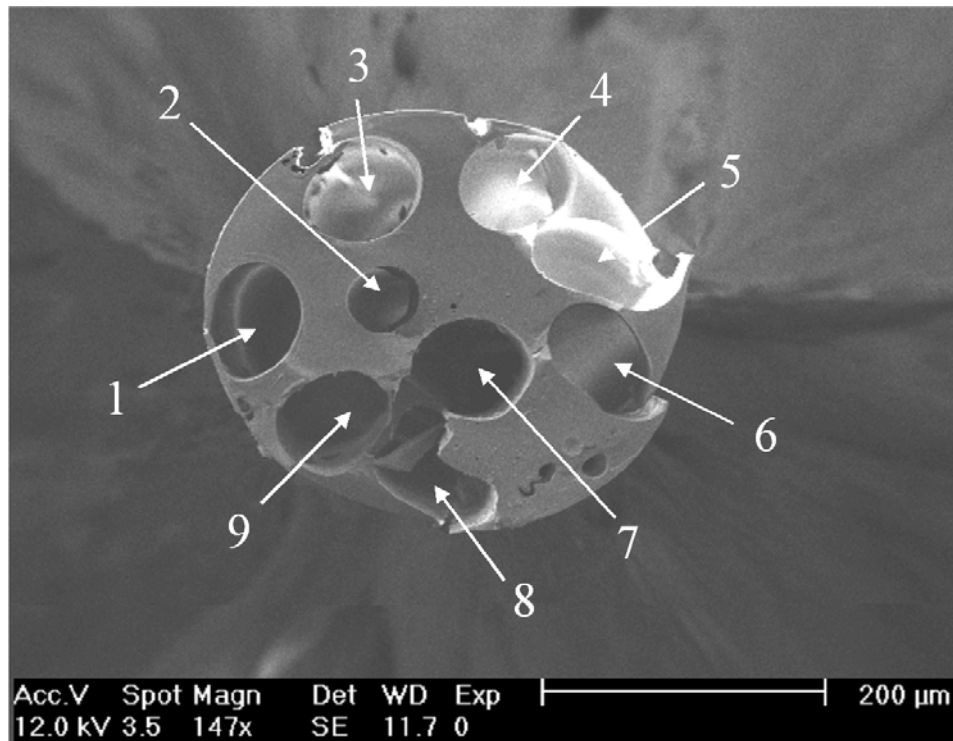


Figure 102. SEM image of a co-extruded multi-lumen microtube, after pyrolysis (H44 and filler #2)

Figure 92 and 93 show an example of ceramic microtubes in which most of the holes deriving from the decomposition of the sacrificial filler filaments were separated from each other, but some were too close to the edge of the microtube to avoid fracturing the surface upon pyrolysis. For the sample shown in figure 94 a similar effect occurred, and thus some grooves are present on the sides of the sample, with the lack of presence of the external layer of SiOC ceramic material. For the sample shown in Figure 95, one can clearly distinguish 9 holes, of different shape and size, with two of them being too close to the edge of the cross-section leading to a fractured surface. In Figures 96 and 97, again, samples in which the holes are clearly distinguishable are shown, with some of them being grouped together. The sample shown in Figure 98 was obtained in a later series of experiments (see paragraph 4.1), and the reported micrograph unmistakably indicates that the grouping of the filler filaments on one edge of the specimen in the preceramic stage led to an uneven distribution of the holes within the microstructure of the ceramic microtube (again, the filaments that were too close to the edge of the microtube led to the fracturing of the surface during pyrolysis).

However, as mentioned before, using the H44 preceramic polymer, it was possible to fabricate samples with a good, albeit not yet perfect, morphology. Figures 99-102 illustrate how in some cases the filler filaments were almost evenly distributed throughout the cross-section of the sample and were more homogeneous in size and shape. Again, the presence of a filament too close to the edge of the microtube led to the formation of a thin crack along the axis of the ceramic microtube (see Figures 99-101). Some occasional defects (voids) deriving from bubbles present in the sample at the preceramic stage are also visible in the cross-section.

The size of the pyrolyzed microtubes, obtained from both SOC-A35 and H44 silicone resins, ranged from about 250 to about 500  $\mu\text{m}$ , while the dimension of the inner axial holes ranged from about 50 to about 90  $\mu\text{m}$ . with respect to the data collected on as-prepared (cross-linked, before pyrolysis) microtubes, a linear shrinkage in the range 25-35 % was observed.

Because most of the samples contained surface defects, as illustrated by the micrographs reported above, it was not possible to measure their mechanical strength. Most of the samples broke during handling to position them on the fixture previously used for single-lumen ceramic microtubes (see Figure 49), and the ones that were tested did not possess any significant strength (suggesting that they contained significant defects as well).

To further clarify the occurrence of axial cracks on the external surface of the multi-lumen microtubes, SEM investigations were also conducted on the as-prepared microtubes still in the preceramic stage (before pyrolysis). In Figure 103 is shown a micrograph for one of the samples, showing what appears to be some longitudinal defects (indicated by the arrows). This finding suggests that at least some of the flaws in the microtubes are not due to the pyrolysis process, but derive from the extrusion process. Again, however, it seems pretty clear that the origin of these flaws is related to the presence of filler filaments too close to the edge of the microtube; the difference in characteristics (e.g. the coefficient of thermal expansion, different mechanical properties in the polymeric state) between the preceramic polymer and the filler material could account for the generation of defects during extrusion.

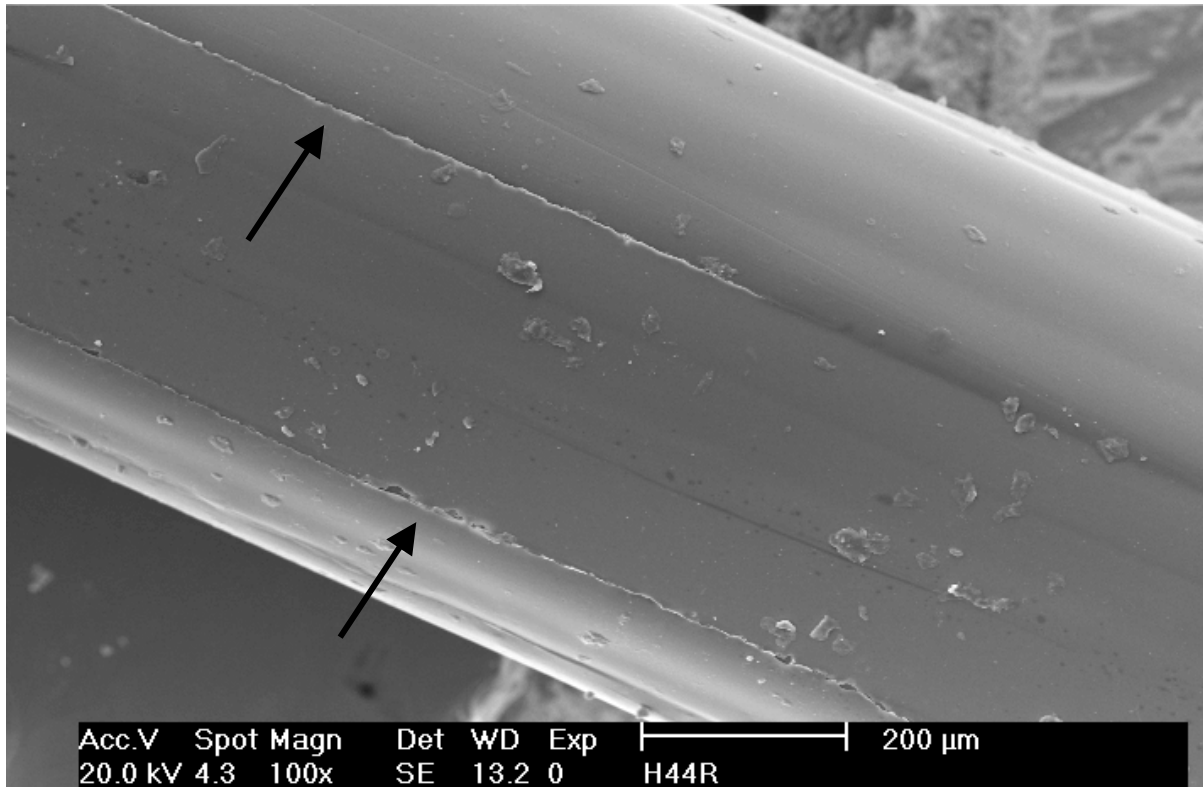


Figure 103. SEM image of a co-extruded multi-lumen microtube, before pyrolysis (H44 and filler #2)

### Conclusive remarks

By co-extrusion of two different types of commercially available silicone resin with suitable fillers it was possible to fabricate composite microtubes, in which the preceramic polymer surrounded the sacrificial filament(s). The microtubes, after cross-linking of the silicone resins, were successfully pyrolyzed to give SiOC ceramic microtubes, with diameters  $< \sim 500 \mu\text{m}$ . During the heat treatment, the sacrificial filler filament(s) decomposed leaving behind a void.

Both single- and multi-lumen microtubes were obtained using two different extruder's heads. Some difference was found between the two preceramic polymers in terms of rheological behavior and processability, resulting in microtubes of variable morphology and quality.

The single-lumen microtubes had a good morphology and possessed an elevated mechanical strength. The multi-lumen microtubes in most cases did not have an homogeneous morphology, and because contained some defects, they did not possess a significant strength.

It can however be observed that no indications that the proposed process is not feasible were found, and thus it can be stated that further experimentation would probably allow to fabricate also multi-lumen microtubes with a suitable morphology. Further work should concentrate on the control of the processing parameters and their relationship to the morphology of the specimens, based also on data for the viscosity as a function of temperature of both preceramic polymers and fillers. For the successful fabrication of multi-lumen ceramic microtubes, it would be advisable

to reduce the number of lumens from 9 to, say, 5 in order to maintain a sufficient amount of ceramic residue around the axial holes after fabrication and pyrolysis.

## References

1. G.M. Renlund, S. Prochazka, R.H. Doremus. Silicon oxycarbide glasses: Part I. Preparation and chemistry. *J. Mater. Res.* 1991;6:2716-2722.
2. Eguchi K. Silicon Oxycarbide Glasses Derived from Polymer Precursors. *J. Sol-Gel Sci.Tech.* 1998;13:945-949.
3. Turquat C, Gregori G, Walter S, Sorarù GD. Transmission Electron Microscopy and Electron Energy-Loss Spectroscopy Study of Nonstoichiometric Silicon-Carbon-Oxygen Glasses. *J. Am. Ceram. Soc.* 2001;84:2189-2196.
4. Rouxel T, Vicens J. Creep Viscosity and Stress Relaxation of Gel-Derived Silicon Oxycarbide Glasses. *J. Am. Ceram. Soc.* 2001;84:1052-1058.
5. T. Rouxel J-CS, J.-P. Guin, V. Keryvin, G.D. Sorarù. Surface Damage Resistance of Gel-Derived Oxycarbide Glasses: Hardness, Toughness, and Scratchability. *J. Am. Ceram. Soc.* 2001;84:2220-2224.
6. Walter S, Brequel H, Enzo S. Microstructural and mechanical characterization of sol gel-derived Si-O-C glasses. *J. Europ. Ceram. Soc* 2002;22:2389-2400.
7. Sorarù GD, Guadagnino E, Colombo P, Egan J, Pantano CG. Chemical Durability of Silicon Oxycarbide Glasses. *J. Am. Ceram. Soc.* 2002;85:1529-1536.
8. P. Colombo, E. Bernardo and L. Biasetto, "Novel Microcellular Ceramics from a Silicone Resin," *J. Am. Ceram. Soc.* 2004;87[1]:152–154.